GLRGROUP.org
Geological Lunar Researches Group

SELENOLOGY TODAY

Plato crater

20060410 - H. 15:06 UT

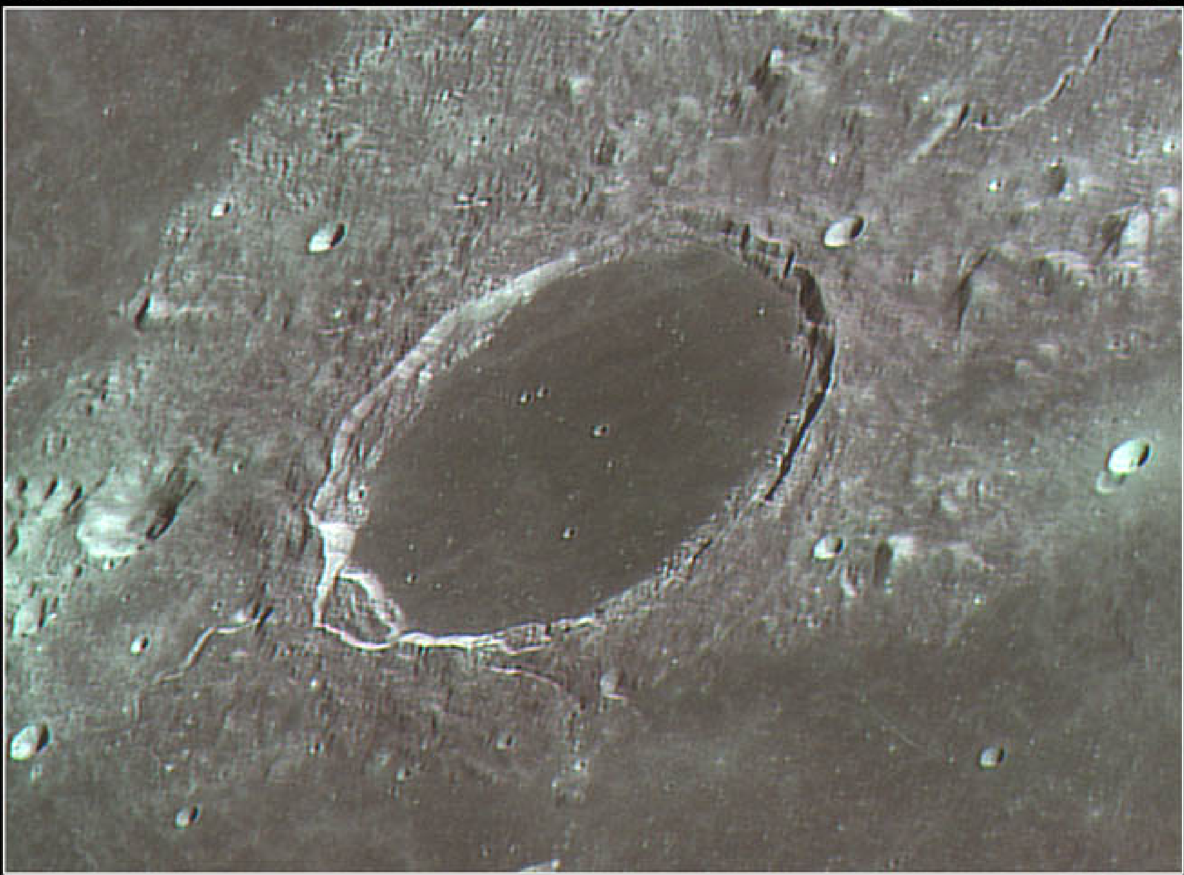

0.11 arcsec/pixel image scale, 500/2000 frames each filter 1.2X resampled
Edmund Optics RGB filters IR blocked, 55 msec. exposure
Lumenera Infinity 2-1M camera and Gladio 315 Lazzarotti Opt. scope

P. Lazzarotti - T. Olivetti
Seeing: 8-9/10 Transparency: 3/5
Bangkok, THAILAND

LUNAR PHOTOELECTRIC PHOTOMETRY HANDBOOK

Selenology Today #2 July 2006

Selenology Today is devoted to the publication of contributions in the field of lunar studies.

Manuscripts reporting the results of new research concerning the astronomy, geology, physics, chemistry and other scientific aspects of Earth's Moon are welcome.

Selenology Today publishes papers devoted exclusively to the Moon.

Reviews, historical papers and manuscripts describing observing or spacecraft instrumentation are considered.

The Selenology Today

Editorial Office

selenology_today@christian-woehler.de

SELENOLOGY TODAY #2
July 2006

Geological Lunar Researches Group

Cover : Paolo Lazzarotti and Tiziano Olivetti, image taken on April 10, 2006 at 15:06 UT Bangkok.

Telescope Gladio 315 Lazzarotti optics, Lumenera Infinity 2-1 M, RGB filters and IR blocked.

LUNAR PHOTOELECTRIC PHOTOMETRY HANDBOOK

by C. A. Kapral

Many thanks for the positive comments sent to us by our readers, amateurs and professional scientists, for the first issue of Selenology Today.

The primary goal of Selenology Today is to promote serious lunar research among dedicated amateur astronomers who are interested in observing and imaging the surface of the Moon as well as in its geologic history and the processes that formed its surface.
In this scenario, a new opportunity is the impact of ESA's Smart-1. With a predicted date of September 03, the spacecraft will slam into the lunar surface in a dramatic culmination of its 18 month orbit around the Moon.

The spacecraft is expected to crash onto the Moon's near side in Lacus Excellentiae, 10° south of Mare Humorum; the exact location and date will be refined closer to the date. It is likely that the impact flash and its plume of ejected material will be bright enough to be visible through amateur telescopes for a short period. However, the Moon will be well south of the ecliptic in the low constellation of Sagittarius on the date of impact, at least for Europe. Technical adjustments of the probe will be executed from
the 26th of June until the beginning of August. Only after this date, a better estimate of the date of impact will be available, now calculated to occur on September 03 at 2:00 UT with +/- 7 hours uncertainty. In this impact project, as in many other astronomical international campaigns, the effective participation of amateur astronomers will be of high importance.

All amateur lunar observers are encouraged to participate and familiarize themselves, both visually and photographically, with the impact area.

The Geologic Lunar Research group (GLR) set out to coordinate its team of observers for this impact event. This will be done completely through the internet, specifically through the use of e-mail. The editorial Board of Selenology Today (active 24 hours on 24) will collect images including primary analysis about the flash, description, timing and if any impact effects will be detected with amateur instrumentation. A possible "special issue" of Selenology Today could be released immediately. Primary analysis will be carried out also in amateur images submitted to our offices using the emails:

lena@glrgroup.org

This second issue of Selenology Today is composed of a single section including an extensive article by Charles Kapral about Lunar Photoelectric Photometry. This work is meant to give an observer sufficiently information to perform lunar photometry, considering that the basic principles described are also valid for CCD photometry of the lunar surface.
Photometry of the lunar surface is of high scientific interest in several respects. Example projects include lunation curves, lunar colors, TLP (transient lunar phenomena), lunar domes, but also lunar eclipses and occultations of stars.

I hope you will enjoy reading the second issue of Selenology Today !

Raffaello Lena, Editor in Chief

Photometry of the lunar surface is an important remote sensing technique that yields insight into the fundamental compositional, structural, and physical surface properties. Based on single-wavelength photometry it is possible to derive measures of the roughness, grain size, porosity, and scattering behaviour of the lunar regolith. Multi-wavelength photometry additionally reveals information about regolith composition, e. g. its iron and titanium content, but also about the exposure age ("maturity") of the surface that may for example allow for a distiction between ancient basalts and fresh impact ejecta.

The traditional way of performing photometric measurements is the photoelectric approach, while in recent times photometry with CCD cameras has become an increasingly important technique. This handbook is an effort to compile as much theory and practical information necessary to perform lunar photoelectric photometry. No explicit emphasis of CCD-based photometry is given in this article, but all described physical principles, measurement techniques, and photometric modelling approaches remain valid when applied to CCD-based photometry. All information is referenced to the original literature so that the researcher may perform an in-depth study of lunar photometry. I apologize to the authors of papers not included here, either because I felt that they weren't pertinent to lunar photometry, or that I simply missed them. The handbook is not meant to be a lunar astronomy text. I have provided enough general astronomy information to enable the researcher to adequately understand the concepts involved in setting up an observing schedule, make the observations, perform the data reduction, and analyze the results. A list of possible photometry projects is presented in the hope that one or more of them will entice a potential photometrist to actively participate in lunar photometry. Example projects include lunation curves, lunar colors, TLP (transient lunar phenomena), lunar domes, but also lunar eclipses and occultations of stars.

A glossary and several appendices are provided in order to provide as much related information as possible to perform the projects.

If this handbook has convinced a lunar observer to attempt lunar photometry, or has induced a stellar photometrist to try lunar photometry, then I feel that I have accomplished my objective.

C.Kapral

LUNAR PHOTOELECTRIC PHOTOMETRY

BY CHARLES A. KAPRAL

1.History

One of the first astronomers to measure the variation of the moon's total brightness throughout a lunation was William Herschel. Later brightness measurements were made by Bond, Zöellner (1865), Pickering (1882), Thomson (1883), Stebbins (1907, 1908), Brown and Wisliscenus (1915). These observers did not correct their measurements accurately for atmospheric extinction. The early visual photometry was based on a scale developed by J.H. Schröter (1791-1802), in which one step was equivalent to 0.15 stellar magnitude. The first reliable visual measurements were made by Wisliscenus (1915) and by N. Barabashev (1922). Barabashev determined that the brightness of all mare areas are brightest at Full Moon, and that the mare brightness at Full Moon is independent of the angle from the moon's center.

Henry N. Russell (1916) recomputed and published these observations and published a lunation curve which was widely used. M.G. Rougier (1933) used a potassium photocell without a telescope and compared the reading to that of an incandescent light placed at a variable distance, and generated an integrated phase curve (See Table 1 & Figure 1). The slight asymmetry seen in the curve is thought to be due to the photometric differences between the maria and the highland areas of the moon.

Table 1 – Lunar Phase Angle

LUNAR PHASE ANGLE		
PHASE ANGLEE	**WAXING**	**WANING**
0	1.00	1.00
10	0.787	0.759
20	0.603	0.586
30	0.466	0.453
40	0.356	0.350
50	0.275	0.273
60	0.211	0.211
70	0.161	0.156
80	0.120	0.111
90	0.0824	0.078
100	0.056	0.0581
110	0.0377	0.0405
120	0.0249	0.0261
130	--------	0.0093
140	--------	0.0046

Figure 1 – Integrated Phase Function – Kopal Z. (Ed);1971 Physics and Astronomy of the Moon. New York: Academic Press, Inc.

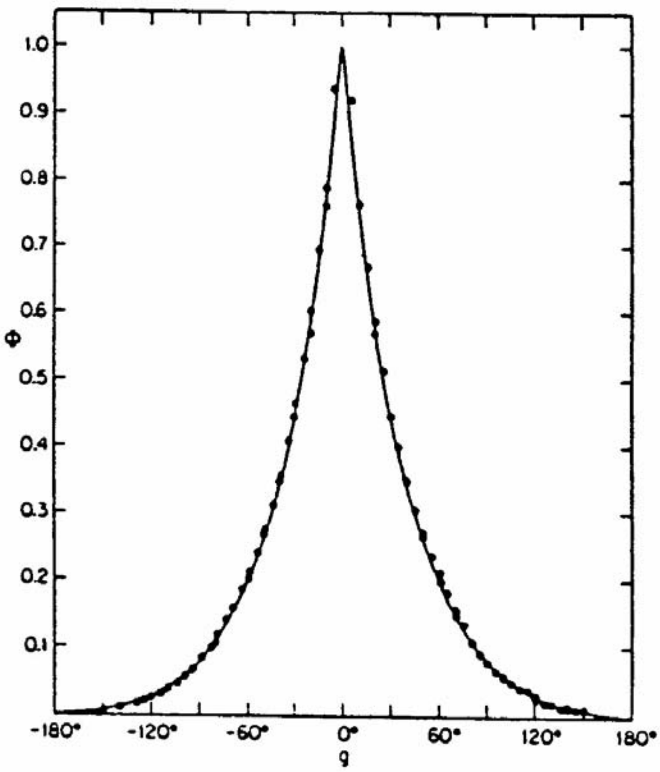

Integral phase function of the Moon. Points—data of Rougier (1933); line—theoretical function of Hapke (1963).

The first application of a multiplier to lunar photometry was by A. Markov (1948). He first studied the integrated light radiance of successive annular areas on the moon, and then studied the radiance of eighteen sites on the surface during a lunation. K. Bullrich (1948) did a rather imprecise visual determination of the integrated phase curve using a Bechstein photometer.

J. van Diggelen of the Utrecht Observatory, in the Netherlands, (1959) studied the moon's photometric properties using five photographs of M. Minnaert's series taken with the Yerkes 40-inch refractor, in the same lunation. He measured the relative brightness of 38 crater floors and tied them into one photometric system, deriving a lunation curve versus phase angle for phase angles of +11 ½°, +24°, +78°, +91°, and +105°.

Richter (1962) investigated the phase functions of particles and found that a selection of phase laws, depending on particle diameters, was recommended to interpret photometric measurements of interplanetary matter.

Bruce Hapke (1963, 1966A, 1981, 1984, 1986) developed a theoretical model which describes the photometric function rather accurately, and which is used in this handbook. The discussion of the full model parameters is too lengthy to include here. The researcher is strongly encouraged to refer to the original papers.

A study was performed (Hapke & Van Horn, 1963) to determine the optical scattering characteristics of various complex surfaces, toward an understanding of how light is reflected from the moon. One object of the study was to determine the types of material that the lunar surface may be composed of. More than 200 different surfaces were studied. They found that the general reflection of a surface may be controlled by: (1) the albedo, (2) the optical scattering characteristics, and (3) the way that the surface material is arranged. A detailed theory was developed to explain optical scattering from dark, porous surfaces, and to mathematically describe the effects of backscatter (Hapke, 1963). The theory was based on a model surface: (1) composed of layers of randomly suspended scattering particles, which are large in comparison to a wavelength of visible light, and whose particles are such that light can freely penetrate from any direction, (2) composed of particles whose individual reflectivity is low, (3) composed of randomly oriented particles, (4) whose light will be gradually attenuated upon penetrating the surface, and (5) upon which all involved solid angles are small. The model was modified to account for the unattenuated backscatter of the incident light, and to include a small forward-scatter component. Wildey (1963) developed a test to verify the validity of the form of the photometric function and to determine if the photometric function is applicable to the inner walls of craters.

Gehrels, Coffeen, & Owings (1964) performed photometric and polari-metric studies of selected lunar regions at several lunar eclipses, comparing their results with Hapke's functions for the "opposition" effect. They found that the intensity is 25% greater at 0°.5 phase angle that at 5° phase angle. The agreement to theory was good only at phase angles greater than 20°.

Irvine (1966) determined an improvement to the model by allowing for the shadows resulting from the scattering if the particles are large enough for the particles to shadow each other. He also observed that the light can escape without being attenuated if it scatters back along the path of incidence. The photometric model developed in 1963 was then modified (Hapke, 1966A) to provide better agreement at the limb areas of the moon. This was accomplished by changing the model surface by wrinkling the 1963 surface into steep-sided depressions whose walls are greater than 45° to the local horizontal. This model agreed with the radar data obtained by radar reflection from the moon's surface. The new model suggested that the "opposition" effect was caused by shadowing within the surface particles. Three parameters were introduced: (1) "h" which represents the porosity of the surface, (2) "f" which represents the fraction of depressions on the lunar surface, and (3) "Gamma" which represents the maximum effective angle between the depression's walls and the local horizontal. The best suggested values for these parameters were: h = 0.40, f = 0.90, and Gamma = Sin(45°). The model is extremely sensitive to these values. The soft landing of the Luna 9 moon probe showed that the model was in agreement with the lunar surface at the Luna 9 site. Oetking (1966) performed a series of reflectivity measurements on samples of various materials using a heavily smoked magnesium oxide surface as the reference to attempt to reproduce the photometric properties of the moon's surface, including the "opposition" effect.

The samples tested were of different composition and particle sizes. He found that the "opposition" effect may not be an unusual property of the moon, but may be a common effect of most substances.

Saari & Shorthill (1967) scanned the moon and produced digitized images throughout a lunation. Theoretically, a phase curve can be produced for any site using this database, although the technique hasn't been widely used. McCord (1967) observed 24 areas with a grating spectrometer to study the visible emissions of the moon, at 3968Å and 3934Å, during 6 lunations in 1965. No significant variations of non-solar radiation were found, but it appeared that changes measured were due to visible emission on or near the surface. Franklin (1967) observed the earthshine in V and B over fourteen nights in 1965. He determined that the Bond Albedo is approximately 0.36 in V and 20% greater in B, in accordance with Danjon's (1954) and Fritz's (1949) measurements.

Hapke (1968) photometrically measured various irradiated and uni-radiated powders to determine which optical characteristics matched those of the moon. He compared his results with the newly derived Surveyor V data, and showed that his results for the iron content of lunar soil agreed with the Surveyor data. Watson (1968) extrapolated photographic and photometric photometry to photoclinometry to calculate relative topographic profiles using spacecraft images. The formulae were based on the Ranger spacecraft data. The reliability of photoclinometric data depends on how precise the photometric function is known.

The study of the "opposition" effect from data acquired by the Apollo 8 and Apollo 10 missions indicated a brightness increase of 19% between 0° and 1.5° phase angle for Apollo 8, and 7% for Apollo 10. Further investigation was required to correlate the magnitude of the "opposition" effect with surface properties. (Pohn, Radin, & Wildey, 1969; U.S. NASA 1969, 1971A). Jones (1969A, 1969B) performed a study which indicated that the uniformity of the light scattering law applied to the lunar surface over the terrestrially visible hemisphere, suggesting that the porosity of the overall surface microstructure is uniform. This was based on a catalog of relative brightness of 199 lunar features, prior to Full Moon. Van Diggelen (1969) accurately measured the ray systems of Tycho, Copernicus, Kepler, and Aristarchus, from photographic plates obtained during a lunar eclipse, to determine their brightness, and to verify the existence of a dark halo around Tycho and Kepler.

Shevchenko (1970) conducted a photometric analysis of 403 equal area sites on the lunar far side utilizing Zond-3 photographs, based on Hapke's (1966A) improved photometric model. The lunar relief was divided into six "types" of photometric relief, and Hapke's "h" and "Gamma" was determined for each type. “Type I” is characteristic of the “average” lunar surface, “Type II” is distinguished by a rise in brightness somewhat retarded relative to the average at small phase angles, “Type III” shows a photometric function that is steeper than average in the range of phase angles close to 90°, “Type IV” exhibits both the above pecularization and the corresponding photometric function departs from the average slope at all phase angles throughout the 0-70° range investigated, “Type V” shows a sharp rise in the slope of the photometric function at large phase angles, and “Type VI” is characterized by a nearly linear brightness range law at small phase angles”

Pohn & Wildey (1970) prepared a 1:5,000,000 map of the normal albedo of the moon based on photographic and concurrent photoelectric scans. Mitchell & Pellicori (1970) observed the moon in the UBVRI system to determine the albedos for the four lunar topographic types: (1) mountains, (2) dark maria, (3) light maria, and (4) cratered terrain. Their results were in agreement with past results that the brighter a feature is, the redder it is.

Adams & McCord (1971) proposed a model of the lunar optical properties which includes the contamination of the surface by aging and composition differences. They compared samples from the Apollo 11 and 12 missions with telescopic spectral reflectivity measurements.

Lane & Irvine (1973) conducted observations of the lunar disk from phase angles of 6° to 120° in nine bands and in UBV. The observations confirmed that the moon gets redder in some areas as the phase angle increases. Bonner & Schmall (1973) extended Watson's (1968) technique for photoclinometry from spacecraft images to include the determination of terrain roughness. Their solution can be applied to either vertical or oblique images and is summarized into a format easily adapted to a computer program.

Bently, De Jonckherre, & Miller (1974) measured five passbands in the near ultraviolet with a rocketborne photometer, and indicated that the geometric albedo decreases towards the shorter wavelengths. Mikhail & Koval (1974) obtained the light curves of thirteen lunar features in five different wavelengths and extrapolated them to zero phase to obtain the luminosity of the features at zero phase. Their study indicated that each individual region's albedo differed at the different wavelengths. Wildey (1974) produced a 1:2,500,000 isodensity mosaic of the Full Moon in five colors, with a control grid used for guiding the mosaicking. He produced a graphical device that allows a researcher to read the true phase angle applicable at any lunar coordinate for either the 1:5,000,000 map or the 1:2,500,000 mosaic.

Evsyukov (1975B) used photographic photometry to determine that "the optical properties of any detail of the lunar surface can be described using five optical characteristics: (1) the normal albedo, (2) color index, (3) brightness phase gradient, (4) maximum degree of polarization, and (5) polaroindex." This was done to explore the possibility of cartography of the optical characteristics of the moon.

Wildey (1976) used a low resolution file of 140 digital samples to determine the geometric albedo of the moon. He also calculated the "super Full Moon", in which the brightness of every lunar area is corrected to zero phase, whose magnitude is $0^m.007$ brighter than the Full Moon. The true Full Moon magnitude determined was −12.76 ± 0.005, with a geometric albedo of 0.1248 and a Bond albedo of 0.072. He also produced (1977) a digital file of the normal albedo of the moon, at a resolution of 6.3 km. The file was produced from five photographs taken with the Northern Arizona Astrophysical Observatory 24" reflector, and gives the lunar longitude, latitude, mean normal albedo, and the standard-deviation-of-the-mean. Clark, et al. (1976) investigated the ratio of Al/Si X-Ray fluores-cence intensity and visible albedos in the Palus Somnii area during the Apollo 15 mission and found a positive correlation. Lucke, Henry, & Fastie (1976) measured the lunar albedo and photo-metric function in the far-ultraviolet with the Apollo 17 orbiting spectrometer. They found that the brightness increases toward shorter wavelengths, in contrast to the visible and near-ultraviolet measurements.

Wildey (1978) analyzed 25 photometric images of the moon to obtain an image of the moon in the Heiligenschein parameter, which is different from the normal albedo images.
Hood & Schubert (1980) studied the effect that lunar magnetic anomalies would have by deflecting the solar wind at the lunar surface. They stated that the high albedo of features such as the Reiner Gamma formation may be the result of the action of the magnetic anomaly situated there.
The scattering of light from a surface was analyzed (Hapke, 1981; Hapke & Wells, 1981; Hapke, 1984, 1986) and equations for the bidirectional reflectance function; radiance factor and coefficient; the normal, hemispherical, Bond, and physical albedos; the integral phase function; phase integral; and limb-darkening profile were derived from an approximate solution of the radiative transfer equation. This theory is used to interpret the reflectance spectroscopy from planetary surfaces, and will allow the average single-scattering albedo, the average particle phase function, the average macroscopic slope, and the porosity to be determined from photometric observations. Hapke (1984) developed a correction to the model for the photometric function to account for the roughness of the surface, and derived the equations for the extinction coefficient and the "opposition" effect (1986). Shkuratov (1981) used a series of photographs at large phase angles to investigate the regional distribution of departures from the correlation between the albedo and the maximum degree of polarization of the moon, and the Fresnel albedo.
Lumme & Irvine (1982) used the newly developed theory of bidirectional reflectance to analyze the data obtained by Wildey & Pohn (1964) and Gehrels, et al. (1964). They discovered that it was only required to add a multiple scattering factor to explain the whole disk observations over a wide range of phase angles and wavelengths. The application of the generalized radiative transfer theory for planetary regoliths (Lumme & Bowell, 1981A, 1981B) showed that the data fits the theory and produces information on both the macroscopic and microscopic lunar properties.
Shevchenko (1982) used data from the Zond-3, Zond-6, Zond-8, and Apollo 13 spacecraft to perform a photometric analysis of 26 lunar phases resulting in an empirical equation for the phase curve of the moon, the integral stellar magnitude of the Full Moon, the phase integral, the light constant, geometric and physical albedos, and the stellar magnitude of the moon at the unity distance from the Earth and Sun.
Davis & Soderblom (1984) devised a new photoclinometric technique to obtain topographic data from single images. It simultaneously uses the brightness data from a pair of profiles along their lengths. A procedure is presented which eliminates the requirement of topographic symmetry along the profiles.
Buratti & Veverka (1985) utilized the Cornell goniometer to measure both low and high albedo surfaces, using a crater roughness model. They found that the decrease in reflected light due to the surface roughness sharply increases with increasing phase angle for low albedo surfaces, and that the effects are constant between 30° and 70° phase angles for high albedo surfaces.
Pinty & Ramond (1986) derived a bidirectional reflectance model for terrestrial surfaces using data from the Nimbus-7 ERB experiment.

Wildey (1986) used the failed prediction of limb-darkening of the Full Moon from brightness versus phase to illustrate the use of operators and their eigenvalue equations to investigate the optical reflection from planetary surfaces.

Helfenstein & Veverka (1987) verified that Hapke's model of the lunar surface can be used to derive the physical and geologic parameters from photometric measurements. They studied the single scattering albedos, backscattering, and the "opposition" effect for various types of lunar terrains by applying Hapke's (1986) equations to the lunar disk-integrated light curve and to the disk-resolved data of Shorthill, et al. (1969). They showed that the single scattering albedos of bright areas are larger than those of the maria.

Helfenstein (1988) studied the photometric behavior of a surface with meter to kilometer scale roughness. He found that "reliable determination of roughness from disk-integrated data or from disk-resolved photometric observations of individual geological features requires observations which extend from small phase angles out to phase angles above 90°. He found that the Hapke model did not accurately describe the photometric behavior of a surface at large incidence and phase angles if the roughness is in the meter to kilometer scale.

Busarev & Shevchenko (1989) used a photometric analysis of Zond-6 photographs to map four mare areas containing Ilmenite by measuring the spectral albedo on the 0.336 - 0.758 μm range. Pinty, Verstraete, & Dickinson (1989) developed a model which is able to predict observed bidirectional reflectance as well as directional-hemispherical reflectance over bare soil. Mustard & Pieters (1989) used Hapke's model to investigate the photometric phase functions of mineral mixtures of common geologic minerals.

McEwen(1991 generated best - fit approximations to the Hapke-function brightness variations for the Minnaert and Lunar-Lambert functions, which are easier to use in photoclinometry than Hapke's function. This simplifies photoclinometry across terrains with variable surface materials. Pinty & Verstraete (1991) investigated the use of bidirectional reflectance measurements to retrieve surface parameters from remotely sensed data. Krisciunas & Schaefer (1991) developed a model of the brightness of moonlight as a function of the moon's phase, the moon's zenith distance, the zenith distance of the sky position, angular separation of the moon and sky position, and the local extinction coefficient.

Hiroi & Pieters (1992) developed the Aisograin ≅ model, which treats reflectance as a series of grain interactions incorporating the real part of the refractive index and the absorption coefficient, and two parameters, ω_1 and ω_2, which model scattering and absorption in the vertical and horizontal directions.

McGuire & Hapke (1995) studied light scattering of large, irregular particles and found that: (1) the Mie theory works for “scattering by a clear, smooth, perfectly spherical particle that is large compared to the wavelength”, (2) almost any change from these ideal characteristics causes major departures from Mie theory. Hence, “Mie theory is a poor predictor of the scattering properties of most large particles encountered in nature”.

Buratti, Hillier & Wang (1996) used multispectral observations from the Clementine spacecraft to study the lunar opposition surge. They found that the brightness of the moon increases more than 40% between solar phase angles of 4° and 0°.

A small wavelength dependence was exhibited suggesting that the principle cause of the opposition surge is shadow hiding. They also found that the surge is about 10% greater in the lunar highlands, attributed to textural variations between the two terrains.

Hillier (1997) defined a model assuming standard radiative transfer theory with correction for macroscopic roughness and a shadow hiding opposition surge. It was shown that extremely narrow opposition surges might be explained by a shadow-hiding model even for relatively compact surfaces if the size of the particles decrease toward the surface. Helfenstein, Veverka & Hillier (1997) tested the hypothesis that the lunar opposition effect is due to shadow hiding, coherent backscatter, or some combination of the two phenomena. They extended Hapke's photometric model to include M.I Mischenko's (1993) description of the coherent backscatter opposition effect. The shape of the Moon's opposition surge is accurately defined by the combination of a narrow coherent backscatter peak and a very broad shadow hiding peak. They proposed that the submicron sized particles that control coherent backscatter do not contribute to the shadow hiding opposition surge and that coherent backscatter cannot be responsible for the broad component of the Moon's opposition surge. Kieffer (1997) studied the photometric stability of the lunar surface using Clementine images to empirically determine small impact events. He found that the Moon can be considered photometrically stable for a fixed illumination and observation geometry to within 1×10^{-8} per year for irradiance, and 1×10^{-7} per year for radiance at a resolution common for spacecraft imaging instruments. Hillier (1997) examined the effects of close packing on the light scattering by spherical particles. He found that classical radiative transfer coupled with the assumption that the composite particle is the fundamental scatterer provides a good approximation in the high porosity limit. However, the radiative transfer calculation underestimates the scattering by approximately 10% at high incidence, emission, and phase angles. Lower porosities can increase the discrepany to 50% or more. Therefore, one should exercise caution in interpreting the results of models based on classical radiative transfer theory in terms of the physical properties of the lunar surface particles.

Nelson, Hapke, Smythe & Horn (1998) studied "the hypothesis that coherent backscattering can be an important contributor to the enhanced reflectance seen in planetary regolith materials when observed at small phase angles." They found "a non-linear relationship between the slope of the opposition curve measured at 2 deg and the single scattering albedo which is the opposite of what is predicted by the shadow hiding model for the opposition effect. Hartman & Domingue (1998) examined the single scattering function and placed constraints on which scattering functions are most appropriate for the Hapke 1986 model. They found that "the correlation between single scattering albedo and the single scattering parameters is not simple, and only general predictions of the value of one based on the others can be made." Hapke, Nelson & Smythe (1998) measured the linearly and circularized polarized reflectances to examine the lunar opposition effect. Shepard & Campbell (1998) used fractal surface statistics as a general model for planetary surface roughness, demonstrating "that a fractal surface model provides a way of quantitatively verifying and extending previous interpretations of the Hapke (1984) roughness parameter." Dollfus (1998) used a video-polarimeter to derive the median grain size and mean roughness slope angle and map them over characteristic lunar features. He discovered terrains of anomalous surface textures and anomalities which may have resulted from seismic action when an impact occurred.

Shkuratov, Starukhina, Hoffmann & Arnold (1999) suggested a model using spectra of optical constants of the medium materials. The model was applied to interpret optical properties of the Moon. The showed that "(1) both color indices and depth of absorption bands for regolith-like surfaces depends on particle size" and "(2) fine-grained reduced iron occurring in regolith particles affects band minima positions in reflectance spectra of lunar pyroxines". Dollfus (1999) analyzed an area around Messier. He found that the highlands are rougher and are made of larger grains. Helfenstein & Shepard (1999) applied computer stereophotogrammetry to Apollo Lunar Surface Closeup Camera photos of the lunar surface and constructed "the first-ever topographic relief maps of undisturbed lunar soil over spatial scales from 85:m to 8.5:m." They confirmed Lumme et al's (1985) results and their findings that the roughnesses of all lunar surfaces increases with decreasing size-scale. They found that "the predicted photometric roughness at size scales of 0.1mm and less significantly exceed photometric estimates and suggests that there exists a measurable size scale below which relief either is not photometrically detectable or is not represented in the Hapke model as macroscopic roughness." Shkuratov, Kreslavsky, Ovcharenko, Stankevich, Zubko, Pieters, & Arnold (1999) performed an analysis of Clementine data and found that the coherent backscatter component is nonzero. They also showed "a flattening of phase-dependent brightness at angles less than 0.25 deg that is caused by the angular size of the solar disk." They show that "the opposition effect of the lunar surface to be substantially formed by the coherent backscatter mechanism." Hillier, Buratti & Hill (1999) used Clementine images to produce a comprehensive study of the lunar surface.They used the calibrated camera data to fit a version of the Hapke photometric model modified to include a new formulation for the lunar opposition surge. They found that most of the surge can be explained by shadow hiding with a halfwidth of approximately 8 deg. Their "results provide an important test for the robustness of photometric models of remote sensing observations."

Considerable work has been done in modeling the surfaces of the moon and other solar system objects. More photoelectric observations must be obtained, both from Earth, and from spacecraft, in order to refine the models. Most of the current amateur photometric work utilizes visual photometry based on a 20-step gray scale set up by T.G. Elger. The Elger scale (Appendix E) is applied primarily to the investigation of Lunar Transient Phenomena (LTP), and lately to determine the albedo of selected lunar features in the A.L.P.O. Selected Areas Program.

2.The Moon’s motion and position

The moon revolves around the Earth in an elliptical orbit which varies between 225,732 miles and 252,007 miles. This causes the moon's horizontal parallax to vary between 33' 30" and 29' 25". The moon's equatorial plane is tilted 6° 51' to it's orbital plane, and the orbital plane is tilted 5° 9' to the ecliptic. This causes the moon's rotational axis to precess in a period of 18.6 years. See Figure 2. Kepler's Laws of motion dictate that the moon move faster at perigee, and slower at apogee.

Figure 2 – Moon’s Motion and Position – British Astronomical Association; Guide to Observing the Moon. Enslow Publisher, Inc., Hillside, NJ.

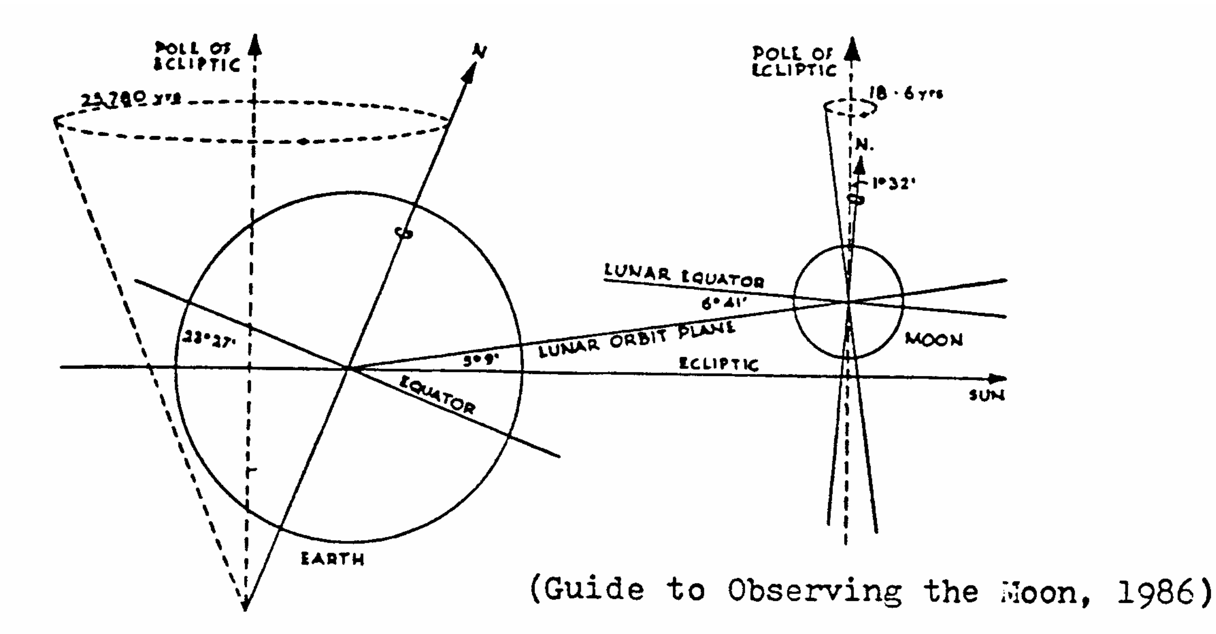

An observer of the moon will soon notice that the moon appears to nod and wobble in it's orbit, allowing up to 59% of it's surface to become visible. These are the moon's librations. Libration has three primary causes:

1. Since the moon's axis is tilted 6° 51' to it's orbital plane, occasionally more of the north or south pole is tilted toward the Earth. This is libration in latitude, and can attain a maximum value of ∀7° 48' 2".6. See Figure 3.

2. Since the moon has a constant rate of rotation about it's axis, and a varying orbital speed, due to Kepler's Laws, an apparent wobble of up to ∀7° 57' may be observed. This causes more of the east or west limb to be observed. This is the libration in longitude. See Figure 4.

3. Since the observer travels around half of the Earth's circumference in half a day, his view of the moon will change slightly due to his seeing it from different places on a 7457 mile baseline. This is the diurnal effect, and is much smaller that either the librations in latitude or longitude, amounting to ∀57' 2".6.

Figure 3 – Moon's Axis – British Astronomical Association; 1986. Guide to ObservingThe Moon. Enslow Publisher, Inc., Hillside, NJ.

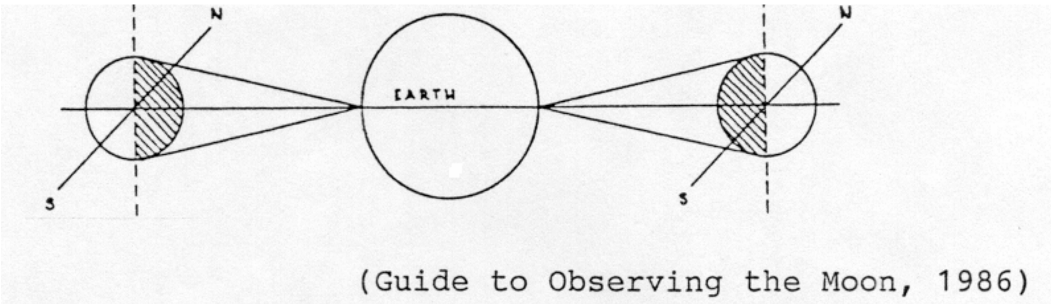

Figure 4 – Moon's Rotation – British Astronomical Association; 1986. Guide to ObservingThe Moon. Enslow Publisher, Inc., Hillside, NJ.

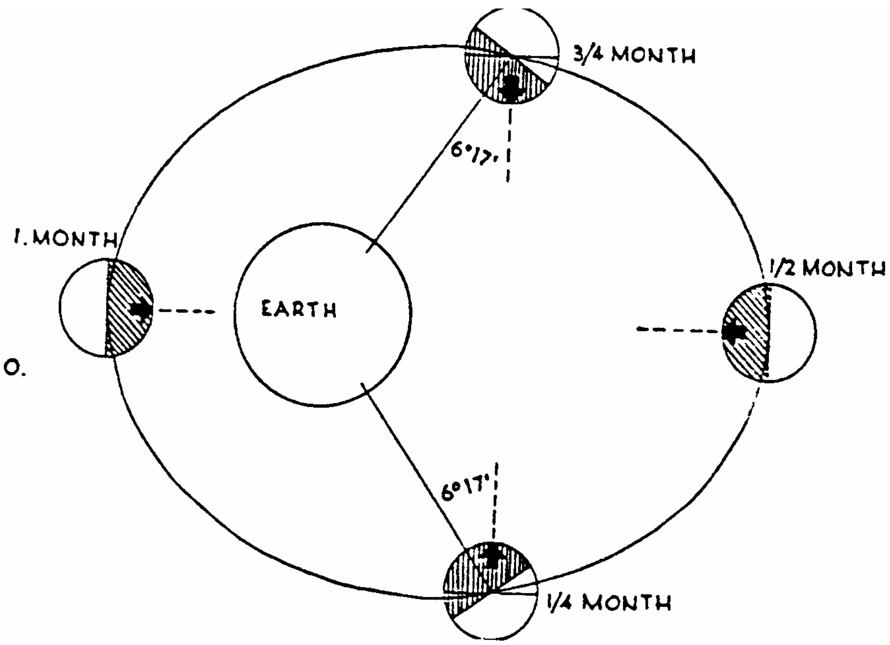

The angular height of the moon at the meridian varies throughout the year, and throughout a lunation. This is caused by the inclination of the moon's orbit to the ecliptic. Because of it's orbital tilt, the moon can pass 5° higher in the sky than the sun, reaching a maximum northern declination of +282° and a maximum southern declination of –282°. Therefore, the moon can vary by as much as 57° in meridian altitude during the year.

The result of this is that (British Astronomical Association, 1986):

1. In the Spring, the First Quarter moon rises high in the sky, the Full Moon is much lower, and the Last Quarter moon is very low.

2. In the Summer, the First Quarter moon is lower than in the Spring, the Full Moon is low, and the Last Quarter moon is higher than in the Spring.

3. In the Autumn, the First Quarter moon is lowest during the year, the Full Moon is higher than in the Summer, and the Last Quarter moon is at it's greatest height.

4. In the Winter, the First Quarter moon is higher than in the Autumn, the Full Moon is highest in the year, and the Last Quarter moon is lower than in the Autumn.

The 5° orbital tilt results in the moon always being within a 10° band parallel to the ecliptic, 5° above it and 5° below it.

3. The Photometric Function

It is known that the surface of the moon scatters the light incident upon it. This scattering is simulated by utilizing a Lambert surface. A matte surface will scatter the light isotopically, that is, equally in all directions. If all light is scattered back, the surface is a Lambert surface. When this type of surface is illuminated by light at a specific angle of incidence, a photometer will indicate a constant reading, regardless of the observing angle or distance. On a Lambert sphere, the brightness is determined by the cosine of the angle of incidence. Therefore, the brightest spot on a Lambert sphere is at the sub-solar point, and the brightness decreases to 0 at the terminator. At full sphere, the terminator is the limb, and the "limb darkening" is greatest.

The moon differs from a Lambert surface in various ways. On the moon:

1. The sub-solar point is not the brightest point.
2. The lines of isophotes are approximately on the meridians of longitude.
3. There is no "limb darkening" on the moon.
4. The lunation curve peaks sharply at Full Moon

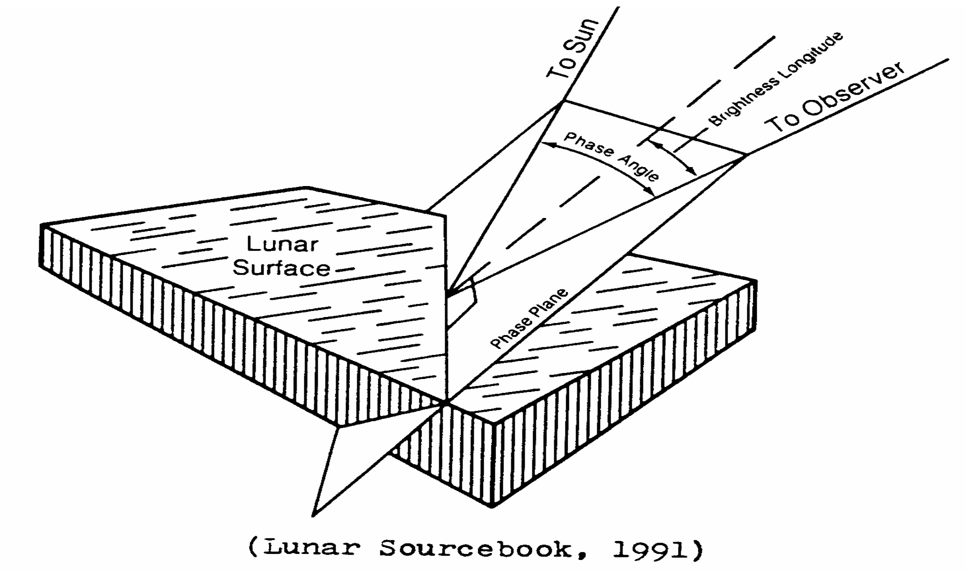

Figure 5 - Photometric Function - Heiken, G.H., Vaniman, D.J., & French,B.M.; 1991. Lunar Sourcebook. NJ. Cambridge University Press.

The photometric function of a site describes the photometric behavior of the site. It relates the intensity of the light scattered in a direction to the intensity of the light incident to the site and arriving from a different direction. It depends upon the angle of incidence of the light, the angle of observation, and the phase angle. See Figure 5.

A plot of the brightness of a site versus the phase angle produces the lunation curve for the site. A study of lunation curves indicates the following photometric properties:

1. The photometric function depends only on the phase angle (g) and the brightness longitude. See Figure 6 and Table 2. Figure 6 shows the relative brightness as a function of phase angle and brightness longitude. It shows the rapid brightening near full moon (phase angle = 0°), the well-known darkening near the terminator (where the brightness longitude = 90° – phase angle), and the relative faintness of all sites for the cresent phases (phase angles greater than 90°).

2. Most sites are brightest at Full Moon. (Wildey & Pohn, 1964).

3. The rate of increase of brightness is very rapid at small phase angles (near Full Moon). This is the "opposition" effect, or Heiligenschein. (Gehrels et al., 1964; Wildey & Pohn, 1969; Pohn et al., 1969).

4. Sites which have a similar albedo have a similar brightness at Full Moon, regardless of their location on the moon. There is no "limb darkening".

5. Sites at the same longitude tend to have similar photometric functions. See Figure 7. Figure 7 shows “brightness contours” mapped onto the apparent lunar disk at phase angle intervals of 15° to indicate the actual brightness variations an observer sees at various phases.

6. The brightness of all sites increases (or decreases) faster than linearly before (of after) Full Moon. Their lunation curves are always concave upward, and peak on, or near, Full Moon. See Figure 8a and Figure 8b. Figure 8a plots the brightness function against colongitude (in this example, Colongitude = g + 90°) for three sites on the Moon’s equator, at longitudes of +45° (E), 0°, and -45° (W). Note that all three curves peak at Full Moon (g = 0°), but only the 0° - longitude curve is symmetric about Full Moon. The eastern hemisphere sites show a gradual brightening before Full Moon and a rapid darkening after Full Moon; the western hemisphere sites show an opposite effect.

The brightness function model and Figures 6, 7, and 8a ignore albedo and express brightness so that the maximum (Full Moon) brightness of a site equals 1.0. The parts of this handbook on observing and data reduction techniques discuss how a site’s albedo may be found using the photometric function.

Table 2 – Days from New Moon Phase

DAYS FROM NEW MOON PHASE				
gE	Days	Lunar Phase	% Illumination of the Visible Hemisphere	
-180	0	New Moon	0	
-170	0.8202941		5.555	
-160	1.6405882		11.111	
-150	2.4608823		16.666	
-140	3.2811764		22.222	
-130	4.1014705		27.777	
-120	4.9217646		33.333	
-110	5.7420587		38.888	
-100	6.5623528		44.444	
-90	7.3826469	1st Qtr	49.999	50.000
-80	8.2029410		55.555	
-70	9.0232351		61.111	
-60	9.8435292		66.666	
-50	10.6638233		72.222	
-40	11.4841174		77.777	
-30	12.3044115		83.333	
-20	13.1247056		88.888	
-10	13.9449997		94.444	
0	14.7652938	Full Moon	99.999	100.000
+10	15.5855879		94.444	
+20	16.4058820		88.888	
+30	17.2264764		83.333	
+40	18.0464702		77.777	
+50	18.8667643		72.222	
+60	19.687058454		66.666	
+70	20.5073525		61.111	
+80	21.3276466		55.555	
+90	22.1479407	3rd Qtr	49.999	50.000
+100	22.9682348		44.444	
+110	23.7885289		38.888	
+120	24.6088230		33.333	
+130	25.4291171		27.777	
+140	26.2494112		22.222	
+150	27.0697053		16.666	
+160	27.8899994		11.111	
+170	28.7102935		5.555	
+180	29.5305876	New Moon	0	

The model lunar surface used in this handbook is based on the Hapke model surface, (Hapke (1963, 1966A)). The model surface uses the following assumptions (Hapke (1963):

1. "The surface consists of a semi-infinite layer of objects large compared with a wavelength of visible light and arranged in an open network into which light from any direction can penetrate freely. The objects are located irregularly enough within this structure so that on a macroscopic scale the medium appears isotropic and homogeneous."
2. "The reflectivity of the individual objects is low, and so only scattered light rays are important."
3. "The reflecting objects are oriented at random. Thus an effective scattering law for an individual object can be used which is a function only of the angle between the directions of illumination and observation and is otherwise independent of these directions. This assumption is valid for a cloud of particles in suspension, but for a nonsuspension the necessity for support of the reflecting objects will introduce some departure from complete randomness. However, it will be assumed that for the dendritic surface structure under consideration here this departure is so slight that to the approximation of this analysis the assumption is justified."
4. "Since the objects that make up the surface are located at random within the array, a typical bundle of light rays penetrating the surface will, owing to absorption and reflection by the objects, experience a gradual attenuation similar to that in a continuous fluid. Thus it will be assumed that the intensity of light is exponentially attenuated in proportion to the path length of the ray through the medium."
5. "All solid angles involved (e.g., those subtended by the light source and detector at the surface and the acceptance cone of the detector) are small."

This model was then improved (Hapke, (1966A)) by the inclusion of “three fitable parameters h, f, and γ; h is related to the porosity of the lunar soil and governs the sharpness of the backscatter peak; f if the fraction of the surface occupied by depressions; γ is the effective maximum angle which the walls of the depressions make with the local horizontal. Best preliminary values of these parameters are $h = 0.40$, $f = 0.90$, and $\gamma = \sin 45^{\circ}$.”

Additional references for the lunar photometric function and albedo are : [Aronson & Emslie (1973); Barabashov & Ezevsky (1962); Bennett (1938); Bohren & Huffman (1993); Chandrasekhar (1960); Dragg & Prior (1969); Draine & Goodman (1993); Drossart (1990, 1993); Emslie & Aronson (1973); Fedoretz (1952); Fessenkov (1962); Fielder (1971); Goguen & Veverka (1979); Gold, Bilson & Baron (1977); Greenberg (1974); Hameen-Antilla, Laakso, & Lumme (1965); Hapke (1966B, 1971, 1977, 1993); Harris (1961); Hawke et al. (1993); Hedervari (1983A); Hess, Menzel & O'Keefe (1966); Holt & Rennilson (1970); Hopfield (1967); Kerker (1969); Kopal (1962, 1966, 1971); Kopal & Goudas (1967); Johnson & Morgan (1953); Kopal & Mikhailov (1962); Kopal & Rackham (1964); Kornienko, Shkuratov, Bychinskii & Stankevich (1982); Kuiper & Middlehurst (1961); Lester, McCall & Tatum (1979); Link (1972); Liou & Hansen (1971); Lucchitta (1971); Lumme (1972); Lumme & Bowell (1981A, 1981B); MacRobert (1984A); Markov (1962); McCord & Adams (1973); McKay, Fruland, & Heiken (1974); Minnaert (1941, 1959, 1961, 1967); Moore, H.L. (1980); Mukai, Mukai, Giese, Weiss & Zerull (1982); Muller (1897); Ney, Woolf & Collins (1966); Novikov, Shkuratov, Popov, & Goryachev (1982); Pohn, Wildey & Offield (1971); Price (1988); Purcell & Pennypacker (1973); Puskar (1983); Rennilson, Holt & Morris (1968); Rukl (1976); Salisbury (1970); Schuerman (1980); Schuerman, Wang, Gustafson, & Schaefer (1981); Shevehenko (1980); Shorthill & Saari (1965); Shkuratov & Kreslavsky (1998); Singer (1967); Skorobogatov & Usoskin (1982); Struve (1960); Sytinskaya (1953); Tanashchus & Gilchuk (1978); U.S. NASA (1971B, 1972); Van Diggelen (1965); Van de Hulst (1957); Veverka, Gougen & Noland (1977); Weiss-Wrana (1983); Westfall (1983B, 1984B); Whitaker (1969); Whitford-Stark (1974); Wildey (1963, 1971, 1972, 1992); Wildey & Pohn (1971); Wilson (1971); Zerull (1976); Zerull & Giese (1974); Zerull, Gustafson, Schulz, & Theile-Corbach (1993)].

Figure 6 - Photometric Function - Westfall, J.E.; 1948B.

Lunar Photoelectric Photometry Handbook.Priv:Pub.

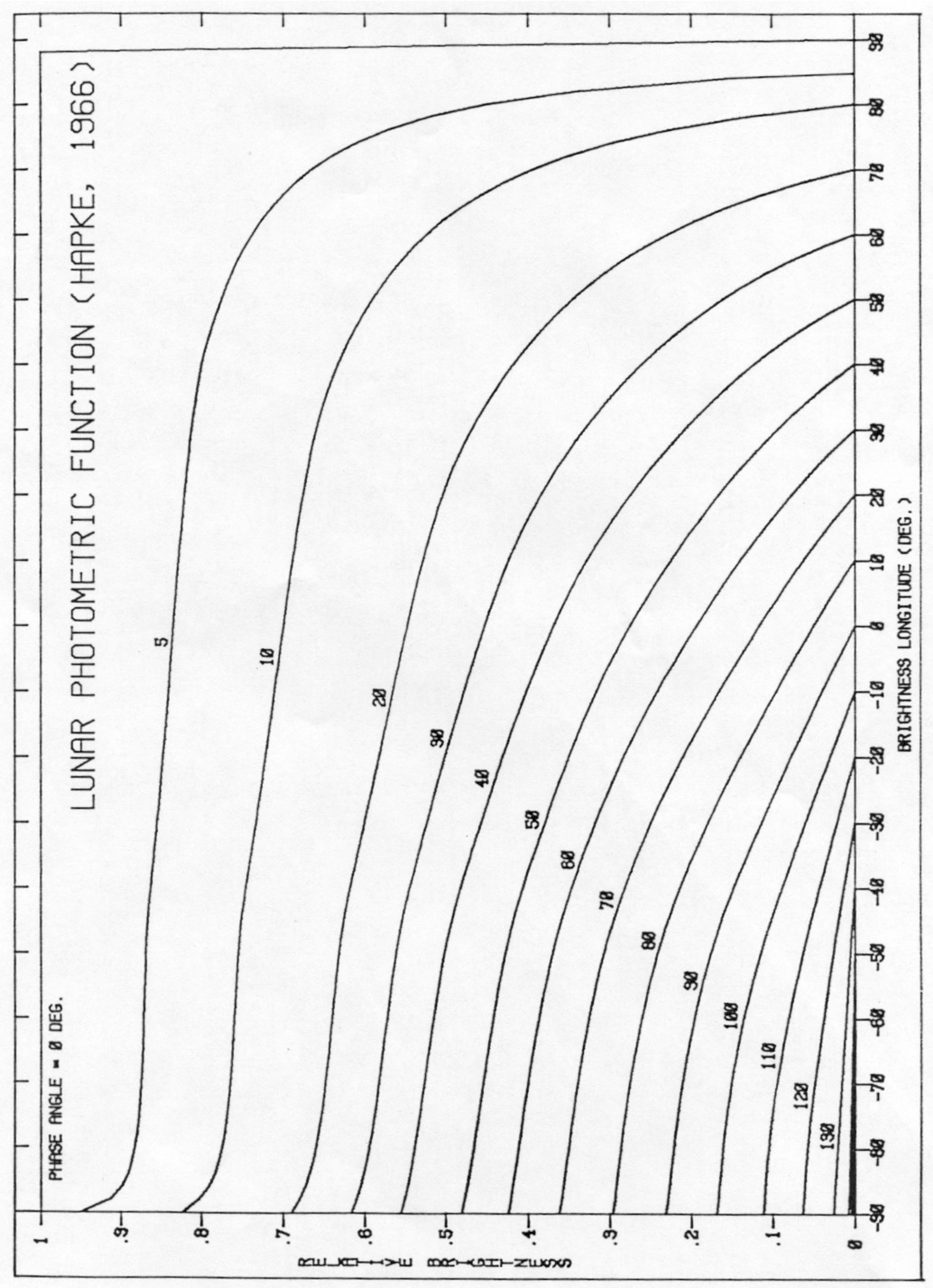

Figure 7 – Lunar Isophot Graph by Phase – Westfall, J.E.; 1948B.

Lunar Photoelectric Photometry Handbook.Priv:Pub.

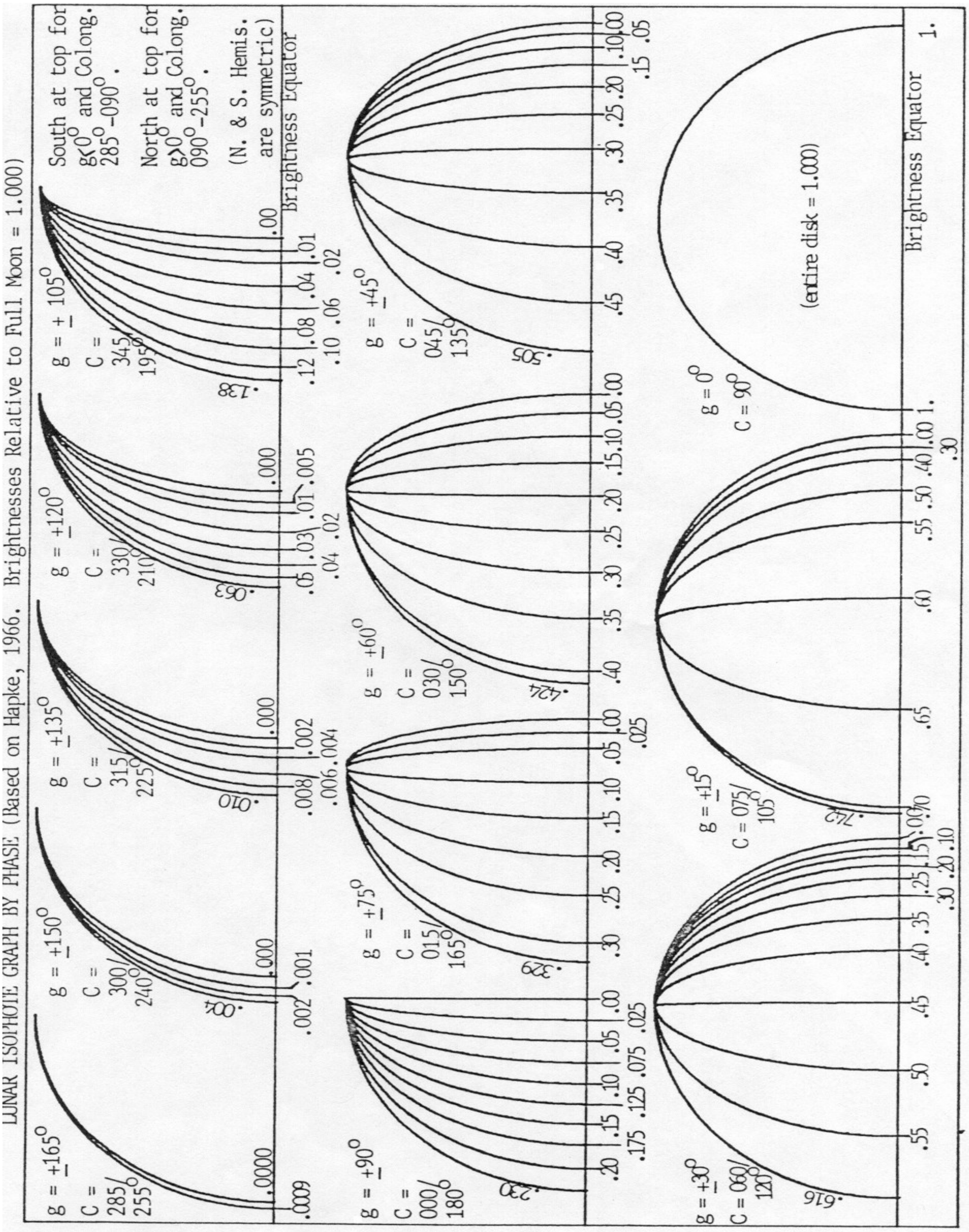

Figure 8a – Theoretical Lunar Photometric Function – Westfall, J.E.; 1948B.

Lunar Photoelectric Photometry Handbook.Priv:Pub.

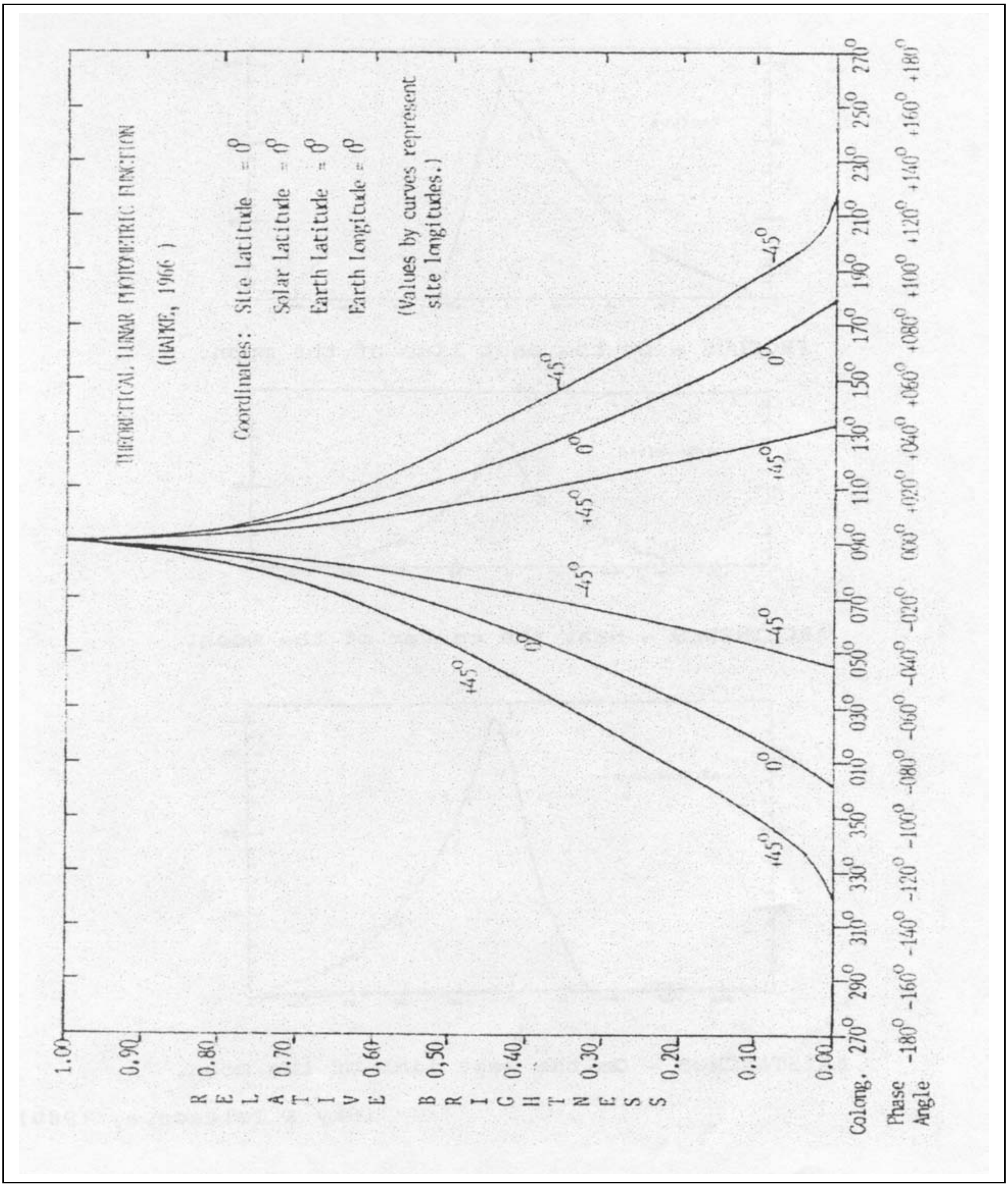

Figure 8b - Lunation Curves - Struve, O.; 1960. Photometry of the Moon

Sky & Telescope, Vol.20, No.2, pp.70-73.

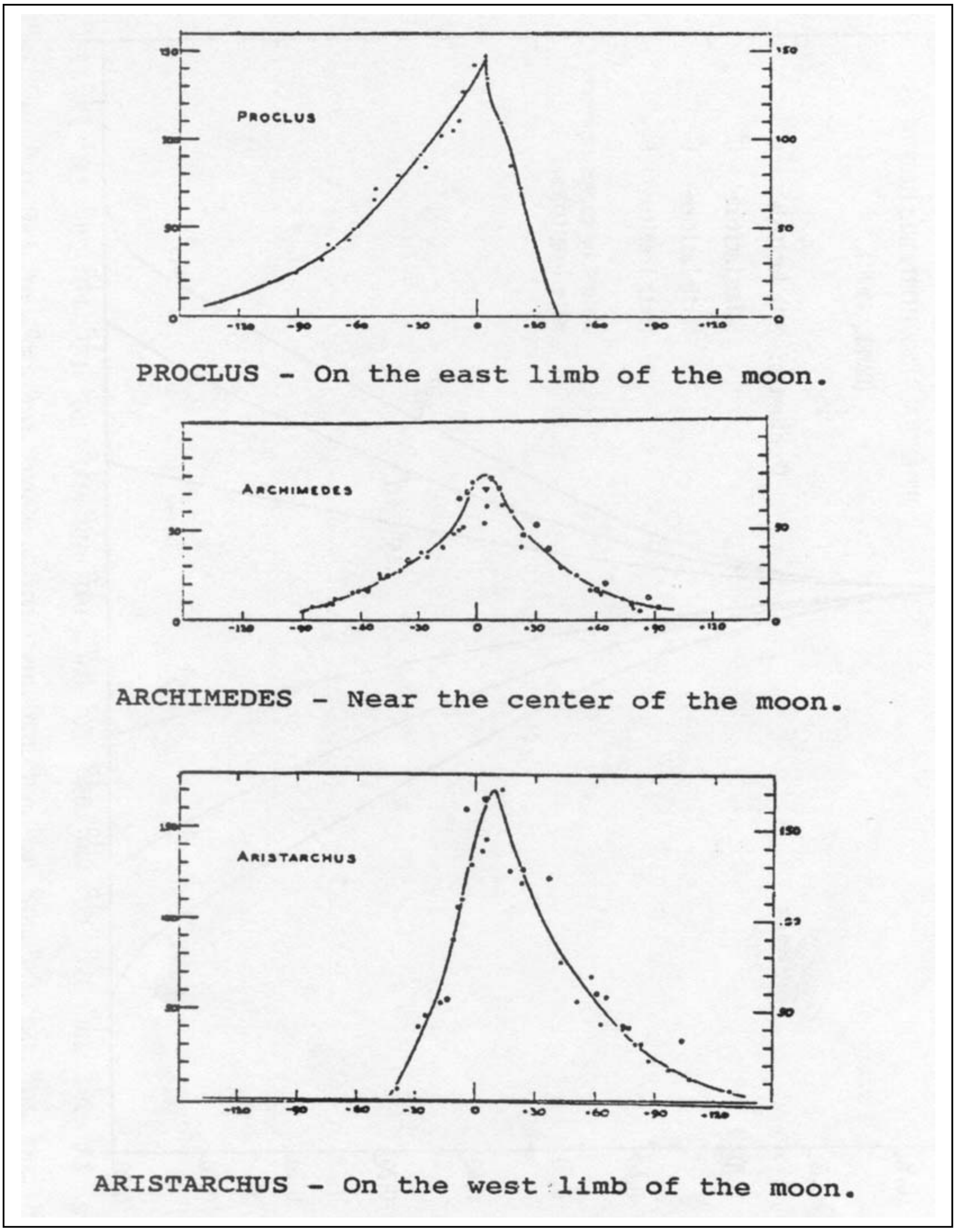

PHOTOMETRIC TECHNIQUES

1. SITE SELECTION.

Experience has shown that it is more efficient to measure several sites in the immediate area, rather than just one site. Therefore, sites may be selected based on "Site Sets", a group of sites in the same area using the same two comparison sites (Kapral, 1991A, 1991B). See Appendix D for examples of site sets. The selection criteria are:

1. The sites should be close together.
2. The area should be easily identifiable throughout a lunation.
3. The local albedo variations in the scan aperture should be small.
4. The site should be reasonably flat with a minimum of local relief, eliminating local shadowing.
5. There should be no high features immediately east or west of the site, eliminating external shadowing.
6. The comparison sites should be at approximately the same longitude as the study sites, to insure that they are visible the entire time that the study sites are visible.
7. The "Site Set" should be located so that it can be observed throughout a lunation. E.G.: east if you work a 1st shift, or west if you work a 2nd shift, unless you don't mind getting up in the middle of the night to make a hour or two of observations.

NOTE:East is toward Mare Crisium, and north is toward Plato (IAU convention).

A number of excellent sources may be used to select the study sites, such as: [Alter (1964); Arthur & Agnieray (1964); Bowker & Hughes (1971); Kuiper (1960); Moore, P.A. (1976); Rükl (1990)].
Several of the comparison sites are also Lunar Transient Phenomenon sites, and should be avoided if possible, since this would be like trying to obtain a variable star's light curve using another variable star as the comparison star. See Appendix F and G. Because this isn't always possible, two comparison sites should be selected to measure against, hoping that only one of the sites may display transient activity.
Once the sites are selected, it is necessary to determine when the sites to be measured will be visible. The terminator is the dividing line between the light and dark portions of the moon. It is the sunrise line from New Moon to Full Moon, and the sunset line from Full Moon to New Moon. The colongitude indicates the position of the terminator. It is the angle at the center of the moon, increasing at approximately 12E per day, that reaches 360E each month when the sun rises at selenographic longitude of 0°.

The colongitude is 0° at Full Moon, 180° at Last Quarter, and 270° at New Moon. Colongitude can be used to determine when to look for a particular lunar site. If L_o is the selenographic longitude of the site, then sunrise occurs when the colongitude (C) = 360° – L_o; noon occurs at C = 90° – L_o; and sunset occurs at C = 180° – L_o. For example: the crater Plato has L_o = –9°, therefore sunrise is at C = 9°, noon is at C = 99°, and sunset is at C = 189°. The corresponding dates may be obtained from the Astronomical Almanac, the A.L.P.O. Solar System Ephemeris, or the B.A.A. Handbook. Table 3 indicates the change in colongitude per each hour or minute of Universal Time.

Table 3 – COLONGITUDE CONVERSION TABLE

COLONGITUDE CONVERSION TABLE			
U.T. (Hours)	COLONGITUDE CHANGE	U.T. (Minutes)	COLONGITUDE CHANGE
1	0.51	0	0.00
2	1.02	1	0.01
3	1.52	2	0.02
4	2.03	3	0.03
5	2.54	4	0.03
6	3.05	5	0.04
7	3.56	6	0.05
8	4.06	7	0.06
9	4.57	8	0.07
10	5.08	9	0.08
11	5.59	10	0.08
12	6.10	20	0.17
13	6.60	30	0.25
14	7.11	40	0.34
15	7.62	50	0.42
16	8.13		
17	8.64		
18	9.14		
19	10.16		
20	10.67		
21	11.18		
22	11.68		
23	12.19		

Colongitude will determine the visibility of most lunar sites. However, for those sites located near the limb of the moon, the librations in longitude and latitude must be accounted for. The Astronomical Almanac, The A.L.P.O. Solar System Ephemeris, and the B.A.A. Handbook list the libration values for 0h UT for each day of the year. The circumstances of the effect of libration on any given day (direction and amount) can be determined by plotting the libration values on a Cartesian graph.

Positive libration in latitude indicates that the north pole is tilted toward the observer, positive libration in longitude indicates that the east (IAU) limb is tilted toward the observer. NOTE: Both the Astronomical Almanac and the B.A.A. Handbook use the "CLASSICAL" east and west, NOT the IAU convention.

The east-west axis of the graph should show a maximum of nine units each way, and the north-south axis should show a maximum of seven units each way, since this is the maximum libration each way. Label the axes: + Latitude - "North"; - latitude - "South"; + Longitude - "East"; - Longitude - "West". Now plot the libration values versus time. It is usually sufficient to plot every 3rd or 4th day. Draw a curve connecting the points, and add the times of New Moon, First Quarter, Full Moon, Last Quarter, and also the times of perigee and apogee. You can now determine the librational aspect of the moon for any day in the lunation. See Figure 9.

Experience will show that the libration curve varies from a severe ellipse to almost a circle. No two curves are alike. The best times to view the limb areas are when the curve is a long, thin ellipse, combined with a favorable Full Moon.

Figure 9 - Libration Chart - by C. Kapral

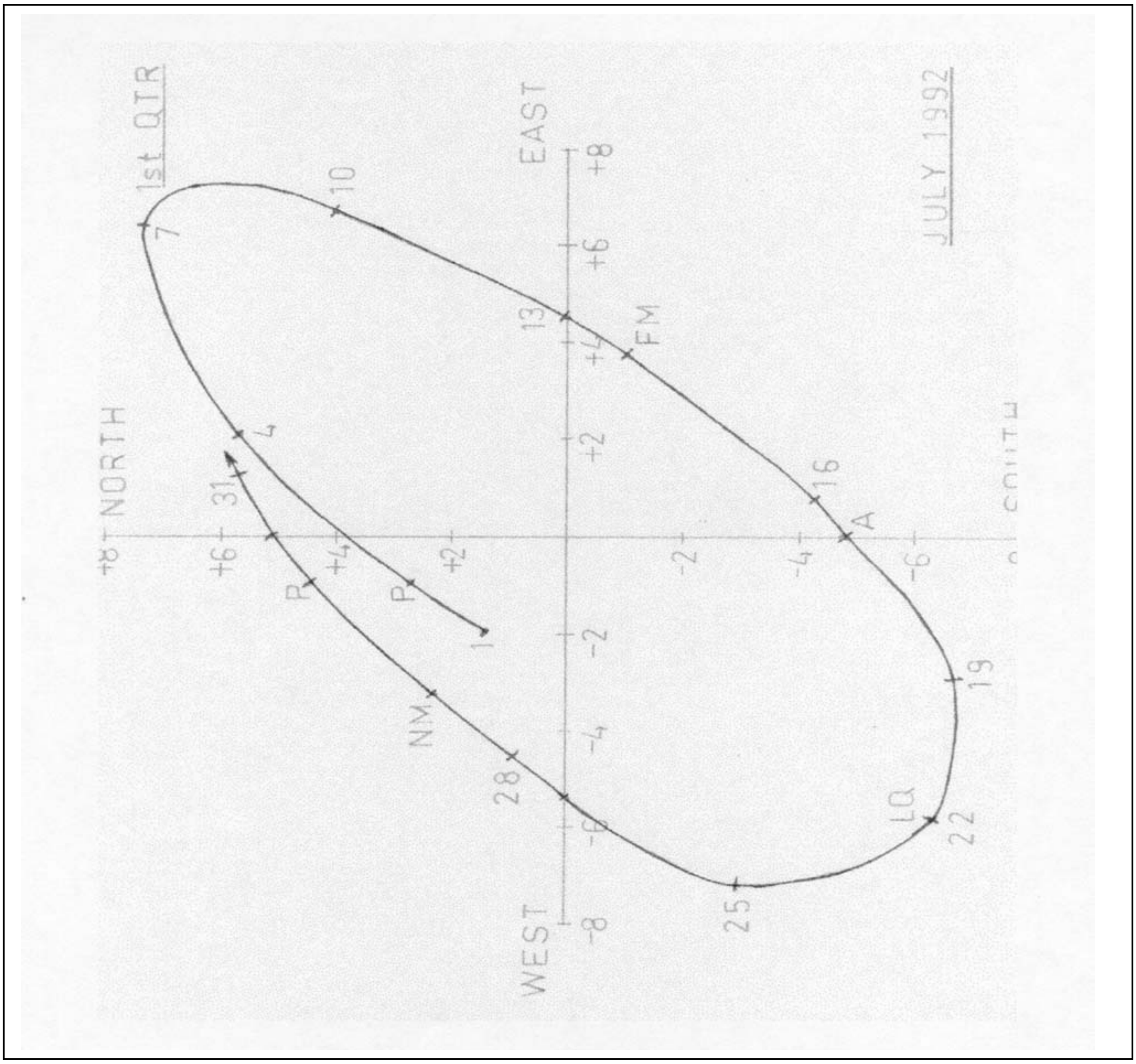

2. PHOTOMETRIC PROCEDURE

There is considerable overlap between the techniques of stellar photometry and lunar photometry. The primary differences are: (i) the Moon's complex and rapid motion in both right ascension and declination, (ii) the Moon is a bright, extended source of light.The motion of the moon in the sky is quite fast, as witnessed when observing a star being occulted by the moon. The motion is approximately 0.5 to 0.6 arc-seconds per second of time in right ascension, and approximately 0 to 0.2 arc-seconds per second of time in declination. Since the site to be measured must be accurately placed in the photometer aperture, a drive corrector must be used to prevent the site from drifting out of the scan aperture. A variable frequency corrector will correct for motion in right ascension, declination motion can be corrected via a declination drive, or by limiting measurement to within a ten to fifteen second window.A small photometer scan aperture is desirable, typically to cover an approximately 15 km area on the moon. This is because lunar albedo varies on a small spatial scale and relatively homogenous tonal features are often of the order of 5 arc-seconds in diameter (about 10 km). Since it is difficult to obtain a suitable aperture, the focal length may be extended by using an achromatic Barlow lens and extension tubes. The moon is an extremely bright object, and the use of the Barlow lens and extension tubes will prevent the off-scale readings which will probably otherwise occur. Also, the use of the small scan area allows the consistently precise location of the aperture on the site that is necessary for photometry.A serious problem for lunar photometry is scattered light. The effect of scattered light is to reduce lunar contrast, making bright areas darker and dark areas brighter. The effect of scattered light is more serious near the terminator, where the surface brightness drops to a value comparable to the scattered light itself.The Moon is a bright, extended object, and it is usually not possible to make "sky background" readings immediately adjacent to the sites being studied. The best that can be done is to take a background reading upon a dark area as close to the site as possible, which should be whichever of these three types of area is closest to the site being measured: (i) the sky immediately adjacent to the Moon's limb; (ii) a fully-shadowed area that is noticeably larger than the photometer aperture; or (iii) an area close to, but not on the dark side of, the terminator.Because the amount of scattered light will vary with position on the Moon's disk, no background reading will be entirely accurate in representing the scattered light present at the site itself. It is essential that all scattered light be reduced as much as possible. Therefore, excellent transparency is necessary (to reduce scattering from particulate matter in the atmosphere), as are clean optics with coatings in good condition. Refractors or off-axis reflectors are preferred. Catadioptics are next best. The least desirable, but unfortunately the most common, are those telescopes with spider supported secondary mirrors, the Newtonians and Cassegrains. Whatever form of telescope you use, all optical surfaces should be clean and the optical path should be well baffled. Any reflecting surfaces, such as the interiors of eyepieces, Barlow lenses, drawtubes, etc. should be flat black and non-reflecting. While scattered light is relatively easy to compensate for in lunar sunlit areas, it becomes a serious issue near the terminator.

Three types of lunar photometry may be undertaken:

1. Absolute Photometry: The measurement of the brightness of a site in standard units, usually stellar magnitudes per square arc-second. This method compares the lunar sites with photometric standard stars. It is widely used for lunar eclipse photometry. The method suffers from the fact that it compares an extended area (the lunar site) with a point source. This necessitates accurately knowing the area of the scan aperture (in square arc-seconds), and insure that the photometer's response does not vary within the scan aperture. Corrections must also be made for the Earth's distance from the Sun. Some uncertainty is caused by the employment of the Sun's apparent visual magnitude as well.

2. Differential Photometry: Measurement of the brightness of a site and comparing it with the known brightness of a comparison site. This utilizes the existing absolute photometry performed on "standard" sites. Appendix G lists sites of known brightness useful for selecting comparison sites. The photometer used for the measurements listed in Appendix G had a peak response at approximately 4400Å, so these measurements are suitable for B-band photometry only.

   The observing sequence is SKY-COMPARISON SITE 1-COMPARISON SITE 2-SITE 1-SITE 2-SITE 3-SITE 4-COMPARISON SITE 1-COMPARISON SITE 2-SKY

A minimum of four sets of measures are taken on each observing session. The SKY reading is taken by placing the closest limb of the moon immediately out of the telescope's field of view, then making the measurement. A V-filter measure is recorded, followed by any other filters used, for each SKY and SITE. The transparency is determined by recording the faintest star visible at the zenith. A typical observing session will last approximately 13 hours. A voice-actuated tape recorder is handy for notes, but taping the measurements will result in a long and tedious transcription process, and is NOT recommended.

A typical data reduction procedure would be to convert the measures into relative brightness units, where a perfect lunar reflector at Full Moon would have a brightness of 1.00. Let R = the photometer reading of the study site, corrected for sky background, and R(o) = the same for the standard site. (Note: Differential extinction corrections will be negligible if the sites are in the same general area of the moon, within 0.5 lunar radius, and the Moon is not at a low altitude, above 30°. Then, let L = relative brightness of the site under study, and L(o) = relative brightness of the standard site. Let A(o) = albedo of the standard site. Then, L = L(o)*A(o)*R/R(o). This value may be graphed against phase angle to show the actual brightness function of the site being studied.

Another mode of data reduction is to determine the study site's parameters for the Hapke (1966A) photometric model. The values of the "Hapke parameters" (except for h) are VERY sensitive to observational errors. A more practical approach might be to assume that h, f, and Gamma have their "normal" values and then use the algorithms in Appendix H to determine the site's theoretical relative brightness (Lt) and then to solve for albedo using A = L/L(t). Obviously, the same standard site should be used in all investigations of the study site.

3. Multiband Photometry: The measurement of the brightness of a site in more than one spectral band. The use of V, B, and R filters is especially useful for the detection of short and long term Lunar Transient Phenomenon color changes. The observing sequence must be modified to include the measurement of a "standard" and an "extinction" star. The "standard" stars are required in order to define a known magnitude with which you can determine the apparent magnitude of the site (Iriarte, Johnson, Mitchell, & Wisniewski; 1965). The "standard" stars are based on the Johnson and Morgan definition of the UBV System (Johnson & Morgan, 1953). The "extinction" stars are used to determine the first-order atmospheric extinction coefficient. This is the loss of light due to attenuation of the light traveling through the changing air mass. The extinction is determined by using a least-squares analysis of the air mass versus magnitude. A list of "standard" and "extinction" stars is given in Appendix B & C.

An observing sequence for multiband photometry might be: (SKY):(STANDARD STAR):(EXTINCTION STAR):(COMPARISON SITE 1):(COMPARISON SITE 2):(SITE 1):(SITE 2):(SITE 3):(SITE4):(COMPARISON SITE 1):(COMPARISON SITE2):(STANDARDSTAR):(EXTINCTIONSTAR):(SKY). The comparison sites are included to provide a total photometry sequence, both differential and multiband, and may be omitted if only multiband photometry is required. The readings are used to determine the "magnitude" of the sites. This "magnitude" is NOT equivalent to a star's magnitude, since the site is an extended source, limited by the photometer's scan area on the moon. This is irrelevant since only the color difference is of interest. The determination of the color index of a site may be averaged over an observing session, or they can be reduced on a observation basis, in the case of a rapid transient color change.

A typical data reduction procedure would begin by correcting the readings for sky background and for differential extinction. Then, let (1), (2), and (3) be the subscripts for the three bands used (Visual, Blue, and Red), let L(1), L(2), and L(3) be the corrected lunar readings, S(1), S(2), and S(3) be the corrected stellar readings, and M(1), M(2), and M(3) be the magnitudes of the standard star in the three spectral bands. Next, find the apparent magnitude of the lunar site in each of the spectral bands, designated LM(1), LM(2), and LM(3):

$$LM(1) = M(1) - 2.5 \cdot \log(L(1)/S(1))$$

$$LM(2) = M(2) - 2.5 \cdot \log(L(2)/S(2))$$

$$LM(3) = M(3) - 2.5 \cdot \log(L(3)/S(3))$$

The V–B color index for the site is:

$$CI(1-2) = LM(1) - LM(2)$$

The value of the color index will vary depending on the two bands chosen, the lunar site, and the phase. Two whole-moon average color indices are approximately (B–V) = +0.92 and (U–B) = +0.46. (Note: These values are absolute color indices; the Moon's intrinsic coloration can be found by subtracting the Sun's color index from the color index at the lunar site).

3. THE PHOTOMETER USED IN THE PROJECT

The photometer used was an OPTEC SSP-3 solid-state photometer. The SSP-3 uses a silicon PIN-photodiode having a 300 to 1100 nm spectral range. It has a 25mm Ramsden eyepiece and is powered by a 9-volt NiCd battery. The photometer has a two-position filter slider mounted between the flip mirror and the detector. V, B, and R filters were used. The filters are made from combinations of Schott colored glass and their responses are as follows: V = 460 to 700 nm, B = 360 to 580 nm, and R = 520 to 1000 nm. These filters closely match the Johnson standard values.

An observer having a photometer that uses a photomultiplier tube, such as a 1P21 photomultiplier tube or any other kind, can also engage in lunar photometry. If you can do stellar photometry, you can do lunar photometry.

PHOTOMETRY PROJECTS

I. Low-Speed Photometry

A. LUNATION CURVES.

The main purposes of lunar photometry are the completion or the establishment of the photometric curves of various lunar features throughout a lunation, and the determination of the color indices of various features in several spectral bands. Most lunar features have not had their lunation curves accurately determined. Therefore, if a suspected anomalous albedo change is reported, not enough data is known about the standard appearance of the feature to verify the change. Also, the macroscopic roughness of the lunar surface is still not yet well known due to the lack of photometric coverage especially in different colors and at large phase angles.

1. Van Diggelen's (1959) study of the Minnaert photograph series, combined with further data, gave the lunation curves for 38 craters. However, the following 10 craters do not seem to have further data available to complete their lunation curves: Eratosthenes, Eudoxus, Maginus, Maurolycus, Piccolomini, Plinius, Pytheas, Stöfler, Thebit, and Walter. Studies should be performed to complete their lunation curves and to determine the lunation curves of other lunar features (e.g.: Benton, 1983; Hedervari, 1982).

2. Elger's Albedo Scale (Appendix E) is used to make rapid brightness estimates of a lunar feature. It is a 20-step gray scale, in half-steps, which is widely used in Lunar Transient Phenomena observations, and in the A.L.P.O. Selected Areas Program. It should be extended to increase it's accuracy.

3. Most features attain their peak brightness at Full Moon. However, some craters attain their maximum brightness after Full Moon, such as: Archimedes, Aristarchus, Aristillus, Arzachel, Billy, Catherina, Clavius, Copernicus, Cyrillus, Gassendi, Grimaldi, Kepler, Lubiniezky, Macrobius, Posidonius, Proclus, Ptolemaeus, Schickard, and Tycho. No site is known which attains it's maximum brightness <u>BEFORE</u> Full Moon. A search should be conducted to determine which other craters attain their maximum brightness after Full Moon, and especially to determine if any feature attains it's maximum brightness <u>BEFORE</u> Full Moon.

4. A study should be conducted on twin craters, craters of approximately the same diameter very close to each other, and crater chains, to determine if their brightness and lunation curves are the same.

5. Creation of an albedo map of a large area, such as Mare Crisium or Sinus Iridium, at Full Moon compared to a geologic map of the same area would be useful, especially if performed at a particular wavelength, such as that of Ilmenite at 0.5 to 0.6 μm (Busarev & Shevchenko; 1989).

B. LUNAR COLORS.

At first sight the moon appears silvery in the sky. More experienced observers notice subtle color differences on the surface. Firsoff (1958) noticed that the diamond-shaped area northwest of Aristarchus was mustard yellow. The southeast foothills of the Apennines appeared greenish-khaki. He states that "color at phases much less than Full Moon are usually stronger and often different from those at Full Moon". He noticed that Mare Frigoris is yellowish. The northwest portion of Mare Imbrium, just north of Sinus Iridium, and in Mare Tranquillitatis and the edges of the plains adjoining it are green or blue. Oceanus Procellarum and in parts of Mare Imbrium and Serenitatis are yellow and red. Brown was noted in the crater Plato. He noted that Mare Crisium, Mare Humorum, and within Grimaldi and Ptolemaeus are greenish. Most of the bright crater rims, floors, and rays are green. Platt (1958) argued that interplanetary dust particles contribute to the low albedo and low thermal conductivity of the moon, and may introduce "radiation-induced coloration".

Sytinskaya (1965) reexamined the geologic data in accordance with their color and reflective properties to determine analogies to the lunar surface, and produced a catalog of brightness coefficients and color-indices for 101 sites.

Roberts (1966) performed a high-resolution 3-color photometric study of Copernicus, Kepler, Aristarchus, and Sinus Iridium, at wavelengths of 6714 Å, 5450 Å, and 7889 Å.

A study of 83 lunar areas (McCord; 1969) showed that there are color differences on the moon. "There are small but real color contrasts within the mare which vary over relatively short distances, as well as regional differences. The highlands appeared uniform in color compared to the maria. The bright craters are some of the most highly colored features on the lunar surface. The disturbed upland regions are redder. It is evident that the color structure of the lunar surface is complex and that the albedo and topographic boundaries are not necessarily color boundaries. Similarly, color boundaries are not necessarily accompanied by striking albedo or topographic boundaries. Very bright craters and very dark maria are some of the bluest features observed. Areas of very similar albedos have very different colors and vice versa".

Mitchell & Pellicori (1970) showed that the greatest color contrast between topographies occurs at long wavelengths. Younkin (1970) measured the color versus iron absorption depths and showed that "the redder the mare, the more the iron".

Whitaker (1972) combined UV and IR photographic negatives to enhance the color differences between various types of lunar terrain. He found that the greatest color variations are in the maria. He also determined that: (1) the various maria were deposited over a considerable length of time, (2) the bluer material is the more recent, and is high in Titanium, (3) the theory that sinuous rilles are lava drainage channels is supported, and (4) the terrae are monotonous, with but a few red isolated areas. Lipskii & Shevchenko (1972) prepared a contour map for the "reddening coefficient" in Mare Imbrium, from spectrozonal photographs taken at 380 μm and 640 μm.

A detailed study of 31 sites in Mare Nubium was performed (Johnson, Pieters, & McCord; 1973) which showed that "the boundaries between these areas of differing relative reflectivity do not correspond with either albedo changes or contacts between U.S.G.S. defined units". They also showed that "the brighter-the redder" measurement does not apply to Mare Humorum.

Asaad & Mikhail (1974) studied 4 color contrasts for 104 lunar sites and found distinct color differences, with the greatest contrast occurring at the longer wavelengths.

A study of the color-index distribution over the lunar surface was performed by Evsyukov (1974, 1975A, 1984). He found large variations of color-indices in the maria. Considering the three conditions for maria location are: (1) adjacent to a continent, (2) near a boundary between two types of continent surfaces, and (3) adjacent to a "red" continent, he concluded that: "(1) the colorimetric structure of the lunar maria is essentially determined by the location of a mare relative to the boundary of continental terrain of various types, (2) maria adjoining neutral continents are bluer than the continents, (3) Mare Frigoris, which adjoins a red continent, is redder than the continent, and (4) maria that are bounded by both types of continental terrain essentially maintain the same color as the adjoining continent". The map produced divides the lunar surface according to the ages of the rocks and their composition.

The whole-moon average color index (B-V) is approximately +0.92 magnitudes, similar to a G8 star, and about +0.3 higher than the sun.

As detailed above, lunar areas do have color.

Areas which reflect in the longer wavelengths (eg: red, yellow, and brown) are: SE Apennines foothills close to the Haemus Mountains, plateau NW of Aristarchus (Wood's Spot), two spots on the NW floor and W glacis of Copernicus, dark spots between Copernicus and Bode, rays of Copernicus, Oceanus Procellarum, Gruithuisen domes, Sinus Iridium, rays of Kepler, Langrenus, Lichtenberg, dark spots S of Manilius, Plato, Ptolemaeus (evening), Riphaen Mountains, Sinus Roris, floor spots of Schickard, interior of Mare Serenitatis, Palus Somnii, Stevinus, light spots of Mare Tranquillitatis, Tycho Walls and nimbus, Mare Veris, Mare Frigoris, Gassendi (south point of north peak), Aristarchus, diamond shaped area NE of Aristarchus, Alphonsus, and Pr. Laplace.

Areas which reflect in the medium or shorter wavelengths (eg: green, blue, violet, ultraviolet) are: Atlas, Mare Crisium, Eratosthenes, Grimaldi, Mt. Hadley, Hercules, Mare Humorum (dark areas), Le Monnier, Sinus Medii (dark spots), Mare Vaporum (dark spots), Oceanus Procellarum, Riccioli, Schickard, Mare Serenitatis, Stadius, Mare Tranquillitatis, Ptolemaeus (morning), Mare Foecunditatis, Sinus Aestuum, Maginus, Rheita Valley, and Mare Imbrium (south of Sinus Iridium).

Clearly, a lot more work needs to be done to establish the color-index of the various areas throughout a lunation, especially since the color of a site may vary throughout the lunation.

Additional references for lunar colors are: [Avigiano (1951); Bell (2000); Firsoff (1962), 1970; McCord & Johnson (1969, 1970); McCord et al. (1972A, 1972B); Mikhail (1970); Peacock (1968); Schaber (1980); Schmitt (1974); Scott (1964); Teyfel (1962); Wright (1929)].

C. LUNAR TRANSIENT PHENOMENON.

Lunar Transient Phenomena (LTP) are short-term changes in the appearance of a site. They manifest themselves in 5 basic types: (1) brightenings, (2) darkenings, (3) red colorations, (4) blue colorations, and (5) obscurations. They have been reported by many amateur and professional observers from as long ago as 557 AD. They have been observed from Earth based sites, as well as by the Apollo astronauts orbiting the moon. Yet, LTPs are a controversial issue. Many believe that they are mere aberrations of the Earth's atmosphere or instrumental effects. However, on November 3, 1958, N.A. Kozyrev (1959) obtained an emission spectrum of carbon vapor originating in the crater Alphonsus. On the nights of November 26, 28, and 30, and December 3, 1961, he obtained spectrograms of the Aristarchus and Herodotus area which showed emission lines of molecular hydrogen at 4634 Å (Kozyrev, 1963). The Aristarchus and Herodotus region account for approximately 1/3 of the transient events reported. Since then, many observations have been made spectroscopically,photographically,photoelectrically, and recently CCD imaging, of strange happenings on the Moon. The literature has many references to observed changes on the Moon: [Blizard (1967); Burley & Middlehurst (1966); Cameron (1972, 1974, 1975, 1977, 1978, 1979, 1980, 1981, 1986, 1991); Cameron & Gilheany (1967); Chapman (1967); Criswell & De (1977); De & Criswell (1977); Firsoff (1962, 1970); Garlick, Steigmann, & Lamb (1972); Geake & Mills (1977); Haas (1937, 1942); Kozyrev (1959, 1963); Matsushima (1967); Middlehurst (1967); Middlehurst & Burley (1966); Middlehurst & Moore (1967); Middlehurst, Burley, Moore, & Welther (1968); Mills (1970); Moore (1971, 1976); Rutkowski (1981); Westfall (1979B)].

Approximately 200 lunar sites have transient activity associated with them (Appendix F). These sites should be observed using short-interval multiband photometry if an LTP is suspected, or using a scheduled multiband program to monitor the sites over long periods. This is an especially rewarding program in that the long-term monitoring of the albedo behavior of the sites is extremely valuable scientifically.

D. LUNAR DOMES.

Lunar domes are features having topography varying from circular to irregular outlines, have a common convex shape, have slopes generally less than 5°, and have diameters up to 30 kilometers. Some domes have craters on their summit. Domes display a large variety of diameters, flank slopes, and volumes, which are caused by different lava effusion rates, lava viscosities (with values spanning at least six orders of magnitude) and durations of the effusion process. A new classification scheme of effusive domes by Woehler et al entitled “A Combined Spectrophotometric and Morphometric Study of the Lunar Mare Dome Fields near Cauchy, Arago, Hortensius and Milichius” is currently in press in the journal Icarus. Almost all domes are associated with the mare, although there are high-albedo highland domes. The mare domes are mostly concentrated in the lunar equatorial belt from 60° W to 40° E and 0° to 20° N, with 3 areas having the highest concentration: (1) the Marius Hills, (2) Hortensius, and (3) Cauchy. Domes are thought to be similar to Earth's shield volcanos. Because domes are only visible when they are within 8° to 10° of the terminator, and can be observed only during a 16 to 18 hour window after lunar sunrise or before lunar sunset each month (Jamieson, 1988). Domes are divided into seven classes (Head & Gifford, 1980).

Additional references to lunar domes are [Cooke (1966); Delano (1969); Greeley (1971); Guest & Murray (1976); Head (1976); Head & Gifford (1980); Head & McCord (1978); Herring (1960, 1961, 1962, 1965A, 1965B); Jamieson (1972, 1974, 1988); Jamieson & Rae (1965); Kitt (1990); MacRobert (1984B); Moore (1958); Phillips (1987, 1989A, 1989B, 1990, 1991); Quaide (1965); Rifaat (1967); Smith (1973, 1974); Sytinskaya (1965); Whitford-Stark (1974)].

It has been suggested that lunar domes are different in color from the lunar hills. A useful project is to measure the domes and hills in V, B, and R to determine the extent of the color differences, if any. A long-term study of the domes should be conducted to discover any transient activity associated with them.

E. EARTHSHINE.

Earthshine is the light that the Earth reflects on the Moon's dark portion of it's disk, visible at very low lunar phase, typically less than 20% phase. It's intensity depends on the amount of cloud cover and dust in the Earth's atmosphere. It's intensity is a measure of the albedo of the Earth, which is greatly determined by meteorological conditions (Link, 1972). Satellite observations (Arking, 1963) show that the continents are more cloudy and brighter than the seas, contrary to Danjon's (1936) findings. Earthshine also varies in intensity during the 11-year solar cycle (Dubois, 1944).

A photometric study could be performed and the results correlated to the amount of cloud cover on the Earth, as well as monitoring the dust from volcanic eruptions, meteor showers, and fires (slash and burn agriculture, etc.)

F. LUNAR ECLIPSES.

The primary reason for eclipse photometry is to determine the density of the Earth's shadow. The variation in density across the shadow is not uniform. One cause of this is the absorption of light in the Earth's ozone layer. [Dobson (1930); Götz (1931); Link (1933, 1946); Mitra (1952); Paetzold (1950, 1951, 1952); Vigroux (1954); Westfall (1972, 1975, 1979A, 1979C, 1980, 1982, 1984A, 1990)].

Kepler was the first astronomer to investigate the photometry of eclipses (Frisch, 1858). He determined that the illumination of the Moon in the shadow was due to refraction of light in the Earth's atmosphere. Recent observations indicate that the density in the central part of the shadow is dependent upon the degree of cloudiness above the Earth's terminator, while the density at the edge of the shadow is dependent upon the thickness of the Earth's ozone layer.

The enlargement of the Earth's shadow compared to theoretical predictions, the "shadow-increase", was discovered and studied by many researchers. [Beer and Mädler (1834); Brosinsky (1888); Cassini (1740); Hartmann (1891); Hepperger (1895); Lahire (1707); Lalande (1783); Lambert (1782); Legentil (1755); Lemonnier (1746); Schmidt (1856); Schober & Schroll (1973); Seeliger (1896)]. The shadow appears enlarged (between 1.7% and 3%) of it's calculated size, and also appears flattened. The flattening is probably caused by a high absorbing layer, probably composed of meteoritic dust (at approximately 100 km above the Earth), which is higher and denser at the equator than at the poles.

[Bauer and Danjon (1923); Bouška (1948); Bouška and Švestka (1950); Cabannes (1929); Fessenkov (1970); Greenstein (1937); Hansa and Zacharov (1958); Koebke (1951); Kühl (1928); Link (1929, 1948, 1950A, 1959); Link and Linková (1954); Paetzold (1953); Švestka (1950); Zacharov (1952)].

Certain lunar features appear brighter than they should during an eclipse, suggesting luminescence, eg: Linné. Solar exciting radiation also makes an eclipse appear brighter, due to changes in the aerosol content in the Earth's atmosphere. [Barbier (1959, 1961); Cimino and Fortini (1953); Cimino and Fresa (1958); Cimino and Gianuzzi (1955); Dubois (1956, 1957, 1959); Fortini (1954, 1955); Heyden (1954); Keen (1983); Kosik (1940); Kozyrev (1956); Link (1946, 1947A, 1947B, 1950B, 1951, 1958); Rocket Panel (1952); Schaefer (1991); Sekiguche (1980); Tsesevich (1940)].

The shadow density should be measured at a well defined point, rather than measure the total magnitude of the eclipsed Moon. A bright feature should be selected (Ex: Aristarchus, Kepler, Proclus, Censorinus, etc.) and measured throughout the penumbral and umbral phases of the eclipse. Some eclipses are very dark, and it may become difficult to keep the site in the scan aperture. Also, measuring more than one site during an eclipse can be very difficult if the eclipse is very dark. Some sites disappear.

Photometry of areas near the edge of the shadow are valuable in that those areas give information about the Earth's upper atmosphere. Eclipse photometry is fun and can provide valuable information about the Earth's atmosphere.

2. HIGH-SPEED PHOTOMETRY

A. LUNAR OCCULTATIONS.

An occultation occurs when a celestial body, in this case the Moon, passes in front of another celestial body, a star, planet, asteroid, etc. Occultations are among the oldest observed astronomical phenomenon. It was an occultation of Mars in 357 B.C. that led Aristotle to conclude that Mars was further from the Earth than the Moon. Other later observers determined that since stars disappeared almost instantly when occulted, they must have a very small angular size.

Occultations enable us to accurately determine the motion of the Moon laterally. This allows a more accurate estimation of the secular acceleration of the Moon, and is important in establishing corrections to the Moon's ephemeris.

Occultations are important in the discovery of close double stars (separations of 0".1 to 0".01) (O'Keefe, 1950). Occultations also allow the determination of the angular diameter of stars. Approximately 50% of all known angular diameters measured were made from occultation data. MacMahon (1909) deduced that by timing the disappearance of a star at the Moon's limb, the diameter of the star could be measured. Eddington (1909) then showed that this method would only be applicable for large stars due to diffraction effects at the Moon's limb. A spinning photographic plate was used to observe an occultation of Regulus and it's diffraction fringes (Arnulf, 1936). His estimation of the diameter of Regulus was in close agreement to the diameter obtained by Brown (1968). Williams (1939) showed that the shape of the diffraction pattern is changed "in a way that can be interpreted directly in terms of stellar diameter". (Nather and Evans, 1970). Whitford (1939, 1946) gave results on four stars which he determined had large diameters.

The first accurate high-speed occultation observations were performed by D.S. Evans and A.W.J. Cousins in the early 1950's, when they observed several occultations of Antares. Evans and R.E. Nather started a photoelectric program to observe occultations in the late 1960's, which resulted in a series of papers describing the occultation process [Africano et al. (1975); Brown (1968); Cousins and Guelke (1953); Dunham et al. (1973); Evans (1951, 1970, 1971); Evans et al. (1954); Nather (1970); Nather and McCants (1970)].
Evans also measured the diameter of μ Geminorum (Evans, 1959), and discussed the effects of irregularities at the Moon's limb on the measurement of large diameter stars [Diercks and Hunger (1952); Evans (1955, 1957); Jackson (1950)].
Scheure (1962) proposed a deconvolution technique for data analysis of the brightness of radio sources, which was then applied to the Antares data, obtaining the brightness distribution across the star (Taylor, 1966).
Occultations can be difficult to observe and there are limitations to the technique. Only 10% of the sky is available for using occultation techniques. Occultations are not easily visible on either side of Full Moon, since scattered light interferes with the observations. Reappearances are very difficult to record, since it is difficult to insure that the star will reappear in the scan aperture. A good description of the theory and process of occultation observations can be found in Blow (1983); Genet (1983).
Any photometer can be used for observing lunar occultations, either a current to frequency or a photon counting photometer. A computer is needed to act as the data acquisition system, with a required integration period of from one to eight milliseconds. This is usually accomplished by using a 4K block of computer memory as a storage buffer. The buffer "rotates" so that only the most recent 4K of data is retained. Therefore, for example, data acquisition at a rate of one millisecond will maintain data for the most recent four second period. A means of monitoring this data is required in order to detect the drop in data corresponding to the occultation, so that the rotation of the buffer can be stopped, and the data "frozen". Usually an oscilloscope or visual observation through a guide telescope is used. It is then a simple matter to count backward from the end of the buffer to determine the time of the event.
The data acquisition system obviously requires an accurate clock. Usually this can be accomplished by comparing the computer's clock with the WWV or CHU time service. Note that any propagation delays in receiving the time service signal must be accounted for.
Obviously, the data can then be stored on a floppy disk, or on the computer's hard drive.

CONCLUSION

Lunar photoelectric photometry is an area where the observer can make a valuable contribution to lunar science. So much remains to be learned about the Moon. We still don’t know if any feature attains full brightness BEFORE full moon. We still don’t know the photometric behavior of most features throughout a lunation. Lunar satellites can provide answers to some questions about the Moon but they only take measurements at a very narrow time window during a lunation. Much more observations are needed and we have the capability of providing the observational results that can be applied to answering some of these questions.

This handbook has given you a brief history of lunar photometric observations, who did what, and when. It also gives some basic information about the Moon in general and about the Moon's photometric function. The parameters and steps for setting up a photometric observing session have been detailed, from the types of photometry, site selection criteria, and the steps required in taking the measurements. Various types of photometric projects have been discussed.

The following pages contain the following:

1. A GLOSSARY of terms used in lunar photometry.
2. An extensive BIBLIOGRAPHY, where an observer can review the papers related to photometry to learn more about what's been done to date and to learn a lot more about the theory involved.
3. A fully WORKED EXAMPLE of the data reduction for differential photometry.
4. Tables are provided for the selection of VBR "STANDARD" and FIRST-ORDER"EXTINCTION" stars for use in Absolute Photometry.
5. A list of SUGGESTED LUNAR SITES AND THEIR COMPARISON SITES is given, by quadrant, although an observer may certainly choose their own sites if they wish.
6. A list of sites in ELGER'S ALBEDO SCALE is included for those who wish to extend the scale.
7. Many observers are involved in LTP (or TLP) observations and a LIST OF LUNAR TRANSIENT PHENOMENON SITES is given. These are sites where at least one suspected change has been observed.
8. A table is included, perhaps the most important table in the book, of the SUMMARY OF PHOTOMETRIC PROPERTIES OF SELECTED LUNAR SITES for 298 lunar sites. These are the "Comparison" sites used in the book.
9. A list of DATA REDUCTION ALGORITHMS used for the data reduction for differential and multi-band observations are given. This begins with the averaging of the readings through the determination of the albedo and, for multi-band photometry, the color index of the measured site.

Lunar photometry is a lot of fun. It's challenging, requires some thought in setting up projects, entails making very careful observations, and gives a lot of personal satisfaction. AND, the results are scientifically VERY useful. I sincerely hope that some observers currently performing variable star or planetary photometry will give lunar photometry a try. It's certainly something to do at full Moon.

GLOSSARY

ABSOLUTE PHOTOMETRY: The measurement of a site in stellar magnitudes per arc-second by comparison with photometric standard stars.

AIRMASS: The mass of the Earth's atmosphere traversed by the moonlight. It is equal to the secant of the zenith distance, $Sec(z) = (Sin(Ø)Sin(\delta) + Cos(Ø)Cos(\delta)Cos(H))^{-1}$, where $Ø$ = the observer's latitude, δ = the moon's declination, and H = the moon's hour angle. $Sec(z) = 1$ at the zenith.

ALBEDO: The ratio of the total quantity of light reflected from the site, in all directions, to the total light incident at the site.

BOND ALBEDO: The ratio of the light scattered in all directions by a spherical moon to the light incident upon it.

BRIGHTNESS FUNCTION: A function which indicates how the brightness of the site changes in relation to the phase angle and the observer's position (brightness longitude).

BRIGHTNESS LONGITUDE: The angle between the local normal to the surface at the site and the observer, measured in the site-sun-observer plane.

COLONGITUDE: The longitude of the sunrise terminator measured eastward from the moon's central meridian around the moon. Let L_0 = the selenographic longitude of the site, then sunrise occurs when the colongitude = 360° – L_0, noon occurs when colongitude = 90° – L_0, and sunset occurs when colongitude = 180° – L_0. The colongitude at New Moon = 270°, at First Quarter = 0°, at Full Moon = 90°, and at Last Quarter = 180°.

COLOR INDEX: The magnitude difference between different filters.

COORDINATES: The location of sites on the lunar surface expressed in longitude (λ) and latitude (β), or in standard direction cosine sets expressed in units of thousandths of the lunar radius (ξ, η, and ζ), where $(\xi^2 + \eta^2)$ is less than or equal to 1. The cardinal points adopted by the International Astronomical Union in 1961 are: North – in the direction of Plato, South – in the direction of Clavius, East – in the direction of Mare Crisium, and West – in the direction of Oceanus Procellarum.

DETAILED LUNAR PHOTOMETRY — The study of a small area which can be considered to be geometrically Placed at one point on the lunar surface.

DIFFERENTIAL PHOTOMETRY: Measuring the brightness of a site and comparing it to the known brightness of a comparison site.

EARTHSHINE: The light that the Earth reflects on the moon's dark side. It varies depending upon the amount of clouds and dust in the Earth's atmosphere.

ELGER'S ALBEDO SCALE: A 20-step scale, in half-steps, from 0 = black to 10 = white, used to determine the visual albedo of lunar sites.

GEOMETRIC ALBEDO: The ratio of the brightness of the moon at 0° phase angle to the brightness of a Lambert sphere of the same radius viewed normally.

INTEGRATED LUNAR PHOTOMETRY: The study of the total emission of the moon.

INTEGRATED PHASE FUNCTION: The relative brightness of the entire moon at phase angle (g), normalized to the brightness at 0° phase angle.

LAMBERT SURFACE: A surface which appears equally bright when viewed from any angle, and which reflects all the light incident on it.

LIBRATION: The slow wobbling of the moon, allowing an observer to see about 59% of the lunar surface. Libration in latitude is caused by the moon's rotation axis not being at a right angle to it's orbital plane. Libration in longitude is caused by the moon's constant rotation speed about it's axis and it's varying orbital velocity, faster at perigee and slower at apogee.

LUNAR TRANSIENT PHENOMENON: Temporary, relatively short-lived abnormalities of the appearance of a lunar site. The most common transient events are: (1) brightenings, (2) Darkenings (3) red, colorations, (4) blue colorations, and (5) obscuration

LUNATION: The period from New Moon to New Moon.

LUNATION CURVE: A Cartesian plot of the brightness of a site versus the phase angle.

MAGNITUDE: The brightness scale, created by Poison, for stars, each magnitude value being 2.512 times brighter than the previous value. EG: A 1st magnitude star is 2,512 times brighter than a 2nd magnitude star. For the moon, it is a relative value which indicates how much brighter a site is compared with a magnitude of 0, or a "brightness" of 1, used for multiband photometry.

NORMAL ALBEDO: The brightness of a surface viewed at 0° phase angle and illuminated at an arbitrary angle relative to a Lambert surface viewed and illuminated normally.

OPPOSITION EFFECT: The surge in surface brightness near 0° phase angle.

PHASE ANGLE: The angle measured from the moon's center between the direction of the Earth and the Sun.

PHASE INTEGRAL: The ratio of the Bond Albedo to the Geometric Albedo.

PHOTOMETRIC FUNCTION: A function which describes the photometric behavior of a site. It is dependent upon the angle of incidence of the light, the angle of observation, and the phase angle.

BIBLIOGRAPHY

Adams, J.B. & McCord, T.B.; 1971. "Alteration of Lunar Optical Properties: Age and Compositional Effects." Science, Vol. 171, pp. 567-571.

Africano, J.L., Cobb, C.L., Dunham, D.W., Evans, D.S., Fekel, F.C., and Vogt, S.S.; 1975. "Photoelectric Measurements of Lunar Occultations VII.: Further Observational Results. " Astron. J., Vol. 80, p. 689.

Alter, D. (Ed); 1964. Lunar Atlas. New York: Dover Publications, Inc.

Arking, A.; 1963. Space Res., COSPAR Symp., Warsaw, Vol. 4, p. 139.

Aronson, J. & Emslie, A.; 1973. "Spectral Reflectance and Emittance of Particulate Materials. 2. Application and Results. " Appl. Opt., Vol. 12, pp. 2573-2584.

Arnulf, M.A.; 1936. Compt. Rend., Vol. 292, p. 115.

Arthur, D.W.G. & Agnieray, A.P.; 1964. Lunar Designations and Positions, Quadrant I, II, III, IV. Tucson: University of Arizona Press.

Arthur, D.W.G. et al.; 1963. "The System of Lunar Craters, Quadrant I. " Comm. of the Lunar and Planetary Lab., Vol. 2, No.30. Tucson: University of Arizona Press.

________; 1964. "The System of Lunar Craters, Quadrant II. " Comm. of the Lunar and Planetary Lab., Vol. 3, No. 40. Tucson: University of Arizona Press.

________; 1965. "The System of Lunar Craters, Quadrant III. " Comm. of the Lunar and Planetary Lab., Vol. 3, No. 50. Tucson: University of Arizona Press.

________; 1966. "The System of Lunar Craters, Quadrant IV. " Comm. of the Lunar and Planetary Lab., Vol. 5, Part 1, No. 70. Tucson: University of Arizona Press.

Asaad, A.S. & Mikhail, J.S.; 1974. "Colour Contrasts of Lunar Grounds." The Moon, Vol. 11, pp. 273-299. D. Reidel Publishing Company, Dordrecht.

Avigliano, D.P.; 1951. "Lunar Colors." J.A.L.P.O., Vol. 8, pp. 50-55 & 62-65.

Barabashov, N.P.; 1922. "Bestimmung der Erdalbedo und des Reflexionsgestzes fur die Oberflache der Mondmeere Theorie der Rillen." Astron. Nachr., Vol. 217, pp. 445-452.

Barabashov, N.P. & Ezevsky, V.I.; 1962. "On the Photometric Homogeneity of the Lunar Surface." pp. 395-398 in Kopal & Mikhailov, 1962.

Barbier, D.; 1959. Private communication, November, 1959.

________; 1961. "Photometry of Lunar Eclipses." CHPT 7, pp. 249-273 in Kuiper & Middlehurst, 1961.

Bauer, E. and Danjon, A.; 1923. Bull. Soc. Astr. Fr., Vol. 37, p. 241.

Beer, W. and Mädler, J.H.; 1834. Astr. Nachr., Vol. 11, p.290.

Bell, J.; 2000. "Colors On The Moon?" Astronomy, Vol. 28, No. 5, pp. 48-51.

Bennett, A.L.; 1938. "A Photovisual Investigation of the Brightness of 59 Areas on the Moon." Astrophy. J., Vol. 88, pp. 1-26.

Bently, A.N., De Jonckheere, C.G., & Miller, D.E.; 1974. "Geometric Albedo of the Moon in the Ultraviolet." Astron. J., Vol. 79, No. 3, pp. 401-403.

Benton, J.L.; 1983. "The Selected Areas Program: A New Beginning." J.A.L.P.O., Vol. 30, pp. 1-5.

Blizard, J.B.; 1967. "A Survey of Lunar Transient Events." Rep't. Denver Res. Inst., U. of Denver, Denver, CO, pp. 573-577.

Blow, G.L.; 1983. "Lunar Occultations." CHPT. 9, pp. 9-1 - 9-25, in Genet, 1983.

Bohren, C. & Huffman, D.; 1993. Absorption and Scattering of Light by Small Particles. Wiley, New York.

Bonner, W.J. & Schmall, R.A.; 1973. "A Photometric Technique for Determining Planetary Slopes from Orbital Photographs." U.S. Geological Survey Professional Paper 812-A. Washington: U.S. Government Printing Office.

Bouška, J.; 1948. Bull. Astr. Insts. Csl., Vol. 1, pp. 37, 75.

Bouška, J. and Švestka, Z.; 1950. Bull. Astr. Insts. Csl., Vol. 2, p. 6.

Bowker, D.E. & Hughes, J.K.; 1971. Lunar Orbiter Photographic Atlas of the Moon. NASA report SP-206. Washington: NASA.

British Astronomical Association; 1986. Guide to Observing the Moon. Enslow Publishers, Inc., Hillside, NJ.

Brown, R.H.; 1968. Ann. Rev. Astron. Astrophys., Vol. 6, p. 13.

Brosinsky, A.; 1888. Über die Vergrösserung, etc. Göttingen.

Bullrich, K.; 1948. Ber. Deutsch. Wetterd., U.S.-Zone, No. 4.

Buratti, B.J., Hillier, J.K., Wang, M.; 1996. "The Lunar Opposition Surge: Observations by Clementine" Icarus, Vol. 124, pp. 490-499.

Buratti, B.J., McConnochie, T.H., Calkins, S.B., Hillier, J.K., Herkenhoff, K.E.; 2000. "Lunar Transient Phenomena: What Do the Clementine Images Reveal." Icarus, Vol. 146, pp. 98-117.

Buratti, B.J. & Veverka, J.; 1985. "Photometry of Rough Planetary Surfaces: The Role of Multiple Scattering." Icarus, Vol. 64, pp. 320-328.

Burley, J.M. & Middlehurst, B.M.; 1966. "Apparent Lunar Activity." Proc. Natl. Acad. Sci., Vol. 55, p. 1007.

Busarev, V.V. & Shevchenko, V.V.; 1989. "Prediction of Lunar Areas Containing Ilmenite Based on Color and Spectroscopic Characteristics." Sov. Astron., Vol. 33, No. 3, pp. 304-308.

Cabannes, J.; 1929. "Sur La Diffusion De La Lumière", p. 167. Paris.

Cameron, W.S.; 1972. "Comparative Analysis of Observations of Lunar Transient Phenomena." Icarus, Vol. 16, pp. 339-387.

________; 1974. "Report on the ALPO Lunar Transient Phenomena Observing Program." J.A.L.P.O., Vol. 25, No. 1-2, pp. 1-14.

________; 1975. "Manifestations and Possible Sources of Lunar Transient Phenomena (LTP)." The Moon, Vol. 14, pp. 187-199. D. Reidel Publishing Company, Dordrecht.

________; 1977. "Lunar Transient Phenomena (LTP): Manifestations, Site Distribution, Correlations, and Possible Causes." Phys. Earth Planet. Inter., Vol. 14, pp. 194-216.

________; 1978. Lunar Transient Phenomena Catalog. NSSDC/WDC-A-R&S 78-03. Greenbelt, MD: NASA Goddard Spaceflight Center.

________; 1979. "Results from the LTP Observing Program for the Association of Lunar and Planetary Observers (ALPO)." J.A.L.P.O., Vol. 27, No. 9-10, pp. 195-240.

________; 1980. "New Results from Old Data: Lunar Photometric Anomalies in Wildey and Pohn's 1962 Observations." Astron. J., Vol. 85, pp. 314-328.

________; 1981. "Report on the A.L.P.O. LTP Observing Program." J.A.L.P.O., Vol. 29, pp. 15-24.

________; 1986. "Comparison of Brightness of Lunar Features By Three Methods of Observations." J.A.L.P.O., Vol. 31, pp. 33-40.

________; 1991. "Lunar Transient Phenomena." Sky & Telescope, Vol. 81, No. 3, pp. 265-268.

Cameron, W.S. & Gilheany, J.J.; 1967. "Operation Moonblink and Report of Observations of Lunar Transient Phenomena." Icarus, Vol. 7, pp. 29-41.

Cassini, J.D.; 1740. Tables Astronomiques, p. 34. Paris.

Chandrasekhar, S.; 1960. Radiative Transfer. New York: Dover Publications, Inc.

Chapman, W.B.; 1967. "Tidal Influences at the Lunar Crater Aristarchus." J. Geophys. Res., Vol. 72, pp. 6293-6298.

Cimino, M. and Fortini, T.; 1953. R. C. Accad. Lincei., Vol. 14, p. 619.

Cimino, M. and Fresa, A.; 1958. R. C. Accad. Lincei., Vol. 25, p. 58.

Cimino, M. and Gianuzzi, M.A.; 1955. R. C. Accad. Lincei., Vol. 18, p. 173.

Clark, P.E. et al.; 1976. "Palus Somnii: Anomalies in the Correlation of Al/Si X-Ray Flourescence Intensity Ratios and Broad-Spectrum Visible Albedos." Geophys. Res. Let., Vol. 3, No. 8, pp. 421-424.

Cooke, S.R.B.; 1966. "An Unusual Lunar Dome." Sky & Telescope, Vol. 32, No. 2, pp. 111.

Cousins, A.W.J. and Guelke, R.; 1953. Monthly Notices Roy. Astron. Soc., Vol. 113, p. 776.

Criswell, D.R. & De, B.R.; 1977. "Intense Localized Photoelectric Charging in the Lunar Sunset Terminator Region 2. Supercharging at the Progression of Sunset." J. Geophys. Res., Vol. 82, pp. 1005-1007.

Danjon, A.; 1936. Ann. Obs. Strasbourg., Vol. 3, III.

________; 1954. "Albedo, Color, and Polarization of the Earth." in The Earth as a Planet, G.P. Kuiper (Ed), pp. 726-738. Chicago: University of Chicago Press.

Davis, P.A. & Soderblom, L.A.; 1984. "Modeling Crater Topography and Albedo from Orthoscopic Viking Orbiter Images. 1. Methodology." J. Geophys. Res., Vol. 89, No. B11, pp. 9449-9457.

De, B.R. & Criswell, D.R.; 1977. "Intense Localized Photoelectric Charging in the Lunar Sunset Terminator Region 1. Development of Potentials and Fields." J. Geophys. Res., Vol. 82, pp. 999-1004.

Delano, K.J.; 1969. "A Revised Catalog of Lunar Domes." J.A.L.P.O., Vol. 21, Nos. 5-6, pp. 76-79.

Diercks, H. and Hunger, K.; 1952. Z. Astrophys., Vol. 31, p. 182.

Dobson, G.M.B.; 1930. Proc. Roy. Soc. A., 129, p. 411.

Dollfus, A.; 1998. “Lunar Surface Imaging Polarimetry: I. Roughness and Grain Size.” Icarus, Vol. 136, pp. 69-103.

Dollfus, A.; 1999. “Lunar Surface Imaging Polarimetry.” Icarus, Vol. 140, pp. 313-327.

Dragg, J.L. & Prior, H.L.; 1969. "Photometric Function Reductions." NASA SP-201, pp. 41-44. Washington: NASA.

Draine, B. & Goodman, J.; 1993. "Beyond Clausius-Massotti: Wave Propagation on a Polarization Point Lattice and the Discrete Dipole Approximation." Astrophy. J., Vol. 405, pp. 685-697.

Drossart, P.; 1990. "A Statistical Model for the Scattering by Irregular Particles." Astrophy. J., Vol. 361, L29-L32.

Drossart, P.; 1993. "Optics on a Fractal Surface and the Phtometry of the Regoliths." Planet. Space Sci., Vol. 41, No. 5, pp. 381-393.

Dubois, J.; 1944. L'Astronomie, Vol. 58, p. 136.

________; 1956. L'Astronomie, Vol. 70, p. 225.

________; 1957. J. Phys. Théor. Appl. Paris, Vol. 18, p. 13, Suppl.

________; 1959. Rozpr. Ceskosl. Akad. V□d., Vol. 69, No. 6.

Dunham, D.W., Evans, D.S., McGraw, J.T., Sandmann, W.H., and Wells, D.C.; 1973. "Photoelectric Measurement of Lunar Occultation. VI. Further Observationsl Results. " Astron. J., Vol. 78, p. 482.

Eddington, A.E.; 1909. Monthly Notices Roy. Astron. Soc. Vol. 69, p. 178.

Emslie, A. & Aronson, J.; 1973. "Spectral Reflectance and Emittance of Particulate Materials. 1. Theory. " Appl. Opt., Vol. 12, pp 2563-2572.

Evans, D.S.; 1951. Monthly Notices Roy. Astron. Soc., Vol. 111, p. 64.

________; 1955. Astron. J., Vol. 75, p. 589 (Paper III).

________; 1957. Astron. J., Vol. 62, p. 83.

________; 1959. Monthly Notices Astron. Soc. S. Africa., Vol. 18, p. 158.

________; 1970. "Photoelectric Measurement of Lunar Occultations. III. Lunar Limb Effects." Astron. J., Vol. 75, pp. 589-599.

________; 1971. "Photoelectric Measurement of Lunar Occultations. V. Observational Results." Astron. J., Vol. 76, pp. 1007-1116.

Evans, D.S., Heydenrych, J.C.R., and Van Wyk, J.D.N.; 1954. Astron. J. Vol. 113, p. 781.

Evsyukov, N.N.; 1974. "Colorimetric Structure of the Lunar Maria." Sov. Astron., Vol. 17, No. 6, pp. 801-804.

________; 1975A. "A Two-Parameter Regional Subdivision of the Lunar Surface." Sov. Astron., Vol. 18, No. 3, pp. 359-362.

________; 1975B. "Possibility of Cartography of the Complex of Optical Characteristics of the Moon." Sov. Astron., Vol. 19, No. 2, pp. 242-244.

________; 1984. "Division of the Lunar Surface into Regions by Albedo and Color in the Spectral Range of 0.62-0.95 μm." Sov. Astron., Vol. 28, No. 2, pp. 212-214.

Fedoretz, V.A.; 1952. "Photographic Photometry of the Lunar Surface." Publ. Astron. Obs. of the Kharkov State University, Vol. 2, pp. 49-172 (in Russian).

Fessenkov, V.; 1962. "Photometry of the Moon," p. 99-130 in Kopal, 1962.

________; 1970. "The Application of Lunar Eclipses for Surveying the Optical Properties of the Atmosphere." Sov. Astron., Vol. 14, No. 2, pp. 195-201.

Fielder, G. (Ed); 1971. Geology and Physics of the Moon. New York: American Elsevier Pub. Co., Inc.

Firsoff, V.A.; 1958. "Color on the Moon." Sky & Telescope, Vol. 17, No. 7, pp. 329-331.

________; 1962. Strange World of the Moon. New York: Science Editions, Inc. (See: CHPT. 8, pp. 76-85, "Realities or Shadows?"; CHPT. 9, pp. 86-97, "Seasonal Changes"; CHPT. 10, pp. 98-110, "Colours and Hues": and CHPT. 12, pp. 122-133, "The Vexed Question of the Lunar Atmosphere.")

________; 1970. The Old Moon and the New. Cranbury, NJ: A.S. Barnes and Co., Inc., (See: CHPT. 13, pp. 178-190, "Seeing is Believing"; CHPT. 14, pp. 191-208, "Colours, Shadows, and Seasons"; and CHPT. 15, pp. 209-228, "For and Against a Lunar Atmosphere".)

Fortini, T.; 1954. R. C. Accad. Lincei., Vol. 17, p. 209.

________; 1955. R. C. Accad. Lincei., Vol. 18, p. 65.

Franklin, F.A.; 1967. "Two-Color Photometry of the Earthshine." J. Geophys. Res., Vol. 72, No. 11, pp. 2963-2967.

Frisch, Cr.; 1858. J. Kepleri Opera Omnia., Vol. 2, p. 297. Francoforti.

Fritz, S.; 1949. "The Albedo of the Planet Earth and of Clouds." J. Meteorol., Vol. 6, pp. 277-282.

Garlick, G.F.J., Steigmann, G.A., & Lamb, W.E.; 1972. "Explanation of Transient Lunar Phenomena Based on Lunar Sample Studies." Nature, Vol. 235, pp. 39-40.

Geake, J.E. & Mills, A.A.; 1977. "Possible Physical Processes Causing Transient Lunar Events." Phys. Earth Planet. Inter., Vol. 14, pp. 299-320.

Gehrels, T., Coffeen, D. & Owings, T.; 1964. "Wavelength Dependence of Polarization. III. The Lunar Surface." Astron. J., Vol. 69, pp. 826-852.

Genet, R.M. (Ed); 1983. Solar System Photometry Handbook. Richmond, Va: Willmann-Bell, Inc.

Goguen, J. & Veverka, J.; 1979. "Scattering of Light from Particulate Surfaces. IV. Photometric Functions for Surfaces of Arbitrary Albedo." NASA TM-80339, p. 405.

Gold, T., Bilson, E., & Baron, R.L.; 1977. "The Search for the Cause of the Low Albedo of the Moon." J. Geophys. Res., Vol. 82, No. 30, pp. 489-498.

Götz, P.; 1931. Gerland's Beitr. Geophys., Vol. 31, p. 119.

Greeley, R.; 1971. "Lava Tubes and Channels in the Lunar Marius Hills." The Moon, Vol. 3, pp. 289-314. D. Reidel Publishing Company, Dordrecht.

Greenberg, J.M.; 1974. "Some Examples of Exact and Approximate Solutions in Small Particle Scattering: A Progress Report. " in Planets, Stars, and Nebulae Studied with Photopolarimetry (T. Gehrels, Ed.), pp 107-134. Univ. Of Arizona Press, Tucson.

Greenstein, J.L.; 1937. Harv. Circ. No. 422.

Guest, J.E. & Murray, J.B.; 1976. "Volcanic Features of the Nearside Equatorial Lunar Maria." J. Geol. Soc. Lond., Vol. 132, pp. 251-258.

Haas, W.H.; 1937. "Color Changes on the Moon." Popular Astronomy, Vol. 45, pp. 337-341.

________; 1942. "Does Anything Ever Happen on the Moon?" J. Roy. Astr. Soc. of Can., Vol. 36, pp. 237-272, 317-328, 361-376, 397-408.

Hameen-Antilla, K.A., Laakso, P., & Lumme, K.; 1965. "The Shadow Effect in the Phase Curves of Lunar Type Surfaces." Ann. Acad. Sci. Fenn., p. 172.

Hansa, M. and Zacharov, I.; 1958. Bull. Astr. Insts. Csl., Vol. 9, p. 236.

Hapke, B.W.; 1963. "A Theoretical Photometric Function for the Lunar Surface." J. Geophys. Res., Vol. 68, No. 15, pp. 4571-4586.

________; 1966A. "An Improved Theoretical Lunar Photometric Function." Astron. J., Vol. 71, pp. 333-339.

________; 1966B. "Optical Properties of the Lunar Surface." pp. 142-153 in Hess, Menzel, & O'Keefe, 1966.

________; 1968. "Lunar Surface Composition Inferred from Optical Properties." Science, Vol. 159, pp. 76-79.

________; 1971. "Optical Properties of the Lunar Surface." CHPT. 5, pp. 155-211, in Kopal, 1971.

________; 1977. "Interpretations of Optical Observations of Mercury and the Moon." Phys. of Earth Planet. Int., Vol. 15, pp. 264-274.

________; 1981. "Bidirectional Reflectance Spectroscopy: 1. Theory." J. Geophys. Res., Vol. 86, No. B4, pp. 3039-3054.

________; 1984. "Bidirectional Reflectance Spectroscopy: 3. Correction for Macroscopic Roughness." Icarus, Vol. 59, pp. 41-59.

________; 1986. "Bidirectional Reflectance Spectroscopy: 4. The Extinction Coefficient and the Opposition Effect." Icarus, Vol. 67, pp. 264-280.

________; 1993. Theory of Reflectance and Emittance Spectroscopy, Cambridge Univ. Press, New York.

Hapke, B. W., Nelson, R., Smythe, W.; 1998. "The Opposition Effect of the Moon: Coherent Backscatter and Shadow Hiding. " Icarus, Vol. 133, pp. 89-97.

Hapke, B.W. & Van Horn, H.; 1963. "Photometric Studies of Complex Surfaces, with Applications to the Moon." J. Geophys. Res., Vol. 68, No. 15, pp. 4545-4570.

Hapke, B.W. & Wells, E.; 1981. "Bidirectional Reflectance Spectroscopy: 2. Experiments and Observations." J. Geophys. Res., Vol. 86, No. B4, pp. 3055-3060.

Harris, D.L.; 1961. "Photometry and Colorimetry of Planets and Satellites," in The Solar System, III. Planets and Satellites (G.P. Kuiper & B.M. Middlehurst, Eds). Chicago: University of Chicago Press.

Hartman, B. & Domingue, D.; 1998. "Scattering of Light by Individual Particles and the Implications for Models of Planetary Surfaces. " Icarus, Vol. 131, pp. 421-448.

Hartmann, J.; 1891. Abh. Sachs. Ges. (Akad.) Wiss. (Math-Phys. KL.)., Vol. 17, p. 365.

Hawke, B.R., Peterson, C.A., Lucey, P.G., Taylor, G.J., Blewett, D.T., Campbell, B.A., Coombs, C.R., Spudis, P.D.; 1993. "Remote Sensing Studies of the Terrain Northwest of Humorum Basin. " Geophys. Res. Letters, Vol. 20, No. 6, pp. 419-422.

Head, J.W.; 1976. "Lunar Volcanism in Space and Time." Rev. of Geophys. and Space Phys., Vol. 14, No. 2, pp. 265-300.

Head, J.W. & Gifford, A.; 1980. "Lunar Mare Domes: Classification and Modes of Origin." The Moon and the Planets, Vol. 22, pp. 235-258.

Head, J.W. & McCord, T.B.; 1978. "Imbrium-Age Highland Volcanism on the Moon: The Gruithuisen and Marian Domes." Science, Vol. 199, pp. 1433-1436.

Hedervari, P.; 1982. "A Proposed Photometric Program for A.L.P.O. Lunar Observers." J.A.L.P.O., Vol. 29, pp. 147-150.

________; 1983A. "On the Albedos of Some Lunar Features." J.A.L.P.O., Vol. 30, pp. 9-10.

________; 1983B. "Lunar Photometry." CHPT. 4, pp. 4-1 - 4-20, in Genet, 1983.

Heiken, G.H., Vaniman, D.J., & French, B.M.; 1991. Lunar Sourcebook. New York: Cambridge University Press.

Helfenstein, P.; 1988. "The Geological Interpretation of Photometric Surface Roughness." Icarus, Vol. 73, pp. 462-481.

Helfenstein, P. & Shepard, M.K.; 1999. “Submillimeter-Scale Topography of the Lunar Regolith.” Icarus, Vol. 141, pp. 107-131.

Helfenstein, P. & Veverka, J.; 1987. "Photometric Properties of Lunar Terrains Derived from Hapke's Equation." Icarus, Vol. 72, pp. 342-357.

Helfenstein, P. Veverka, J., Hillier, J.; 1997. "The Lunar Opposition Effect: A Test of Alternative Models." Icarus, Vol. 128, pp. 2-14.

Henden, A.A. & Kaitchuck, R.H.; 1982. Astronomical Photometry. New York: Van Nostrand Reinhold Company.

Hepperger, J.; 1895. S. B. Akad. Wiss. Wein (Math-Phys. KL)., Vol. 54/II.

Herring, A.K.; 1960. "Observing the Moon - Rumker." Sky & Telescope, Vol. 20, No. 4, p. 219.

________; 1961. "Observing the Moon - Kies." Sky & Telescope, Vol. 21, No. 5, p. 281.

________; 1962. "Observing the Moon - Hortensius." Sky & Telescope, Vol. 23, No. 1, pp. 33-34.

________; 1965A. "Observing the Moon - Marius." Sky & Telescope, Vol. 29, No. 1, p. 59.

________; 1965B. "Observing the Moon - Milichius." Sky & Telescope, Vol. 29, No. 4, p. 252.

Hess, W., Menzel, D.H., & O'Keefe, J. (Eds); 1966. The Nature of the Lunar Surface. Baltimore: Johns Hopkins University Press.

Heyden, F.J.; 1954. Astrophy. J., Vol. 118, p. 412.

Hillier, J.K.; 1997. "Shadow-Hiding Opposition Surge for a Two-Layer Surface. " Icarus, Vol. 128, pp. 15-27.

Hillier, J.K.; 1997. "Scattering of Light by Composite Particles in a Planetary Surface." Icarus, Vol. 130, pp. 328-335.

Hillier, J.K., Buratti, B.J., Hill, K.; 1999. “Multispectral Photometry of the Moon and Absolute Calibration of the Clementine UV/Vis Camera.” Icarus, Vol. 141, pp. 205-225.

Hiroi, T. & Pieters, C.M.; 1992. Effects of Grain Size and Shape in Modeling Reflectance Spectra of Mineral Mixtures. " Proceedings of Lunar and Planetary Science, Vol. 22, pp. 313-325. Lunar and Planetary Institute.

Holt, H.E. & Rennilson, J.J.; 1970. "Photometric and Polarimetric Properties of the Lunar Regolith." NASA SP-235, pp. 157-161. Washington: NASA.

Hood, L.L. & Schubert, G.; 1980. "Lunar Magnetic Anomalies and Surface Optical Properties." Science, Vol. 208, pp. 49-51.

Hopfield, J.J.; 1967. "Optical Properties and Infrared Emission of the Moon." pp. 101-120 in Singer, 1967.

Iriarte, B., Johnson, H.L., Mitchell, R.I., & Wisniewski, W.K.; 1965. "Five-Color Photometry of Bright Stars: The Arizona-Tonanzintla Catalog-Multicolor Photometry UBVRI." Sky & Telescope, Vol. 30, p. 21. (Available as a reprint).

Irvine, W.M.; 1966. "The Shadowing Effect in Diffuse Reflection." J. Geophys. Res., Vol. 71, No. 12, pp. 2931-2937.

Jackson, J.; 1950. Observatory, Vol. 70, p. 215.

Jamieson, H.D.; 1972. "The Lunar Dome Survey: A Progress Report." J.A.L.P.O., Vol. 23, No. 11-12, pp. 212-215.

________; 1974. "The Lunar Dome Survey: A Progress Report (II)." J.A.L.P.O., Vol. 24, No. 9-10, pp. 187-192.

________; 1988. "Observing Lunar Domes." J.A.L.P.O., Vol. 33, No. 1-3, pp. 23-24.

Jamieson, H.D. & Rae, W.L.; 1965. "The Joint A.L.P.O.-B.A.A. Lunar Dome Project." J.A.L.P.O., Vol. 18, No. 9-10, pp. 179-182.

Johnson, H.L. & Morgan, W.W.; 1953. Astrophy. J., Vol. 117, p. 313.

Johnson, T.V., Pieters, C. & McCord, T.B.; 1973. "Mare Humorum: An Integrated Study of Spectral Reflectivity." Icarus, Vol. 19, pp. 224-229.

Jones, M.T.; 1969A. "A Quantitative Evaluation of the Uniformity of the Light Scattering Properties of the Lunar Surface." The Moon, Vol. 1, pp. 31-58. D. Reidel Publishing Company, Dordrecht.

________; 1969B. "A Single-Color Investigation into the Uniformity of the Light Scattering Properties of the Lunar Surface." Icarus, Vol. 10, pp. 66-89.

Kapral, C.A.; 1991A. "Practical Lunar Photometric Photometry." Selenology, Vol. 10, No. 1, pp. 12-26.

________; 1991B. "Practical Lunar Photoelectric Photometry." J.A.L.P.O., Vol. 35, No. 3, pp. 104-110.

Keen, R.A.; 1983. "Volcanic Aerosols and Lunar Eclipses." Science, Vol. 222, pp. 1011-1013.

Kerker, M.; 1969. The Scattering of Light. Academic Press, New York.

Kieffer, H.H.; 1997. "Photometric Stability of the Lunar Surface. " Icarus, Vol. 130, pp. 323-327.

Kitt, M.T.; 1990. "How to Find a Lunar Volcano." Astronomy, Vol. 18, No. 12, pp. 62-66.

Koebke, F.; 1951. Bull. Soc. Amis. Sci., Poznan, p.11.

Kopal, Z. (Ed); 1962. Physics and Astronomy of the Moon. New York: Academic Press, Inc.

________; 1966. An Introduction to the Study of the Moon. New York: Gordon & Breach. (See CHPT. 19, pp. 323-336, "Photometry of Scattered Moonlight").

________; 1971. Physics and Astronomy of the Moon. New York: Academic Press, Inc.

Kopal, Z. & Goudas, C.L. (Eds); 1967. Measure of the Moon. New York: Academic Press, Inc.

Kopal, Z. & Mikhailov, Z.K. (Eds); 1962. The Moon. New York: Academic Press, Inc.

Kopal, Z. & Rackham, T.; 1964. "Lunar Luminescence and Solar Flares." Nature, Vol. 202, p. 171.

Kornienko, Yu.V., Shkuratov, Yu.G., Bychinskii, V.I. & Stankevich, D.G.; 1982. "Correlation Between Albedo and Polarization Characteristics of the Moon. Application of Digital Image Processing." Sov. Astron., Vol. 26, No. 3, pp. 345-348.

Kosik, S.M.; 1940. Bull. Tashkent Astr. Obs., Vol. 2, p. 79.

Kozyrev, N.A.; 1956. Izv. Crim. Astrophys. Obs., Vol. 16, p. 148.

________; 1959. "Observation of a Volcanic Process on the Moon." Sky & Telescope, Vol. 18, No. 4, pp. 184-186.

________; 1963. "Volcanic Phenomenon on the Moon." Nature, Vol. 198, pp. 979-980.

Krisciunas, K. & Schaefer, B.E.; 1991. "A Model of the Brightness of Moonlight." Pub. Astron. Soc. Pac., Vol. 103, No. 667, pp. 1033-1039.

Kühl, A.; 1928. Phys. Z., Vol. 29, p. 1.

Kuiper, G.P. (Ed); 1960. Photographic Lunar Atlas. Chicago: University of Chicago Press.

Kuiper, G.P. & Middlehurst, B.M.; 1961. Planets and Satellites. Chicago: University of Chicago Press.

Lahire, P.; 1707. Tabulae Astronomicae, Paris.

Lalande, J.F.; 1783. Astronomie, Vol. 2, p. 337.

Lambert, F.; 1782. Briefwechsel, Berlin.

Lane, A.P. & Irvine, W.M.; 1973. "Monochromatic Phase Curves and Albedos for the Lunar Disk." Astron. J., Vol. 78, pp. 267-277.

Legentil, G.J.H.; 1755. Mém. Acad. Sci., p. 36, Paris.

Lemonnier, P.C.; 1746. Institutions Astronomiques, p. 251, Paris.

Lester, T.P., McCall, M.L. & Tatum, J.B.; 1979. "Theory of Planetary Photometry." J. Roy. Astr. Soc. Can., Vol. 73, No. 5, pp. 233-257.

Link, F.; 1929. Bull. Obs. Lyon., Vol. 11, p. 229.

________; 1933. Bull. Astr., Vol. 8, p. 77, Paris.

________; 1946. Ann. Astrophys., Vol. 9, p. 227.

________; 1947a. J. Soc. Math. Phys. Tchèque., Vol. 72, p. 65.

________; 1947b. Coll. Lyon. C.N.R.S., Vol. 1, p. 308, Paris.

________; 1948. Ann. Geophys., Vol. 4, pp. 47, 211.

________; 1950a. Trans. I.A.U., Vol. 7, p. 135.

________; 1950b. Bull. Astr. Insts. Csl., Vol. 2, p. 1.

________; 1951. Bull. Astr. Insts. Csl., Vol. 2, p. 131.

________; 1958. Bull. Astr. Insts. Csl., Vol. 9, p. 169.

________; 1959. Bull. Astr. Insts. Csl., Vol. 10, p. 105.

________; 1969. Eclipse Phenomena in Astronomy. New York: Springer-Verlag.

________; 1972. "Photometry of the Lunar Surface." The Moon, Vol. 5, pp. 265-285. D. Reidel Publishing Company, Dordrecht.

Link, F. and Linkova, Z.; 1954. Publ. Obs. Nat., Prague, No. 25.

Liou, K. & Hansen, J.; 1971. "Intensity and Polarization for Single Scattering by Polydisperse Spheres: A Comparison of Ray Optics and Mie Theory. " J. Atmos. Sci., Vol. 28, pp. 995-1004.

Lipskii, Yu.N. & Shevchenko, V.V.; 1972. "Preparation of a Spectrozonal Map for an Area on the Lunar Surface." Sov. Astron., Vol. 16, No. 1, pp. 132-136.

Lucchitta, B.K.; 1971. "Evaluation of Photometric Slope Deviation." NASA SP-232, pp. 31-35. Washington: NASA.

Lucke, R.L., Henry, R.C. & Fastie, W.G.; 1976. "Far-Ultraviolet Albedo of the Moon." Astron. J., Vol. 81, pp. 1162-1169.

Lumme, K.; 1972. "On Surface Photometry of the Moon." The Moon, Vol. 5, pp. 447-456. D. Reidel Publishing Company, Dordrecht.

Lumme, K. & Bowell, E.; 1981A. "Radiative Transfer in the Surfaces of Atmosphereless Bodies: I. Theory." Astron. J., Vol. 86, pp. 1694-1704.

________; 1981B. "Radiative Transfer in the Surfaces of Atmosphereless Bodies: II. Interpretation of Phase Curves." Astron. J., Vol. 86, pp. 1705-1721.

Lumme, K. & Irvine, W.M.; 1982. "Radiative Transfer in the Surfaces of Atmosphereless Bodies: III. Interpretation of Lunar Photometry." Astron. J., Vol. 87, pp. 1076-1082.

MacMahon, P.A.; 1909. Monthly Notices Roy. Astron. Soc., Vol. 69, p. 126.

MacRobert, A.; 1984A. "A Guided Tour of the Moon." Sky & Telescope, Vol. 68, No. 3, pp. 211-213.

________; 1984B. "Lunar Domes." Sky & Telescope, Vol. 68, No. 4, pp. 340-341.

Markov, A.V.; 1948. Russ. A.J., Vol. 4, p. 60.

Markov, A.V. (Ed); 1962. The Moon: A Russian View. Chicago: University of Chicago Press.

Matsushima, S.; 1967. "Transient Lunar Brightening." Nature, Vol. 213, pp. 481-482.

McCord, T.B.; 1967. "Observational Study of Lunar Visible Emission." J. Geophys. Res., Vol. 72, No. 8, pp. 2087-2097.

________; 1969. "Color Differences on the Lunar Surface." J. Geophys. Res., Vol. 74, pp. 3131-3142.

McCord, T.B. & Adams, J.B.; 1973. "Progress in Remote Optical Analysis of Lunar Surface Composition." The Moon, Vol. 7, pp. 453-474. D. Reidel Publishing Company, Dordrecht.

McCord, T.B. & Johnson, T.V.; 1969. "Relative Spectral Reflectivity (0.4 to 1.0 Microns) of Selected Areas of the Lunar Surface." J. Geophys. Res., Vol. 74, pp. 4395-4401.

________; 1970. "Lunar Spectral Reflectivity (0.30 to 2.50 Microns) and Implications for Remote Mineralogical Analysis." Science, Vol. 169, pp. 855-858.

McCord, T.B. et al; 1972A. "Spectrophotometry (0.3 to 1.1 Microns) of Visited and Proposed Apollo Landing Sites." The Moon, Vol. 4, pp. 52-89. D. Reidel Publishing Company, Dordrecht.

________; 1972B. "Lunar Spectral Types." J. Geophys. Res., Vol. 77, pp. 1349-1359.

McEwen, A.S.; 1991. "Photometric Functions for Photoclinometry and Other Applications." Icarus, Vol. 92, pp. 298-311.

McEwen, A.S.; 1996. "A Precise Lunar Photometric Function. " Lunar and Planet. Sci., Vol. 27, pp. 841.

McGuire, A.F. & Hapke, B.W.; 1995. "An Experimental Study of Light Scattering by Large, Irregular Particles." Icarus, Vol. 113, pp. 134-155.

McKay, D., Fruland, R. & Heiken, G.; 1974. "Grain Size and the Evolution of Lunar Soils." Proc. Lunar. Sci. Conf. 5th, pp. 887-906.

Melendrez, D.E., Johnson, J.R., Larson, S.M., Singer, R.B.; 1994. "Remote Sensing of Potential Lunar Resources. 2. High Spatial Resolution Mapping of Spectral Reflectance Ratios and Implications for Nearside Mare TiO2 Content." J. Geophys. Res., Vol. 99 (E3), pp. 5601-5619.

Meeus, J.; 1982. Astronomical Formulae for Calculators. Richmond, Va: Willmann-Bell, Inc.

________; 1991. Astronomical Algorithms. Richmond, Va: Willmann-Bell, Inc.

Middlehurst, B.M.; 1967. "An Analysis of Lunar Events." Rev. of Geophysics, Vol. 5, No. 2, pp. 173-189.

Middlehurst, B.M. & Burley, J.M.; 1966. "Chronology Listing of Lunar Events." NASA X-Document 641-66-178. Washington: NASA.

Middlehurst, B.M. & Moore, P.A.; 1967. "Lunar Transient Phenomena: Topographical Distribution." Science, Vol. 155, pp. 449-451.

Middlehurst, B.M., Burley, J.M., Moore, P.A. & Welther, B.L.; 1968. "Chronological Catalog of Reported Lunar Events." NASA TR R-277. Washington: NASA.

Mikhail, J.S.; 1970. "Colour Variations with Phase of Selected Regions of Lunar Surface." The Moon, Vol. 2, pp. 167-201. D. Reidel Publishing Company, Dordrecht.

Mikhail, J.S. & Koval, I.K.; 1974. "Dependence of Normal Albedo of Lunar Regions on Wavelength." The Moon, Vol. 11, pp. 323-326. D. Reidel Publishing Company, Dordrecht.

Mills, A.A.; 1970. "Transient Lunar Phenomenon and Electrostatic Glow Discharges." Nature, Vol. 225, p. 929.

Minnaert, M.; 1941. "The Reciprocity Principle in Lunar Photometry." Astrophys. J., Vol. 93, pp. 403-410.

Minnaert, M.; 1959. "Photometry of the Moon" in The Moon, IAU Symp. no. 47, D. Reidel Publishing Company, Dordrecht.

________; 1961. "Photometry of the Moon." CHPT. 6, pp. 213-248, in: Kuiper & Middlehurst, 1961.

________; 1967. "Photometric Methods for Determination of Lunar Relief." pp. 383-395, in: Kopal & Goudas, 1967.

Mishchenko, M.I.; 1993. “On the Nature of the Polarization Opposition Effect Exhibited by Saturn’s Rings.” Astrophys. J., Vol. 411, pp. 351-361.

Mitchell, R.I. & Pellicori, S.F.; 1970. "UBVRI Photometry of Some Lunar Topographies." The Moon, Vol. 2, pp. 3-9. D. Reidel Publishing Company, Dordrecht.

Mitra, S.K.; 1952. The Upper Atmosphere. p. 152. Calcutta.

Moore, H.L. et al.; 1980. "Lunar Remote Sensing and Measurements." U.S.Geological Survey Professional Paper 1046-B. Washington: U.S. Government Printing Office.

Moore, P.A.; 1958. "Lunar Domes." Sky & Telescope, Vol. 18, No. 12, pp. 91-95.

________; 1971. "Transient Phenomena on the Moon." Q.J. Roy. Astr. Soc., Vol. 12, pp. 45-47.

________; 1976. New Guide to the Moon. New York: W.W. Norton & Co., Inc. (See: CHPT. 10, pp. 120-134, "Atmosphere and Life"; and CHPT. 15, pp. 197-212, "Flashes, Glows, and Moonquakes").

Mukai, S., Mukai, T., Giese, R.H., Weiss, K., Zerull, R.H.; 1982. "Scattering of Radiation by a Large Particle with a Random Rough Surface." Moon and Planets, Vol. 26, pp. 197-208.

Muller, G.; 1897. Die Photometrie der Gestirne, p. 344. (Leipzig: Engelmann).

Mustard, J.F. & Pieters, C.M.; 1989. "Photometric Phase Functions of Common Geologic Minerals and Applications to Quantitative Analysis of Mineral Mixture Reflectance Spectra." J. Geophys. Res., Vol. 94, No. B10, pp. 13,619-13,634.

Nather, R.E.; 1970. "Photoelectric Measurement of Lunar Occultations. II. Instrumentation." Astron. J., Vol. 75, pp. 583-588.

Nather, R.E. & Evans, D.S.; 1970. "Photoelectric Measurement of Lunar Occultations. I. The Process." Astron. J., Vol. 75, pp. 575-582.

Nather, R.E. & McCants, M.M.; 1970. "Photoelectric Measurement of Lunar Occultations. IV. Data Analysis." Astron. J., Vol. 75, pp. 963-968.

Nelson, R.M., Hapke B.W., Smythe, W.D., Horn, L.J.; 1998. "Phase Curves of Selected Particulate Materials: The Contribution of Coherent Backscattering to the Opposition Surge." Icarus, Vol. 131, pp. 223-230.

Ney, E.P., Woolf, N.J. & Collins, R.J.; 1966. "Mechanism for Lunar Luminescence." J. Geophys. Res., Vol. 71, No. 7, pp. 1787-1793.

Novikov, V.V., Shkuratov, Yu.G., Popov, A.P. & Goryachev, M.V.; 1982. "Correlation Between Albedo and Polarization Properties of the Moon (Heterogeneity of the Relative Porosity of the Surface of the Western Part of the Visible Hemisphere)." Sov. Astron., Vol. 26, No. 1, pp. 79-83.

O'Keefe, J.A.; 1950. Astron. J., Vol. 55, p. 177.

Oetking, P.; 1966. "Photometric Studies of Diffusely Reflecting Surfaces with Applications to the Brightness of the Moon." J. Geophys. Res., Vol. 71, No. 10, pp. 2505-2513.

Paetzold, H.K.; 1950. Z. Naturf., Vol. 5a, p. 661.

________; 1951. Z. Naturf., Vol. 6a, p. 639.

________; 1952. Z. Naturf., Vol. 7a, p. 325.

________; 1953. Z. Astrophys., Vol. 32, p. 303.

Peacock, K.; 1968. "Multicolor Photoelectric Photometry of the Lunar Surface." Icarus, Vol. 9, pp. 16-66.

Phillips, J.H.; 1987. "Lunar Domes - First Observed by Johann Hieronymus Schroter." J.A.L.P.O., Vol. 32, No. 3-4, pp. 67-73.

________; 1989A. "The New Lunar Dome Survey: The Hortensius-Milichius-Tobias Mayer Region." J.A.L.P.O., Vol. 33, No. 4-6, pp. 61-72.

________; 1989B. "Observations of Lunar Domes North-Northwest of Milichius: An Interpretation." J.A.L.P.O., Vol. 33, No. 4-6, pp. 73-74.

________; 1990. "The Marius Hills Region - A Unique Lunar Dome Field." J.A.L.P.O., Vol. 34, No. 3, pp. 104-108.

________; 1991. "The New Lunar Dome Survey - An Update." J.A.L.P.O., Vol. 35, No. 2, pp. 70-71.

Pickering, E.C.; 1882. Selenograph. J. This paper is difficult to find. See G. Muller (1897, p. 345) for a good summary.

Pinty, B. & Ramond, D.; 1986. "A Single Bidirectional Reflectance Model for Terrestrial Surfaces." J. Geophys. Res., Vol. 91, No. D7, pp. 7803-7808.

Pinty, B. & Verstraete, M.M.; 1991. "Extracting Information on Surface Properties from Bidirectional Reflectance Measurements." J. Geophys. Res., Vol. 96, No. D2, pp. 2865-2874.

Pinty, B., Verstraete, M.M. & Dickinson, R.E.; 1989. "A Physical Model for Predicting Bidirectional Reflectances Over Bare Soil." Remote Sens. Environ., Vol. 27, pp. 273-288.

Platt, J.B.; 1958. "On the Nature and Color of the Moon's Surface." Science, Vol. 127, pp. 1502-1503.

Pohn, H.A., Radin, H.W. & Wildey, R.L.; 1969. "The Moon's Photometric Function Near Zero Phase Angle from Apollo 8 Photography." Astrophy. J., Vol. 157, L193-L195.

Pohn, H.A. & Wildey, R.L.; 1970. "A Photoelectric-Photographic Study of the Normal Albedo of the Moon." U.S.

Geological Survey Professional Paper 599-E. Washington: U.S. Government Printing Office.

Pohn, H.A., Wildey, R.L. & Offield, T.W.; 1971. "Correlation of the Zero-Phase Brightness Surge (Heiligenschein) with Lunar Surface Roughness." NASA SP-272, pp. 296-297. Washington: NASA.

Price, F.W.; 1988. The Moon Observer's Handbook. New York: Cambridge University Press.

Purcell, E. & Pennypacker, C.; 1973. "Scattering and Absorption of Light by Nonspherical Dielectric Grains." Astrophy. J., Vol. 186, pp. 705-714.

Puskar, R.J.; 1983. "The Opposition Effect in Optical Scattering from Rough Surfaces." The Ohio State University Journal (PHD Thesis).

Quaide, W.; 1965. "Rilles, Ridges, and Domes - Clues to Maria History." Icarus, Vol. 4, pp. 374-389.

Rennilson, J.J., Holt, H.E. & Morris, E.C.; 1968. "In Situ Measurements of the Photometric Properties of an Area on the Lunar Surface." J. Opt. Soc. Amer., Vol. 58, pp. 747-755.

Richter, N.B.; 1962. "The Photometric Properties of Interplanetary Matter." Q.J. Roy. Astr. Soc., Vol. 3, pp. 179-186.

Rifaat, A.S.; 1967. "Photometric Studies of Two Lunar Domes." Icarus, Vol. 7, pp. 267-273.

Roberts, G.L.; 1966. "Three-Color Photometric Photometry of the Moon." Icarus, Vol. 5, pp. 555-564.

Rocket Panel; 1952. Phys. Rev., Vol. 88, p. 1027.

Rougier, M.G.; 1933. "Photometrie Photoelectrique Globale de la Lune." Strasbourg 2, Part 3, pp. 205-339.

Rükl, A.; 1976. Moon, Mars, and Venus. London: Paul Hamlyn Publishing.

________; 1990. Atlas of the Moon. London: Paul Hamlyn Publishing.

Russell, H.N.; 1916. "The Stellar Magnitudes of the Sun, Moon, and Planets." Astrophy. J., Vol. 43, pp. 103-129.

Rutkowski, C.; 1981. "What is Happening on the Moon? Lunar Transient Phenomena." J. Roy. Astr. Soc. of Can., Vol. 75, No. 5, pp. 237-241.

Saari, J.W. & Shorthill, R.W.; 1967. "Isothermal and Isophotic Atlas of the Moon." NASA CR-855, prepared by Boeing Scientific Research Laboratories under contract NASW-982. 186 pp.

Salisbury, J.W.; 1970. "Albedo of Lunar Soil." Icarus, Vol. 13, pp. 509-512.

Schaber, G.C.; 1980. "Reflection of Solar Radiation with Wavelength from 0.3 Microns to 2.2 Microns." pp. 41-52 in Moore et al., 1980.

Schaefer, B.E.; 1991. "Eclipse Earthshine." Pub. Astr. Soc. Pac., Vol. 103, No. 661, pp. 315-316.

Scheuer, P.A.G.; 1962. Australian J. Phys., Vol. 15, p. 333.

Schmidt, J.; 1856. Der Mond, p. 141, Leipzig.

Schmitt, H.H.; 1974. "Lunar Mare Color Provinces as Observed by Apollo 17." Geology, Vol. 2, pp. 55-56.

Schober, H.J. & Schroll, A.; 1973. "Photoelectric and Visual Observation of the Total Eclipse of the Moon of August 6, 1971." Icarus, Vol. 20, pp. 48-51.

Schröter, J.H.; (1791-1802). Selenographische Fragmente (Göttingen: Lilienthal).

Schuerman, D.; 1980. Light Scattering by Irregularly Shaped Particles. Plenum, New York.

Schuerman, D., Wang, R., Gustafson, B., & Schaefer, R.; 1981. "Systematic Studies of Light Scattering. 1. Particle Shape." Appl. Opt., Vol. 20, pp. 4039-4050.

Scott, N.W.; 1964. "Colour on the Moon." Nature, Vol. 204, pp. 1075-1076.

Seeliger, H.; 1896. Abh. Bayer. Akad. Wiss., II K1, 19/2.

Sekiguche, N.; 1980. "Photometry of the Lunar Surface During Lunar Eclipses." The Moon and Planets, Vol. 23, pp. 90-107. D. Reidel Publishing Company, Dordrecht.

Shepard, M.K., Campbell, B.A.; 1998. "Shadows on a Planetary Surface and Implications for Photometric Roughness." Icarus, Vol. 134, pp. 279-291.

Shevchenko, V.V.; 1970. "Physical Mapping of the Moon from Photometric Data." Sov. Astron., Vol. 14, No. 3, pp. 478-486.

________; 1980. "Formulas and Diagrams for the Definition of the Average Lunar Photometric Function." Trudy.

Gos. Astron. Inst. P.K. Sternberga Vol. 50, pp. 105.

________; 1982. "The Lunar Photometric Constant in the System of True Full Moon." in Sun & Planetary Systems (W. Fricke & G. Teleki, Eds.), pp. 263-264. D. Reidel Publishing Company, Dordrecht.

Shkuratov, Yu.G.; 1981. "Connection Between the Albedo and Polarization Properties of the Moon. Freznel Component of Reflected Light." Sov. Astron., Vol. 25, No. 4, pp. 490-494.

Shkuratov, Yu.G., Kreslavsky, M.A.; 1998. 29th Ann.Lunar and Planet. Conf., March 16-20.

Shkuratov, Yu.G., Kreslavsky, M.A., Ovcharenko, A.A., Stankevich, D.G., Zubko, E.S., Pieters, C., Arnold, G.; 1999. "Opposition Effect from Clementine Data and Mechanisms of Backscatter.", Icarus, Vol. 141, pp. 132-155.

Shkuratov, Yu.G., Starukhina, L., Hoffmann, D., & Arnold, G.; 1999. “A Model of Spectral Albedo of Particulate Surfaces: Implications for Optical Properties of the Moon.” Icarus, Vol. 137, pp. 235-246.

Shorthill, R.W. et al.; 1969. "Photometric Properties of Selected Lunar Features." NASA CR-1429. Washington: NASA.

Shorthill, R.W. & Saari, J.M.; 1965. "Radiometric and Photometric Observations of the Moon Through a Lunation." Ann. of the N.Y. Acad. of Scien., Vol. 123, Art. 2, pp. 722-739.

Singer, S.F.; 1967. Physics of the Moon. Washington: American Astronautical Society.

Skorobogatov, B. & Usokin, A.; 1982. "Optical Properties of Ground Surfaces of Nonabsorbing Materials." Opt. Spectrosc., Vol. 52, pp. 310-313.

Smith, E.I.; 1973. "Identification, Distribution and Significance of Lunar Volcanic Domes." The Moon, Vol. 6, pp. 30-31. D. Reidel Publishing Company, Dordrecht.

________; 1974. "Rümker Hills: A Lunar Volcanic Dome Complex." The Moon, Vol. 10, pp. 175-181. D. Reidel Publishing Company, Dordrecht.

Stebbins, J. & Brown, F.C.; 1907. "Determination of the Moon's Light with a Selenium Photometer." Astrophy. J., Vol. 26, No. 5, p. 326.

________; 1908. "Determination of the Moon's Light with a Selenium Photometer." Nature, Vol. 77, No. 1996, p. 302. This is an explanation to the Stebbins & Brown (1907) method.

Struve, O.; 1960. "Photometry of the Moon." Sky & Telescope, Vol. 20, No. 2, pp. 70-73.

Švestka, Z.; 1950. Bull. Astr. Insts. Csl., Vol. 2, p. 41.

Sytinskaya, N.N.; 1953. "Summary Catalog of the Absolute Values of the Visual Reflecting Power of 104 Lunar Features.", Russian. Astr. Zhur., Vol. 30, p. 295.

________; 1965. "Photometric Data For and Against the Presence of Widely Distributed Volcanic Activity on the Moon." Ann. of the N.Y. Acad. of Scien., Vol. 123, Art. 2, pp. 756-767.

Tanashchuk, M. & Gilchuk, L.; 1978. "Experimental Scattering Matrices of Ground Glass Surfaces." Opt. Spectrosc., Vol. 45, pp. 658-662.

Taylor, J.H.; 1966. Nature, Vol. 210, p. 1105.

Teyfel, V.G.; 1962. "Colour and Spectral Characteristics of the Lunar Surface." pp. 399-407, in Kopal & Mikhailov, 1962.

Thomson, W.; 1883. "Approximate Photometric Measures of the Sun, Moon, Cloudy Sky, and Electric and Other Artificial Lights." Nature, Vol. 27, No. 679, pp. 277-279.

Tsesevich, V.P.; 1940. Publ. Astr. Inst. Univ. Leningrad, No. 50.

U.S. NASA (United States. National Aeronautic and Space Administration. Manned Spacecraft Center.); 1969. "Analysis of Apollo 8 Photography and Visual Observations." NASA SP-201. Washington: U.S. Government Printing Office. (See: pp. 35-38 (Colorimetry) & 38-44 (Photometry).)

________; 1971A. "Analysis of Apollo 10 Photography and Visual Observations." NASA SP-232. Washington: U.S. Government Printing Office. (See: pp. 31-36 (Photometry).)

________; 1971B. "Apollo 14 Preliminary Science Report." NASA SP-272. Washington: U.S. Government Printing Office.

________; 1972. "Apollo 16 Preliminary Science Report." NASA SP-315. Washington: U.S. Government Printing Office.

Van Diggelen, J.; 1959. "Photometric Properties of Lunar Crater Floors." Recherches Astronomiques de L'Observatoire D'Utrecht, Vol. 14, No. 2, pp. 1-14. Translated to English as NASA Technical Translation F-209 (1964).

________; 1965. Planetary Space Science, Vol. 13, p. 271.

________; 1969. "A Photometric Investigation of the Lunar Crater Rays." The Moon, Vol. 1, pp. 67-84. D. Reidel Publishing Company, Dordrecht.

Van de Hulst, H.; 1957. Light Scattering by Small Particles. Wiley, New York.

Veverka, J., Goguen, J. & Noland, M.; 1977. "Photometry of Planetary Surfaces: Studies of the Validity of a Minnaert Description." NASA TM X-3511, p. 275.

Vigroux, E.; 1954. Ann. Astrophys., Vol. 17, p. 399.

Watson, K.; 1968. "Photoclinometry from Spacecraft Images." U.S. Geological Survey Professional Paper 599-B. Washington: U.S. Government Printing Office.

Weiss-Wrana, K.; 1983. "Optical Properties of Interplanetary Dust: Comparison with Light Scattering by Larger Meteoritic and Terrestrial Grains." Astron. Astrophy., Vol. 126, pp.240-250.

Westfall, J.E.; 1972. "Photometry Methods and the Total Lunar Eclipse of January 30, 1972." J.A.L.P.O., Vol. 23, pp. 113-118.

________; 1975. "Observing Lunar Eclipses". J.A.L.P.O., Vol. 25, pp. 85-88.

________; 1979A. A.L.P.O. Lunar Eclipse Handbook. Priv. Pub. (See: pp. 5-7 Photometry).)

________; 1979B. "A Comprehensive Catalog of Lunar Transient Phenomena." J.A.L.P.O., Vol. 27, pp. 192-195. (See: Map on p. 194.)

________; 1979C. "The Total Lunar Eclipse of September 6, 1979." J.A.L.P.O., Vol. 27, pp. 225-227.

________; 1980. "Photographic Photometry of the Total Lunar Eclipse of September 6, 1979." J.A.L.P.O., Vol. 28, pp. 5-6.

________; 1982. "Photoelectric Photometry of the July 6, 1982 Total Lunar Eclipse." J.A.L.P.O., Vol. 29, pp. 168-171.

________; 1983A. "Photoelectric Photometry of the December 30, 1982 Total Lunar Eclipse." J.A.L.P.O., Vol. 30, pp. 6-9.

________; 1983B. "An Invitation to Lunar Photometry." I.A.P.P.P. Comm., No. 14, pp. 64-68.

________; 1984A. "Three Color Photometry: Penumbral Lunar Eclipse, May 15, 1984." J.A.L.P.O., Vol. 30, pp. 209-211.

________; 1984B. Lunar Photoelectric Photometry Handbook. Priv. Pub.

________; 1990. The A.L.P.O. Solar System Ephemeris: 1991. Priv. Pub.

Whitaker, E.A.; 1969. "An Investigation of the Lunar Heiligenschein." NASA SP-201, pp. 38-39. Washington: NASA.

________; 1972. "Lunar Color Boundaries and Their Relationship to Topographic Features: A Preliminary Survey." The Moon, Vol. 4, pp. 348-355. D. Reidel Publishing Company, Dordrecht.

Whitford, A.E.; 1939. Astrophys. J., Vol. 89, p. 472.

________; 1946. Sky and Telescope, Vol. 6, p. 7.

Whitford-Stark, J.L.; 1974. "A Detailed Structural Analysis of the Deslandres Area of the Moon." Icarus, Vol. 21, pp. 457-465.

Wildey, R.L.; 1963. "The Moon's Photometric Function." Nature, Vol. 200, No. 4911, pp. 1056-1058.

________; 1971. "Limited-Interval Definitions of the Photometric Functions of Lunar Crater Walls by Photography from Orbiting Apollo." Icarus, Vol. 15, pp. 93-99.

________; 1972. "Regional Variations in the Magnitude of Heiligenschein and Causal Connections." NASA SP-289, pp. 25-86. Washington: NASA.

________; 1974. "Astronomical Supplement to the 1:5,000,000 Albedo Map of the Moon and the Establishment of a 1:2,500,000 Auxiliary Mosaic." Astron. J., Vol. 79, pp. 1471-1478.

________; 1976. "The Lunar Geometric Albedo and the Magnitude of the Full Moon." The Observatory, Vol. 96, pp. 235-239.

________; 1977. "A Digital File of the Lunar Normal Albedo." The Moon, Vol. 16, pp. 231-277. D. Reidel Publishing Company, Dordrecht.

________; 1978. "The Moon in Heiligenschein." Science, Vol. 200, pp. 1265-1267.

________; 1986. "Optical Reflection from Planetary Surfaces as an Operator-Eigenvalue Problem." Earth, Moon, and Planets, Vol. 36, pp. 103-116.

________; 1992. "On Blackbody Behavior and the Transformation from Instrumental to Standard Magnitudes and Color Indices." Pub. Astron. Soc. Pac., Vol. 104, pp. 290-300.

Wildey, R.L. & Pohn, H.A.; 1964. "Detailed Photoelectric Photometry of the Moon." Astron. J., Vol. 69, pp. 619-634.

________; 1969. "The Normal Albedo of the Apollo 11 Landing Site and Intrinsic Dispersion on the Lunar Heiligenschein." Astrophy. J., Vol. 158, L129-L130.

________; 1971. "The Normal Albedo of the Apollo 11 Landing Site and Intrinsic Dispersion on the Lunar Heiligenschein." NASA SP-232, pp. 35-36. Washington: NASA.

Wilkins, G.A. (Ed) & Springett, A.W. (Ed); 1961. Explanatory Supplement to the Astronomical Ephemeris and the American Ephemeris and Nautical Almanac. Prepared jointly by the Nautical Almanac Office of the United Kingdom and the United States of America.

Williams, J.D.; 1939. Astrophys. J., Vol. 89, p. 467.

Wilson, L.W.; 1971. "Photometric Studies." pp. 115-123, in Fielder, 1971.

Wisliscenus-Wirtz, C.; 1915. Astron. Nachr., pp. 201-289.

Wollard, E.W. & Clemence, G.M.; 1966. Spherical Astronomy. New York: Academic Press.

Wright, W. H.; 1929. "The Moon as Photographed by Light of Different Colors." Pub. Astr. Soc. Pac., Vol. 41, pp. 125-132.

Younkin, R.L.; 1970. "Optical Reflectance of Local Areas of the Moon." Astron. J., Vol. 75, pp. 831-841.

Zacharov, I.; 1952. Bull. Astr. Insts. Csl., Vol. 3, p. 82.

Zoellner, F.; 1865. Photometrische Untersuchungen (Leipzig: Engelmann).

Zerull, R.; 1976. "Scattering Measurements of Dielectric and Absorbing Nonspherical Particles." Contrib. Atmos. Phys., Vol. 49, pp 168-188.

Zerull, R. & Giese, R.; 1974. "Microwave Analogue Studies." in Planets, Stars, and Nebulae Studied with Photopolarimetry (T. Gehrels, Ed.), pp. 901-915. Univ. Of Arizona Press, Tucson.

Zerull, R., Gustafson, B., Schulz, K., & Thiele-Corbach; 1993. "Scattering by Aggregates with and without an Absorbing Mantle: Microwave Analog Experiments". Astron. Astrophy., Vol. 32, pp. 4088-4100

APPENDIX A – WORKED EXAMPLE

LUNAR PHOTOMETRY OBSERVATION FORM

DATE: 8/4/90 SEEING: 6 TRANSPARENCY: 5

COMPARISON 1: D27 COMPARISON 2: C88

ξ: +0.8169	η: +0.2349	ξ: +0.7209	η: +0.0973
Lo: +57°.18	La: +13°.58	Lo: +46°.42	La: +05°.58

SET	OBJECT	TIME (UT)	"V" READING	"B" READING	COMMENTS
1	SKY	01:58	187	53	
	C1	02:00	1981	599	
	C2	02:02	2542	782	
	CAPE AGARUM	02:04	2711	843	
	PROCLUS	02:06	4549	1409	
	PALUS SOMNII	02:08	2890	903	
	LYELL	02:12	2303	762	
	C1	02:14	2064	646	
	C2	02:15	2696	839	
	SKY	02:16	198	58	
2	C1	02:17	2143	554	
	C2	02:19	2626	819	
	CAPE AGARUM	02:20	2822	849	
	PROCLUS	02:22	4836	1486	
	PALUS SOMNII	02:24	2921	943	
	LYELL	02:25	2552	755	
	C1	02:27	2101	674	
	C2	02:29	2740	855	
	SKY	02:30	194	58	
3	C1	02:34	2181	681	
	C2	02:35	2732	875	
	CAPE AGARUM	02:36	2996	950	

	PROCLUS	02:38	4505	1610
	PALUS SOMNII	02:40	3049	961
	LYELL	02:42	2676	786
	C1	02:44	2228	710
	C2	02:46	2835	894
	SKY	02:47	212	61
4	C1	02:48	2214	709
	C2	02:50	2790	880
	CAPE AGARUM	02:52	3036	957
	PROCLUS	02:55	4932	1677
	PALUS SOMNII	02:56	3171	1015
	LYELL	02:59	2747	840
	C1	03:02	2269	704
	C2	03:04	2847	876
	SKY	03:06	173	58

APPENDIX A (CONT'D)

LUNAR PHOTOMETRY DATA REDUCTION FORM – FORM 1

DATE: 8/4/90 AVERAGE SKY (V): 196 AVERAGE SKY (B): 58

SET	OBJECT	TIME(UT)	(V-SKY)	(B-SKY)	V	B
1	C1	02:00	1789	543	1830	566
	C2	02:02	2350	726	2427	754
	CAPE AGARUM	02:04	2519	787	2519	787
	PROCLUS	02:06	4357	1353	4357	1353
	PALUS SOMNII	02:08	2698	847	2698	847
	LYELL	02:12	2111	706	2111	706
	C1	02:14	1872	590	------	-----
	C2	02:15	2504	783	------	------
2	C1	02:17	1947	796	1926	606
	C2	02:19	2430	761	2487	779
	CAPE AGARUM	02:20	2626	791	2626	791
	PROCLUS	02:22	4640	1428	4640	1428
	PALUS SOMNII	02:24	2725	865	2725	865
	LYELL	02:25	2356	697	2356	697
	C1	02:27	1905	616	------	-----
	C2	02:29	2544	621	-----------	
3	C1	02:33	1978	621	2002	636
	C2	02:35	2529	815	2580	824
	CAPE AGARUM	02:36	2793	890	2793	890
	PROCLUS	02:38	4302	1550	4302	1550
	PALUS SOMNII	02:40	2846	901	2846	901
	LYELL	02:42	2473	726	2473	726
	C1	02:44	2025	650	------	-----
	C2	02:46	2632	834	------	-----
4	C1	02:48	2022	649	2050	646
	C2	02:50	2598	820	2626	818
	CAPE AGARUM	02:52	2844	897	2844	897
	PROCLUS	02:55	4740	1617	4740	1617

PALUS SOMNII	02:56	2979	955	2979	955
LYELL	02:59	2555	780	2555	780
C1	03:02	2077	644	------	-----
C2	03:04	2655	816	------	-----

AVERAGE SKY READINGS

SET	V	B
1	192	56
2	196	58
3	203	60
4	192	60

APPENDIX A (CONT'D)

LUNAR PHOTOMETRY DATA REDUCTION FORM - FORM 2

DATE: 8/4/90 FILTER: V

SET	U.T.	OBJECT	R'	ALT.	SUN CLNG.	SUN B-SUN.	EARTH L-EAR.	EARTH B-EAR.	AMAS CORR	R"
1	02:00	C1	1830	21.85	64.12	-0.08	-3.21	3.85	2.6715	4889
	02:02	C2	2427	21.95	64.20	-0.08	-3.21	3.84	2.6606	6457
	02:04	CAPE AGARUM	2519	22.05	64.20	-0.08	-3.22	3.84	2.6483	6674
	02:06	PROCLUS	4357	22.14	64.20	-0.08	-3.23	3.84	2.6385	11496
	02:08	PALUS SOMNII	2698	22.24	64.24	-0.08	-3.23	3.85	2.62813	7091
	02:12	LYELL	2111	22.42	64.24	-0.08	-3.26	3.85	2.60807	5506
2	02:17	C1	1946	22.63	64.28	-0.08	-3.27	3.84	2.5857	5032
	02:19	C2	2487	22.70	64.32	-0.08	-3.28	3.84	2.5778	6411
	02:20	CAPE AGARUM	2626	22.74	64.32	-0.08	-3.28	3.84	2.57379	6759
	02:22	PROCLUS	4640	22.81	64.32	-0.08	-3.29	3.84	2.5657	11905
	02:24	PALUS SOMNII	2725	22.89	64.36	-0.08	-3.30	3.83	2.55824	6971
	02:25	LYELL	2356	22.92	64.36	-0.08	-3.31	3.83	2.55472	6019
3	02:33	C1	2002	23.16	64.45	-0.08	-3.33	3.83	2.5295	5064
	02:35	C2	2580	23.22	64.49	-0.08	-3.34	3.82	2.5238	6511
	02:36	CAPE AGARUM	2793	23.25	64.49	-0.08	-3.34	3.82	2.52119	7042
	02:38	PROCLUS	4302	23.30	64.49	-0.08	-3.35	3.82	2.5159	10823
	02:40	PALUS SOMNII	2846	23.34	64.49	-0.08	-3.36	3.82	2.51323	7147
	02:42	LYELL	2473	23.39	64.53	-0.08	-3.36	3.82	2.50700	6200
4	02:48	C1	2050	23.50	64.57	-0.08	-3.39	3.81	2.4954	5116
	02:50	C2	2626	23.53	64.57	-0.08	-3.40	3.81	2.4925	6545
	02:52	CAPE AGARUM	2844	23.56	64.65	-0.08	-3.41	3.81	2.48938	7080
	02:55	PROCLUS	740	23.60	64.65	-0.08	-3.42	3.80	2.4856	11782
	02:56	PALUS SOMNII	2979	23.61	64.65	-0.08	-3.42	3.80	2.48469	7402
	02:59	LYELL	2555	23.64	64.65	-0.08	-3.44	3.80	2.48193	6341

OBJECT	MEAN CLNG.	MEAN B-SUN	MEAN L-EAR	MEAN B-EAR	SUN ALT.	EARTH ALT.	P.A. G	BRGT FUNC	PHOT FUNC
C1	64.36	-0.08	-3.33	3.83	55.91	29.55	-29.21	-58.82	0.576390
C2	64.40	-0.08	-3.31	3.83	68.46	40.42	-29.15	-49.04	0.565440
CAPE AGARUM	64.42	-0.08	-3.31	3.83	48.80	21.98	-29.13	-66.81	0.584681
PROCLUS	64.42	-0.08	-3.32	3.82	63.46	39.19	-29.14	-48.09	0.564174
PALUS SOMNII	64.44	-0.08	-3.33	3.82	66.63	42.36	-29.13	-45.11	0.559629
LYELL	64.44	-0.08	-3.34	3.82	69.77	45.56	-29.14	-42.15	0.554187

Observer's Longitude: +74°.4125 Latitude: +40°.53425

APPENDIX A (CONT'D)

LUNAR PHOTOMETRY DATA REDUCTION FORM – FORM 3

DATE: 8/4/90 FILTER: V

A(0) = 0.0640 L(0)*A(0) = 0.036889

L = L(0)*A(0)*R"/R"(0) A = L/PHOT FUNC

R"(0) = D27

SET	R"(0)	OBJECT	R"	L	A	OBJECT	R"	L	A
1	4889	CAPE AGARUM	6674	0.05036	0.086128	PROCLUS	11496	0.08674	0.153748
	5032		6759	0.04955	0.084746		11905	0.08727	0.154686
	5064		7042	0.05130	0.087736		10823	0.07884	0.139745
	5116		7080	0.05105	0.087313		11782	0.08495	0.150582

Mean g = -29.13 N = 4 Mean g = -29.14 N = 4

Mean A = 0.086481 Mean A = 0.149690

SET	R"(0)	OBJECT	R"	L	A	OBJECT	R"	L	A
1	4889	PALUS SOMNII	7091	0.05350	0.095606	LYELL	5506	0.04154	0.074965
	5032		6971	0.05110	0.091317		6019	0.04412	0.079620
	5064		7147	0.05206	0.093031		6200	0.04516	0.081496
	5116		7402	0.05337	0.095371		6341	0.04572	0.082503

Mean g = -29.13 N = 4 Mean g = -29.14 N = 4

Mean A = 0.093831 Mean A = 0.079646

APPENDIX A (CONT'D)

LUNAR PHOTOMETRY DATA REDUCTION FORM – FORM 4

A(0) = 0.0874 L(0)*A(0) = 0.049419

L = L(0)*A(0)*R"/R"(0) A = L/PHOT FUNC

R"(0) = C88

SET	R"(0)	OBJECT	R"	L	A	OBJECT	R"	L	A
2	6457	CAPE AGARUM	6674	0.05108	0.087364	PROCLUS	11496	0.08799	0.155956
	6411		6759	0.05210	0.089111		11905	0.09177	0.162663
	6511		7042	0.05345	0.091416		10823	0.08215	0.145608
	6545		7080	0.05346	0.091432		11782	0.08896	0.157686

Mean g = –29.13 N = 4 Mean g = –29.14 N = 4

Mean A = 0.089831 Mean A = 0.155478

SET	R"(0)	OBJECT	R"	L	A	OBJECT	R"	L	A
2	6457	PALUS SOMNII	7091	0.05427	0.096977	LYELL	5506	0.04214	0.076040
	6411		6971	0.05374	0.096020		6019	0.04640	0.083721
	6511		7147	0.05425	0.096933		6200	0.04706	0.084914
	6545		7402	0.05589	0.099870		6341	0.04788	0.086394

Mean g = –29.13 N = 4 Mean g = –29.14 N = 4

Mean A = 0.097450 Mean A = 0.082767

APPENDIX B –VBR STANDARD STARS

NORTHERN VBR STANDARD STARS (Epoch 1950.0)

NAME	Hr	RA h m s	DEC ° ' "	m_V	B–V	V–R	U–V	U–B	U2000
Gamma Peg.	0039	00 10 39.4	+14 54 20.6	2.83	–0.23	–0.08	+1.08	–0.87	170
Eta Psc.	0437	01 28 48.2	+15 05 19.4	3.62	+0.97	+0.71	+1.69	+0.76	173
107 Psc.	0493	01 39 46.6	+20 01 34.3	5.23	+0.83	+0.68	+1.29	+0.50	128
Beta Ari.	0553	01 51 52.3	+20 33 52.0	2.65	+0.13	+0.12	+0.23	+0.10	129
Alpha Ari.	0617	02 04 20.9	+23 13 37.0	2.00	+1.15	+0.84	+2.27	+1.12	129
Chi 2 Cet.	0718	02 25 29.8	+08 14 13.1	4.28	–0.06	0.04	–0.19	–0.13	175
Kappa Cet.	0996	03 16 44.1	+03 11 17.3	4.82	+0.68	+0.56	+0.89	+0.18	221
Omicron Tau.	1030	03 22 07.1	+08 51 15.2	3.59	+0.89	+0.67	+1.51	+0.62	176
Gamma Tau.	1346	04 16 56.7	+15 30 30.6	3.65	+0.99	+0.73	+1.77	+0.82	178
Delta Tau.	1373	04 20 02.8	+17 25 36.8	3.76	+0.98	+0.73	+1.82	+0.82	178
Epsilon Tau.	1409	04 25 41.6	+19 04 16.4	3.54	+1.02	+0.73	+1.88	+0.88	133
Pi 3 Ori.	1543	04 47 07.4	+06 47 07.4	3.19	+0.45	+0.42	+0.45	–0.01	179
Pi 4 Ori.	1552	04 48 32.4	+05 31 16.3	3.69	–0.17	–0.02	–0.96	–0.80	179
Gamma Ori.	1790	05 02 26.8	+06 18 21.6	1.64	–0.23	–0.09	–1.09	–0.87	180
Beta Tau.	1791	05 03 07.7	+28 34 01.7	1.65	–0.13	–0.01	–0.62	–0.49	135
134 Tau.	2010	05 06 44.3	+12 38 13.6	4.90	–0.07	–0.03	–0.21	–0.18	181
Gamma Gem.	2421	06 04 49.4	+16 26 37.3	1.93	0.00	+0.07	+0.07	+0.03	182
Lambda Gem.	2763	07 05 13.2	+16 37 56.1	3.58	+0.11	+0.12	+0.21	+0.10	184
Rho Gem.	2852	07 05 53.8	+31 53 08.3	4.16	+0.32	+0.34	+0.29	–0.03	100
Kappa Gem.	2985	07 01 25.9	+24 31 10.5	3.57	+0.93	+0.71	+1.62	+0.68	140
Beta Cnc.	3249	08 03 48.3	+09 20 27.7	3.52	+1.48	+1.13	+3.26	+1.78	186
Eta Hya.	3454	08 00 36.7	+03 34 45.7	4.30	–0.19	–0.06	–0.94	–0.74	231
Theta Hya.	3665	09 01 45.8	+02 31 34.6	3.88	–0.06	–0.01	–0.19	–0.13	232
Alpha Leo.	3982	10 05 42.6	+12 12 44.5	1.36	–0.11	0.00	–0.47	–0.36	189
Rho Leo.	4133	10 30 10.8	+09 33 52.2	3.85	–0.14	–0.04	–1.09	–0.95	190
90 AB Leo.	4456	11 32 06.4	+17 04 24.6	5.95	–0.16	–0.07	–0.80	–0.64	147
Beta Leo.	4534	11 46 30.6	+14 51 05.8	2.14	+0.09	+0.06	+0.16	+0.07	192
Beta Vir.	4540	11 48 05.4	+02 02 47.6	3.61	+0.55	+0.46	+0.67	+0.10	237
70 Vir.	5072	13 25 59.0	+14 02 42.8	4.98	+0.71	+0.61	+0.99	+0.26	195
109 Vir.	5511	14 43 43.1	+02 06 09.0	3.74	0.00	+0.07	–0.04	–0.03	243
Alpha Ser.	5854	15 41 48.2	+06 34 53.9	2.65	+1.17	+0.81	+2.41	+1.24	199
Beta Ser.	5867	15 43 52.7	+15 34 37.4	3.67	+0.06	+0.06	+0.15	+0.07	199
Lambda Ser.	5868	15 44 00.8	+07 30 30.7	4.43	+0.60	+0.51	+0.70	+0.10	199
Gamma Ser.	5933	15 54 08.5	+15 49 24.8	3.85	+0.48	+0.47	+0.44	–0.03	200
Alpha Oph.	6556	17 32 36.7	+12 35 41.9	2.08	+0.15	+0.14	+0.25	+0.10	203
Beta Oph.	6603	17 41 00.0	+04 35 11.8	2.77	+1.16	+0.81	+2.40	+1.24	248
Gamma Oph.	6629	17 45 23.0	+02 43 28.3	3.75	+0.04	+0.05	+0.08	+0.04	248
Zeta Aql.	7235	19 03 06.6	+13 47 15.9	2.99	0.00	+0.04	+0.03	–0.01	206
Alpha Aql.	7557	19 48 20.6	+08 44 05.8	0.77	+0.22	+0.14	+0.31	+0.08	207

NORTHERN VBR STANDARD STARS (Epoch 1950.0, Continued)

NAME	RA Hr	h m s	DEC ° ' "	m_V	B-V	V-R	U-V	U-B	U2000
Beta Aql.	7602	19 52 51.4	+06 16 49.8	3.71	+0.86	+0.66	+1.34	+0.48	207
Alpha Del.	7905	20 37 18.9	+15 58 04.3	3.77	-0.06	+0.03	-0.25	-0.22	209
Alpha Peg.	8781	23 02 16.1	+14 56 09.2	2.49	-0.05	+0.01	-0.06	-0.06	213
Iota Psc.	8969	23 37 22.6	+05 21 18.6	4.13	+0.51	+0.43	+0.53	0.00	259
Tau Cet.	0509	01 41 44.7	-16 12 00.5	3.50	+0.72	+0.62	+0.95	+0.20	263
Epsilon Eri	1084	03 30 34.4	-09 37 34.8	3.73	+0.89	+0.73	+1.46	+0.57	267
Beta Eri.	1666	05 05 23.4	-05 08 58.5	2.80	+0.13	+0.15	+0.25	+0.10	225

SOUTHERN VBR STANDARD STARS (Epoch 1950.0)

NAME	RA Hr	h m s	DEC ° ' "	m_V	B-V	V-R	U-V	U-B	U2000
Upsilon Ori.	1855	05 29 30.6	-07 20 12.9	4.63	-0.26	-0.06	-1.33	-1.07	270
Epsilon Ori.	1903	05 33 40.5	-01 13 56.1	1.70	-0.19	-0.01	-1.21	-1.04	225
Zeta Lep.	1998	05 44 41.3	-14 50 21.2	3.55	+0.10	+0.13	+0.16	+0.06	271
Gamma Crv.	4662	12 13 13.8	-17 15 52.0	2.60	-0.11	-0.02	-0.45	-0.35	283
61 Vir.	5019	13 15 47.1	-18 01 01.3	4.75	+0.71	+0.58	+0.98	+0.25	330
Alpha Vir.	5056	13 22 33.3	-10 03 03.4	0.96	-0.23	-0.09	-1.18	-0.94	285
Alpha 2 Lib.	5531	14 48 06.4	-15 06 06.6	2.75	+0.15	+0.17	+0.26	+0.08	288
Beta Lib.	5685	15 14 18.7	-09 58 58.9	2.61	-0.11	-0.04	-0.48	-0.37	289
Zeta Oph.	6175	16 34 24.1	-10 02 02.8	2.56	+0.02	+0.10	-0.82	-0.86	291
Kappa Aql.	7446	19 34 12.1	-07 24 24.7	4.96	-0.01	-0.10	-0.87	-0.87	297
Epsilon Aqr.	7950	20 44 58.2	-09 48 48.2	3.77	+0.01	+0.07	+0.01	+0.04	299

(From: Henden & Kaitchuck, 1982)

NOTE:U2000 column is the page in Uronometria 2000 where the star chart is found.

APPENDIX C – FIRST-ORDER EXTINCTION STARS

Northern First-Order Extinction Stars (Epoch 1950.0)

NAME	Hr	RA h m s	DEC ° ' "	m_V	B-V	V-R	U-V	U-B	U2000
Upsilon Psc.	0383	01 16 42.7	+27 00 06.6	4.76	+0.03	+0.08	+0.13	+0.10	128
Chi 2 Cet.	0718	02 25 29.8	+08 14 13.1	4.28	-0.06	+0.04	-0.19	-0.13	175
Zeta Ari.	0972	03 12 01.3	+20 51 37.9	4.89	-0.02	+0.08	-0.03	-0.01	131
Kappa Tau.	1387	04 22 23.1	+22 10 51.9	4.23	+0.12	+0.16	+0.27	+0.15	133
68 Tau.	1389	04 22 35.6	+17 48 55.2	4.29	+0.04	+0.09	+0.12	+1.08	133
Pi 2 Ori.	1544	04 47 53.0	+08 48 57.6	4.35	+0.01	+0.06	+0.04	+0.03	179
Pi 1 Ori.	1570	04 52 08.4	+10 04 22.5	4.66	+0.08	+0.11	+0.16	+0.08	179
136 Tau.	2034	05 50 11.0	+27 36 08.5	4.61	-0.02	+0.04	-0.01	+0.01	136
Phi Gem.	3067	07 50 26.4	+26 53 48.7	4.99	+0.09	+0.13	+0.21	+0.12	140
Delta Hya.	3410	08 35 00.6	+05 52 45.6	4.17	0.00	+0.04	+0.02	+0.02	186
Gamma Cnc.	3449	08 40 23.7	+21 38 58.8	4.66	+0.02	+0.07	+0.03	+0.01	231
Rho Hya.	3492	08 45 47.1	+06 01 25.1	4.37	-0.05	+0.05	-0.10	-0.05	186
60 Leo.	4300	10 59 39.8	+20 26 54.2	4.41	+0.04	+0.08	+0.08	+0.04	146
Sigma Leo.	4386	11 18 33.5	+06 18 13.1	4.06	-0.07	+0.01	-0.19	-0.12	191
Pi Vir.	4589	11 58 18.6	+06 53 35.1	4.67	+0.13	+0.16	+0.23	+0.10	192
23 Com.	4789	12 32 21.6	+22 54 15.4	4.81	0.00	+0.07	-0.01	-0.01	148
Rho Vir.	4828	12 39 21.2	+10 30 39.2	4.88	+0.09	+0.08	+0.12	+0.06	194
Tau Vir.	5264	13 59 05.9	+01 47 08.5	4.27	+0.09	+0.14	+0.23	+0.14	241
Pi Ser.	5972	16 00 08.4	+22 56 31.0	4.83	+0.07	+0.10	+0.12	+0.05	155
68 Oph.	6723	17 59 12.9	+01 18 17.3	4.42	+0.04	+0.06	+0.06	+0.02	249
Zeta Sge.	7546	19 46 45.4	+19 00 55.5	5.00	+0.10	+0.14	+0.16	+1.06	162
13 Vul.	7592	19 51 20.1	+23 56 52.8	4.58	-0.06	+0.02	-0.19	-0.13	162
Rho Aql.	7724	20 11 57.7	+15 02 38.4	4.95	+0.09	+0.10	+0.10	+0.01	208
Zeta Del.	7871	20 32 58.2	+14 30 02.2	4.69	+0.11	+0.15	+0.22	+0.11	208
29 Vul.	7891	20 36 17.2	+21 01 28.7	4.82	-0.02	+0.02	-0.09	-0.07	164
Omicron Peg.	8641	22 39 24.3	+29 02 46.1	4.79	-0.01	+0.05	-0.01	0.00	123
Rho Peg.	8717	22 52 42.5	+08 32 55.9	4.91	0.00	+0.05	-0.01	-0.01	213

APPENDIX C (CONT'D)

Southern First-Order Extinction Stars (Epoch 1950.0)

NAME	Hr	RA h m s	DEC ° ' "	m_V	B-V	V-R	U-V	U-B	U2000
Rho Cet.	0708	02 23 32.0	-12 50 54.3	4.89	-0.02	-0.01	-0.06	-0.04	265
49 Ori.	1937	05 36 27.8	-07 14 21.4	4.81	+0.14	+0.15	+1.23	+0.09	270
Theta Lep.	2155	06 03 53.5	-14 55 45.5	4.67	+0.05	+0.10	+0.05	0.00	271
Chi 2 CMa.	2414	06 32 57.6	-22 55 26.1	4.54	-0.04	+0.05	-1.06	-0.02	317
Delta Mon.	2714	07 09 18.6	-00 24 30.4	4.15	0.00	+0.08	+1.03	+0.03	228
Tau 2 Hya.	3787	09 29 26.0	-00 57 48.0	4.56	+0.11	+0.14	+0.20	+0.09	233
Alpha Sex.	3981	10 05 22.7	-00 07 35.5	4.49	-0.04	+0.07	-0.11	-0.07	234
Psi Sco.	6031	16 09 15.8	-09 56 10.2	4.92	+0.09	+0.09	+0.19	+0.10	290
Nu Ser.	6446	17 18 00.7	-12 47 52.1	4.31	+0.03	+0.07	+1.06	+0.03	292
Omicron Ser.	6581	17 38 36.1	-12 51 01.0	4.24	+0.08	+0.09	+0.18	+0.10	293
Gamma Sct.	6930	18 26 20.8	-14 35 58.0	4.71	+0.07	+0.08	+0.11	+0.04	295
14 Aql.	7029	19 00 16.5	-03 46 40.0	5.42	0.00	-0.14	-----	-0.07	251
Nu Cap.	7773	20 17 53.5	-12 55 04.5	4.76	-0.04	0.00	-0.15	-0.11	298
Theta Cap.	8075	21 03 08.3	-17 25 57.8	4.07	-0.01	+0.01	0.00	+0.01	300
Sigma Aqr.	8573	22 28 00.1	-10 56 04.1	4.82	-0.06	-0.06	-0.18	-0.12	302

(From: Henden & Kaitchuck, 1982)

NOTE: U2000 column is the page in Uranometria 2000 where the star chart is found.

APPENDIX D – SUGGESTED LUNAR SITES AND THEIR COMPARISON SITES

(Arthur & Agnieray, 1964; Arthur, et al. 1963, 1964, 1965, 1966)

The following is a list of suggested lunar sites to be measured photoelectrically, with suggested comparison sites, two sets for the waxing moon, and two sets for the waning moon. The list is by no means exhaustive. The sites were selected based on the following criteria:

1. The sites are close together.
2. The sites are visible, or easily located, at Full Moon.
3. The sites are not strongly affected by libration, except for selected sites.
4. The sites are relatively easy to find.
5. The sites are interesting sites (LTP sites, domes, etc.).

The Xi and Eta coordinates for each site are given as well as the selenographic longitude and latitude. The comparison sites not in parenthesis are for the waxing moon, while those in parenthesis are for the waning moon.

QUADRANT I

SET	FEATURE	XI	ETA	LONG	LAT	COMPARSON
		COORDINATES				
1	Proclus	+0.702	+0.278	+46.9	+16.1	D27, C88
	Palus Somnii	+0.670	+0.255	+46.9	+13.0	(P10, P1)
	Lyell	+0.633	+0.230	+40.6	+13.6	
	Cape Agarum	+0.885	+0.230	+65.4	+13.3	
2	Auzout	+0.885	+0.178	+69.7	+12.1	D27, C88
	Condorcet	+0.917	+0.211	+69.7	+12.1	(D27, C88)
	Hansen	+0.926	+0.242	+72.6	+14.0	
	Alhazen	+0.914	+0.274	+71.8	+15.9	
3	Firmicius	+0.887	+0.127	+63.4	+ 7.2	D27, C88
	Apollonius	+0.872	+0.078	+61.0	+ 4.4	(C88, D23)
	Dubiago	+0.937	+0.078	+70.0	+ 4.2	
	Apollonius > Dubiago	+0.900	+0.075	+64.5	+ 4.3	
4	Eimmart	+0.826	+0.406	+64.6	+23.9	D27, C88
	Cleomedes	+0.730	+0.465	+55.5	+27.7	(D20, M23)
	Newcomb A	+0.800	+0.490	+43.6	+29.3	
	Eimmart > Cleomedes	+0.800	+0.430	+62.4	+25.5	
5	Macrobius	+0.671	+0.363	+46.0	+21.2	D27, C88
	Macrobius L	+0.624	+0.366	+42.1	+21.4	(D20, M23)
	Macrobius B	+0.611	+0.357	+40.8	+20.9	
	Macrob. > Macrobius L	+0.650	+0.370	+44.3	+21.7	
6	Atlas	+0.481	+0.727	+44.4	+46.6	D27, C88
	Hercules	+0.434	+0.728	+39.2	+46.7	(A15, T104)
	Endymion	+0.495	+0.805	+56.5	+53.6	
	Atlas D	+0.486	+0.770	+49.6	+50.3	
7	Bürg	+0.334	+0.708	+28.2	+45.0	M22, M23
	Plana	+0.350	+0.672	+28.2	+42.2	(A15, T104)
	Bürg A	+0.373	+0.729	+33.0	+46.8	
	Rima Bürg	+0.300	+0.700	+24.8	+44.4	
8	Posidonius	+0.424	+0.528	+29.9	+31.8	M22, M23
	Daniell	+0.422	+0.579	+31.1	+35.3	(D17, T104)
	Grove	+0.415	+0.647	+32.9	+40.3	
	Grove Y	+0.417	+0.608	+31.6	+37.4	
9	Cepheus	+0.543	+0.653	+45.8	+40.7	M22, M23
	Franklin	+0.576	+0.627	+47.6	+38.8	(A15, T104)
	Maury	+0.510	+0.603	+39.7	+37.0	
	Franklin	+0.546	+0.613	+43.7	+37.8	

QUADRANT I (Cont'd)

SET	FEATURE	COORDINATES XI	ETA	LONG	LAT	COMPARSON
10	Chacornac	+0.456	+0.498	+31.7	+29.8	M23, D19
	Le Monnier	+0.455	+0.447	+30.5	+26.5	(D17, T104)
	Römer	+0.537	+0.429	+36.4	+25.4	
	Chacornac > Le Monnier	+0.458	+0.470	+31.2	+28.0	
11	Littrow	+0.485	+0.367	+31.4	+21.5	M23, D20
	Vitruvius	+0.495	+0.303	+31.2	+17.6	(T87, T104)
	Dawes	+0.424	+0.296	+26.3	+17.2	
	Plinius	+0.387	+0.265	+23.6	+15.3	
12	Cauchy	+0.616	+0.167	+38.6	+ 9.6	D21, C88
	Cauchy M	+0.570	+0.133	+35.1	+ 7.6	(P23, P2)
	Maskelyne	+0.500	+0.038	+30.0	+ 4.9	
	Maskelyne H	+0.532	+0.086	+32.2	+ 4.9	
13	Dionysius	+0.297	+0.049	+17.2	+ 2.8	P28, P25
	Sabine	+0.343	+0.024	+20.0	+ 1.3	(M15,T7)
	Ritter	+0.329	+0.035	+19.2	+ 2.0	
	Ariadaeus	+0.296	+0.080	+17.2	+ 4.5	
14	Sosigenes	+0.299	+0.151	+17.6	+ 8.6	S1, T76
	Maclear	+0.338	+0.183	+20.1	+10.5	(M15, T7)
	Ross	+0.363	+0.202	+21.7	+11.6	
	Tacquet A	+0.336	+0.248	+20.2	+14.3	
15	Cassini	+0.061	+0.646	+ 4.5	+40.2	A15, T104
	Theaetetus	+0.084	+0.602	+ 6.0	+37.0	(M10, T71)
	Aristillus	+0.018	+0.557	+ 1.2	+33.8	
	Theaet. > Aristillus	+0.060	+0.650	+ 4.5	+40.5	
16	Aristoteles	+0.191	+0.768	+17.3	+50.1	D19, M22
	Eudoxus	+0.201	+0.698	+16.3	+44.2	(D14, M15)
	Alexander	+0.178	+0.646	+13.4	+40.2	
	Calippus	+0.145	+0.629	+10.7	+38.9	
17	Archimedes	+0.060	+0.496	+ 4.0	+29.7	M16, T92
	Autolychus	+0.022	+0.510	+ 1.4	+30.6	(D13, D14)
	Linné	+0.181	+0.465	+11.7	+27.7	
	Linné > Autolychus	+0.100	+0.475	+ 6.5	+28.4	
18	Menelaus	+0.264	+0.280	+15.9	+16.2	D17, T92
	Manilius	+0.153	+0.250	+ 9.0	+14.4	(M15, T77)
	Menelaus > Manilius	+0.225	+0.270	+13.5	+15.7	
	Menelaus > Manilius	+0.180	+0.255	+10.7	+14.8	

QUADRANT I (Cont'd)

SET	FEATURE	COORDINATES XI	ETA	LONG	LAT	COMPARSON
19	Triesnecker	+0.063	+0.073	+ 3.6	+ 4.1	P23, P28
	Agrippa	+0.182	+0.072	+10.5	+ 4.1	(P29, S8)
	Godin	+0.177	+0.032	+10.2	+ 1.8	
	Triesnecker > Agrippa	+0.125	+0.090	+ 7.2	+ 5.2	
20	Ukert	+0.024	+0.134	+ 1.3	+ 7.7	T77, M15
	Bode	+0.042	+0.117	– 2.4	+ 6.7	(M4, P38)
	Murchison	+0.002	+0.089	– 0.1	+ 5.1	
	Ukert > Bode	+0.010	+0.125	+ 0.6	+ 7.2	

QUADRANT II

SET	FEATURE	XI	ETA	LONG	LAT	COMPARSON
		COORDINATES				
1	Plato	-0.100	+0.782	- 9.2	+51.4	A15, T104
	Mare Frigoris	-0.150	+0.820	-15.1	+55.1	(M10, T71)
	Teneriffe Mountains	-0.150	+0.760	-13.4	+49.5	
	Teneriffe Mountains	-0.110	+0.740	- 9.4	+47.7	
2	Piton	-0.010	+0.655	- 0.8	+40.9	A15, T104
	Piazzi Smyth	-0.042	+0.667	- 3.2	+41.8	(M10, T71)
	Pico	-0.110	+0.715	- 9.0	+45.6	
	Plato > Pico	-0.110	+0.750	- 9.6	+48.6	
3	Le Verrier	-0.268	+0.647	-20.6	+40.3	M10, T71
	Helicon	-0.298	+0.648	-23.0	+40.4	(T27, M8)
	Pr. Laplace	-0.300	+0.725	-25.8	+46.5	
	Pr. Laplace > Helicon	-0.300	+0.680	-24.1	+42.8	
4	Pico β	-0.075	+0.685	- 5.9	+43.2	A15, T10
	Pico E	-0.131	+0.681	-10.3	+42.9	(D8, R12)
	Le Verrier D	-0.164	+0.639	-12.3	+39.7	
	Pico E > Le Verrier D	-0.148	+0.650	-11.2	+40.5	
5	Timocharis	-0.202	+0.449	-13.1	+26.7	D13, D14
	Beer	-0.140	+0.455	- 9.0	+27.1	(M8, T27)
	Feuillée	-0.146	+0.459	- 9.5	+27.3	
	Beer > Timocharis	-0.160	+0.450	-10.5	+16.0	
6	Wallace	-0.142	+0.346	- 8.7	+20.2	M13, D14
	Eratosthenes F	-0.163	+0.304	- 9.9	+17.7	(P19, R1)
	Erat. F > Eratosthenes	-0.175	+0.275	-10.5	+26.7	
	Eratosthenes	-0.190	+0.250	-11.3	+14.5	
7	Mösting	-0.101	+0.012	- 5.9	+ 0.7	P49, P5
	Schröter	-0.120	+0.045	- 6.9	+ 2.6	(P20, P30)
	Turner	-0.228	+0.024	-13.2	+ 1.4	
	Gambart B	-0.200	+0.038	-11.5	+ 2.2	
8	Bianchini	-0.372	+0.752	-34.4	+48.8	M8, T27
	Bianchini > Foucault	-0.390	+0.760	-36.9	+49.5	(D8, R12)
	Foucault	-0.408	+0.770	-39.8	+50.4	
	Harpalus	-0.417	+0.795	-43.3	+52.7	
9	Mairan	-0.514	+0.664	-43.4	+41.6	M8, T27
	Mairan > Sharp D	-0.490	+0.680	-41.0	+42.8	(D8, R12)
	Sharp D	-0.476	+0.704	-42.1	+44.7	
	Sharp	-0.451	+0.716	-40.2	+45.7	

QUADRANT II (Cont'd)

SET	FEATURE	COORDINATES XI	ETA	LONG	LAT	COMPARSON
10	Heraclides A	-0.425	+0.654	-34.2	+40.8	M8, T27
	Hera. A > Laplace D	-0.385	+0.680	-31.6	+42.8	(D8, R12)
	Hera. A > Laplace D	-0.345	+0.700	-28.9	+44.4	
	Laplace D	-0.293	+0.734	-25.6	+47.2	
11	Carlini	-0.339	+0.555	-24.0	+33.7	M8, T27
	Carlini > C. Herschel	-0.370	+0.560	-26.5	+34.1	(D8, R12)
	Carlini > C. Herschel	-0.400	+0.565	-29.0	+34.4	
	C. Herschel	-0.427	+0.566	-31.2	+34.5	
12	Pytheas	-0.329	+0.351	-20.6	+20.5	D13, M13
	Pytheas W	-0.373	+0.370	-23.7	+21.7	(R12, R13)
	Pytheas W > Euler	-0.410	+0.385	-26.4	+22.6	
	Euler	-0.447	+0.395	-29.1	+23.3	
13	Diophantus	-0.499	+0.463	-34.3	+27.6	D13, M13
	Diophantus D	-0.528	+0.452	-36.3	+26.9	(D7, S11)
	Diophantus D > Prinz	-0.570	+0.445	-39.5	+26.4	
	Prinz	-0.628	+0.430	-44.1	+25.5	
14	Copernicus	-0.337	+0.168	-20.0	+ 9.7	P30, P41
	Tobias Mayer H	-0.420	+0.202	-25.4	+11.7	(R12, P41)
	Tobias Mayer	-0.469	+0.268	-29.1	+15.5	
	Milichius	-0.495	+0.174	-30.2	+10.0	
15	Lansberg	-0.448	+0.006	-26.6	+ 0.3	P30, P41
	Lansberg > Reinhold	-0.410	+0.030	-24.2	+ 1.7	(P9, P33)
	Reinhold	-0.387	+0.057	-22.8	+ 3.3	
	Reinhold A	-0.369	+0.072	-21.7	+ 4.1	
16	Briggs	-0.835	+0.445	-68.8	+26.4	D8, R13
	Briggs > Lichtenberg	-0.800	+0.500	-67.5	+30.0	(---)
	Lichtenberg	-0.785	+0.527	-67.5	+31.8	
	Naumann	-0.719	+0.578	-61.8	+35.3	
17	Eddington	-0.883	+0.367	-71.7	+21.5	R12, R13
	Eddington	-0.875	+0.390	-71.9	+23.0	(---)
	Briggs	-0.835	+0.445	-68.8	+26.4	
	Russell	-0.864	+0.449	-75.2	+26.7	
18	Aristarchus	-0.676	+0.402	-47.6	+23.7	R12, R13
	Herodotus	-0.701	+0.394	-49.7	+23.2	(D7, S11)
	Schröter Valley	-0.690	+0.415	-49.3	+24.5	
	Schröter Valley	-0.720	+0.425	-52.7	+25.2	

QUADRANT II (Cont'd)

SET	FEATURE	XI	ETA	LONG	LAT	COMPARSON
		COORDINATES				
19	Hevelius	−0.923	+0.017	−67.4	+ 1.0	P9, D7
	Hevelius	−0.923	+0.038	−67.5	+ 2.2	(−−−)
	Hevelius	−0.923	+0.060	−67.6	+ 3.4	
	Cavalerius	−0.916	+0.089	−66.9	+ 5.1	
20	Reiner	−0.812	+0.120	−54.9	+ 6.9	R13, P9
	Reiner H	−0.805	+0.158	−54.6	+ 9.1	(D8, S11)
	Reiner H > Marius	−0.782	+0.190	−52.8	+11.0	
	Marius	−0.758	+0.206	−50.8	+11.9	

QUADRANT III

SET	FEATURE	XI	ETA	LONG	LAT	COMPARSON
		COORDINATES				
1	Alphonsus	-0.046	-0.233	- 2.7	-13.5	M14, P29
	Alphonsus > Davy	-0.080	-0.225	- 4.7	-13.0	(R6, T107)
	Alphonsus > Davy	-0.110	-0.215	- 6.5	-12.4	
	Davy	-0.138	-0.205	- 8.1	-11.8	
2	Ptolemaeus	-0.031	-0.161	- 1.8	- 9.3	M14, P29
	Ptolemaeus	-0.036	-0.125	- 2.1	- 7.2	(R6, T107)
	Ptolemaeus	-0.036	-0.148	- 2.1	- 8.5	
	Herschel	-0.036	-0.099	- 2.1	- 5.7	
3	Mösting	-0.101	-0.012	- 5.9	- 0.7	P49, S8
	Mösting B	-0.128	-0.047	- 7.4	- 2.7	(P18, P30)
	Lalande	-0.149	-0.078	- 8.6	- 4.5	
	Lalande A	-0.169	-0.115	- 9.8	- 6.6	
4	Guericke	-0.239	-0.200	-14.1	-11.5	P49, P18
	Parry	-0.269	-0.136	-15.8	- 7.8	(C64, M9)
	Bonpland	-0.295	-0.145	-17.3	- 8.3	
	Fra Mauro	-0.290	-0.104	-17.0	- 6.9	
5	Arzachel	-0.031	-0.313	- 1.9	-18.2	M14, P29
	Alpetragius	-0.075	-0.276	- 4.5	-16.0	(R6, T107)
	Alpetragius > Lassell	-0.105	-0.370	- 6.5	-21.7	
	Lassell	-0.132	-0.266	- 7.9	-15.4	
6	Birt	-0.137	-0.380	- 8.5	-22.3	P49, A10
	Birt B	-0.164	-0.378	-10.2	-22.2	(C64, R6)
	Thebit D	-0.134	-0.338	- 8.2	-19.8	
	Nicollet	-0.200	-0.373	-12.4	-21.9	
7	Pitatus	-0.190	-0.500	-13.5	-29.8	A10, T107
	Pitatus	-0.215	-0.495	-14.3	-29.7	(C64, R6)
	Pitatus G	-0.171	-0.497	-11.4	-29.8	
	Hesiodus	-0.245	-0.491	-16.3	-29.4	
8	Lansberg	-0.448	-0.006	-26.6	- 0.3	M9, S6
	Lansberg C	-0.487	-0.026	-29.2	- 1.5	(P9, P33)
	Lansberg C > Euclides	-0.487	-0.078	-29.2	- 4.5	
	Euclides	-0.488	-0.128	-29.5	- 7.4	
9	Darney C	-0.425	-0.244	-26.0	-14.4	A10, T107
	Darney	-0.386	-0.252	-23.5	-14.6	(P9, P33)
	Darney J	-0.354	-0.248	-21.4	-14.4	
	Darney J > Guericke	-0.295	-0.215	-17.6	-12.4	

QUADRANT III (Cont'd)

SET	FEATURE	COORDINATES				COMPARSON
		XI	ETA	LONG	LAT	
10	Herigonius	−0.543	−0.231	−33.9	−13.4	M9, S6
	Herigonius K	−0.578	−0.222	−36.4	−12.8	(D7, M3)
	Letronne A	−0.616	−0.210	−39.1	−12.1	
	Letronne	−0.662	−0.184	−42.3	−10.6	
11	Gassendi	−0.611	−0.301	−39.8	−17.5	C64, R6
	Gassendi	−0.611	−0.345	−40.6	−20.2	(D7, M3)
	Gassendi	−0.590	−0.300	−38.2	−17.5	
	Gassendi A	−0.616	−0.268	−39.7	−15.5	
12	Bullialdis	−0.353	−0.354	−22.2	−20.7	C64, R6
	Bull. > Agatharchides	−0.385	−0.358	−24.4	−21.0	(D7, P9)
	Bull. > Agatharchides	−0.450	−0.348	−28.7	−20.4	
	Agatharchides	−0.483	−0.338	−30.9	−19.8	
13	Hippalus	−0.457	−0.420	−30.2	−24.8	C64, R6
	Campanus A	−0.430	−0.438	−28.6	−26.0	(D7, P9)
	Campanus	−0.411	−0.469	−27.7	−28.0	
	Mercator	−0.384	−0.488	−26.1	−29.2	
14	Vitello	−0.525	−0.506	−37.5	−30.4	C64, R6
	Lee	−0.560	−0.510	−40.6	−30.7	(M3, D7)
	Vitello > Doppelmayer	−0.550	−0.490	−39.1	−29.3	
	Doppelmayer	−0.581	−0.477	−41.4	−28.5	
15	Schickard R	−0.578	−0.696	−53.6	−44.1	C64, M3
	Schickard F	−0.538	−0.744	−53.6	−48.1	(D7, M3)
	Schickard	−0.608	−0.682	−56.2	−43.0	
	Schickard	−0.623	−0.665	−56.6	−41.7	
16	Drebbel	−0.570	−0.655	−49.0	−40.9	C64, M3
	Drebbel C	−0.518	−0.649	−42.9	−40.5	(D7, M3)
	Drebbel > Clausius	−0.570	−0.625	−46.9	−38.7	
	Clausius	−0.554	−0.601	−43.9	−36.9	
17	Capuanus	−0.372	−0.560	−26.7	−34.1	C64, M3
	Elger	−0.405	−0.578	−29.8	−35.3	(D7, M3)
	Capuanus > Ramsden	−0.416	−0.548	−29.8	−33.2	
	Ramsden	−0.442	−0.543	−31.8	−32.9	
18	Grimaldi	−0.920	−0.035	−67.0	− 2.0	D7, P9
	Grimaldi	−0.920	−0.073	−67.3	− 4.2	(−−−)
	Grimaldi	−0.920	−0.110	−67.8	− 6.3	
	Grimaldi	−0.920	−0.140	−68.3	− 8.0	

QUADRANT III (Cont'd)

SET	FEATURE	XI	ETA	LONG	LAT	COMPARSON
		COORDINATES				
19	Hermann	−0.842	−0.015	−57.4	− 0.9	D7, P9
	Damoiseau	−0.872	−0.086	−61.1	− 4.9	(D7, M3)
	Lohrmann A	−0.888	−0.013	−62.6	− 0.7	
	Lohrmann	−0.923	−0.008	−67.4	− 0.5	
20	Billy	−0.744	−0.239	−50.0	−13.8	P9, P33
	Hansteen	−0.771	−0.200	−51.9	−11.5	(D7, M3)
	Hansteen > Sirsalis	−0.800	−0.200	−54.7	−11.5	
	Hansteen > Letronne	−0.735	−0.200	−48.6	−11.5	

QUADRANT IV

SET	FEATURE	XI	ETA	LONG	LAT	COMPARSON
		COORDINATES				
1	Messier	+0.738	-0.033	+47.6	- 1.9	D24, M26
	Messier D	+0.722	-0.062	+46.3	- 3.6	(P10, P47)
	Messier > Taruntius H	+0.750	-0.017	+48.6	- 1.0	
	Taruntius H	+0.764	-0.006	+49.8	- 0.3	
2	Langrenus	+0.863	-0.155	+60.9	- 8.9	R23, D24
	Langrenus C	+0.862	-0.098	+60.0	- 5.6	(R23, D24)
	Langrenus C > Webb	+0.864	-0.048	+59.9	- 2.8	
	Webb	+0.865	-0.016	+59.9	- 0.9	
3	Maclaurin	+0.927	-0.033	+68.0	- 1.9	C88, D27
	Maclaurin > Dubiago P	+0.910	-0.010	+65.5	- 0.6	(C88, D27)
	Dubiago P	+0.920	-0.014	+66.9	- 0.8	
	Dubiago P > Apollonius	+0.898	-0.020	+63.9	- 1.1	
4	Goclenius	+0.696	-0.174	+45.0	-10.0	D24, R23
	Goclenius > Gutengerg	+0.680	-0.160	+43.5	- 9.2	(M17, P3)
	Gutenberg	+0.652	-0.151	+41.3	- 8.7	
	Gutenberg > Lubbock	+0.655	-0.118	+41.3	- 6.8	
5	Bellot	+0.728	-0.215	+48.2	-12.4	D24, R23
	Magelhaens	+0.681	-0.206	+44.1	-11.9	(M17, P3)
	Magelhaens A	+0.690	-0.220	+45.0	-12.7	
	Magelhaens > Goclenius	+0.700	-0.200	+45.6	-11.5	
6	Mädler	+0.487	-0.191	+29.7	-11.0	D24, R23
	Mädler > Theophilus	+0.470	-0.175	+28.5	-10.1	(P28, P23)
	Theophilus	+0.439	-0.198	+26.3	-11.4	
	Theophilus	+0.445	-0.180	+26.9	-10.4	
7	Censorinus	+0.540	-0.007	+32.7	- 0.4	D23, M26
	Maskelyne A	+0.560	-0.001	+34.0	+ 0.0	(M17, P3)
	Censorinus C	+0.561	-0.053	+34.2	- 3.0	
	Isidorus B	+0.543	-0.078	+33.0	- 4.5	
8	Isidorus	+0.547	-0.139	+33.5	- 8.0	D24, R23
	Capella	+0.567	-0.133	+34.9	- 7.6	(M17, P3)
	Capella A	+0.599	-0.133	+37.2	- 7.6	
	Capella A > Gutenberg	+0.620	-0.138	+38.8	- 7.9	
9	Cyrillus	+0.397	-0.231	+24.1	-13.4	M17, P3
	Cyrillus B	+0.362	-0.202	+21.7	-11.7	(S8, T14)
	Kant	+0.340	-0.184	+20.2	-10.6	
	Zöllner	+0.321	-0.140	+18.9	- 8.0	

QUADRANT IV (Cont'd)

SET	FEATURE	COORDINATES XI	ETA	LONG	LAT	COMPARSON
10	Toricelli	+0.476	−0.082	+28.5	− 4.7	P10, P47
	Toricelli > Hypatia	+0.430	−0.080	+25.6	− 4.6	(S8, T14)
	Hypatia H	+0.407	−0.078	+24.1	− 4.5	
	Hypatia	+0.384	−0.074	+22.6	− 4.2	
11	Rosse	+0.545	−0.307	+34.9	−17.9	D24, R23
	Rosse > Fracastorius	+0.530	−0.326	+34.1	−19.0	(M17, P3)
	Rosse > Fracastorius	+0.517	−0.430	+34.9	−25.5	
	Fracastorius	+0.509	−0.363	+33.1	−21.3	
12	Bohnenberger	+0.619	−0.279	+40.1	−16.2	D24, R23
	Bohnenberger A	+0.614	−0.305	+40.1	−17.8	(M17, P3)
	Bohnenberger F	+0.618	−0.253	+39.7	−14.7	
	Bohnen. > Gaudibert	+0.608	−0.232	+38.7	−13.4	
13	Beaumont	+0.458	−0.310	+28.8	−18.1	D24, R23
	Beaumont > Catherina	+0.430	−0.308	+26.9	−17.9	(P23, P28)
	Catherina	+0.381	−0.311	+23.6	−18.1	
	Catherina G	+0.402	−0.300	+24.9	−17.5	
14	Polybius	+0.400	−0.382	+25.6	−22.5	D24, R23
	Polybius > Rothmann	+0.400	−0.400	+25.8	−23.4	(T14, U20)
	Polybius > Rothmann	+0.400	−0.420	+26.1	−24.8	
	Polybius > Rothmann	+0.400	−0.440	+26.5	−26.1	
15	Tacitus	+0.313	−0.279	+19.0	−16.2	M17, P3
	Tacitus G	+0.299	−0.300	+18.3	−17.5	(S8, T14)
	Tacitus > Fermat	+0.300	−0.320	+18.5	−18.7	
	Tacitus > Fermat	+0.300	−0.340	+18.6	−19.9	
16	Colombo	+0.696	−0.261	+46.1	−15.1	D24, R23
	Colombo A	+0.679	−0.244	+44.4	−14.1	(M17, P3)
	Crozier	+0.753	−0.234	+50.8	−13.5	
	McClure	+0.742	−0.264	+50.3	−15.3	
17	Goclenius > Langrenus	+0.730	−0.170	+47.8	− 9.8	D24, R23
	Goclenius > Langrenus	+0.760	−0.150	+50.2	− 8.6	(M17, P3)
	Goclenius U	+0.757	−0.162	+50.1	− 9.3	
	Langrenus DA	+0.793	−0.154	+53.4	− 8.9	
18	Albategnius	+0.070	−0.195	+ 4.1	−11.2	M17, P28
	Albategnius B	+0.069	−0.174	+ 4.0	−10.0	(S8, T14)
	Albategnius P	+0.076	−0.224	+ 4.5	−12.9	
	Klein	+0.044	−0.207	+ 2.6	−11.9	

QUADRANT IV (Cont'd)

SET	FEATURE	XI	ETA	LONG	LAT	COMPARSON
		COORDINATES				
19	Hind	+0.127	−0.138	+ 7.4	− 7.9	M17, P28
	Halley	+0.100	−0.140	+ 5.8	− 8.0	(S8, P29)
	Hipparchus	+0.084	−0.096	+ 4.8	− 5.5	
	Horrocks	+0.102	−0.069	+ 5.9	− 4.0	
20	Abulfeda	+0.234	−0.239	+13.9	−13.8	M17, P28
	Descartes	+0.265	−0.203	+15.7	−11.7	(S8, T14)
	Dolland	+0.246	−0.182	+14.5	−10.5	
	Andel	+0.212	−0.181	+12.4	−10.4	

SELECTED FEATURES

SET	FEATURE	COORDINATES XI	ETA	LONG	LAT	COMPARSON
A	Galle	+0.213	+0.827	+22.2	+55.7	T91, T92
	Galle B	+0.170	+0.824	+17.4	+55.4	(T86, T87)
	Sheepshanks C	+0.169	+0.838	+18.0	+56.9	
	Sheepshanks	+0.150	+0.859	+17.0	+59.2	
B	Egede	-0.122	+0.751	-10.6	+48.6	A15, T104
	Egede A	-0.113	+0.782	-10.4	+51.4	(M14, M15)
	Egede G	-0.074	+0.787	- 6.8	+51.9	
	Protagoras	-0.071	+0.828	- 7.2	+55.8	
C	Tycho	-0.141	-0.685	-11.2	-43.2	A10, T14
	Tycho R	-0.175	-0.667	-13.6	-41.8	(A6, T107)
	Heinsius M	-0.199	-0.656	-15.3	-41.0	
	Heinsius	-0.234	-0.636	-17.7	-39.5	
D	Schiller	-0.368	-0.800	-37.8	-53.1	R6, T107
	Schiller	-0.390	-0.790	-39.4	-52.1	(M3, M9)
	Schiller T	-0.416	-0.773	-41.0	-50.6	
	Schiller	-0.430	-0.765	-41.9	-49.9	
E	Wargentin	-0.550	-0.770	-59.6	-50.4	C64, R6
	Wargentin	-0.565	-0.760	-60.4	-49.5	(M3, P33)
	Wargentin	-0.572	-0.750	-59.9	-48.6	
	Schickard F	-0.538	-0.744	-53.6	-48.1	
F	Liebig	-0.679	-0.412	-48.2	-24.3	C64, M9
	Cavendish	-0.733	-0.417	-53.8	-24.6	(D7, P9)
	Mercenius	-0.704	-0.367	-49.2	-21.5	
	Mercenius D	-0.670	-0.392	-46.7	-23.1	
G	Petavius	+0.805	-0.395	+61.2	-23.3	D24, R23
	Petavius	+0.786	-0.427	+60.4	-25.3	(D24, R23)
	Petavius C	+0.767	-0.464	+60.0	-27.6	
	Wrottesley	+0.765	-0.405	+56.8	-23.9	
H	Stevinus	+0.684	-0.537	+54.2	-32.5	D24, R23
	Stevinus L	+0.690	-0.556	+56.1	-33.8	(D24, R23)
	Furnerius E	+0.690	-0.570	+57.1	-34.8	
	Furnerius	+0.701	-0.592	+60.4	-36.3	

SELECTED FEATURES (Cont'd)

		COORDINATES				
SET	FEATURE	XI	ETA	LONG	LAT	COMPARSON
I	Rümker	−0.634	+0.663	−57.9	+41.5	D8, R12
	Rümker K	−0.614	+0.671	−55.9	+42.1	(D8, R12)
	Rümker S	−0.655	+0.676	−62.7	+42.5	
	Rümker E	−0.655	+0.623	−56.9	+38.5	
J	Reiner Gamma	−0.850	+0.130	−59.0	+ 7.5	D7, P9
	Reiner	−0.812	+0.120	−54.9	+ 6.9	(D7, P9)
	Reiner N	−0.840	+0.093	−57.5	+ 5.3	
	Cavalerius F	−0.899	+0.141	−65.2	+ 8.1	

APPENDIX E – ELGER'S ALBEDO SCALE

Cameron, W.S.; private communication

SCALE	FEATURE	XI	ETA	LONG	LAT
0	Black Shadows	--------	--------	--------	-------
1.0	Darkest part of Grimaldi	−0.925	−0.091	68.3W	5.2S
	Darkest part of Riccioli	−0.961	−0.054	74.2W	3.1S
1.5	Interior of Boscovich	+0.190	+0.171	11.1E	9.8N
	Interior of Billy	−0.744	−0.239	50.0W	13.8S
	Interior of Zupus	−0.755	−0.295	52.2W	17.2S
2.0	Floor of Endymion	+0.495	+0.805	56.5E	53.6N
	Floor of Le Monnier	+0.455	+0.447	30.5E	26.5N
	Floor of Julius Caesar	+0.262	+0.157	15.3E	9.0N
	Floor of Cruger	−0.880	−0.287	66.7W	16.7S
	Floor of Fourier A	−0.657	−0.503	49.5W	30.2S
2.5	Interior of Azout	+0.885	+0.178	64.0E	10.2N
	Interior of Vitruvius	+0.495	+0.303	31.2E	17.6N
	Interior of Pitatus	−0.203	−0.497	13.5W	29.8S
	Interior of Hippalus	−0.457	−0.420	30.2W	24.8S
	Interior of Marius	−0.758	+0.206	50.8W	11.9N
3.0	Interior of Taruntius	+0.722	+0.098	46.5E	5.6N
	Interior of Plinius	+0.387	+0.265	23.6E	15.3N
	Interior of Theophilus	+0.435	−0.198	26.3E	11.4S
	Interior of Parrot	+0.057	−0.252	3.4E	14.6S
	Interior of Flamsteed	−0.696	−0.078	44.3W	4.5S
3.5	Interior of Hansen	+0.926	+0.242	72.6E	14.0N
	Interior of Archimedes	−0.060	+0.496	4.0W	29.7N
	Interior of Mersenius	−0.704	−0.367	49.2W	21.5S
4.0	Interior of Manilius	+0.153	+0.250	9.0E	14.4N
	Interior of Ptolemaeus	−0.031	−0.161	1.8W	9.3S
	Interior of Guericke	−0.239	−0.200	14.1W	11.5S
4.5	Surface around Aristillus	+0.018	+0.557	2.0E	34.0N
	Sinus Medii	+0.050	+0.050	0.5E	1.0N

APPENDIX E (CONT'D)

ELGER'S ALBEDO SCALE

SCALE	FEATURE	XI	ETA	LONG	LAT
5.0	Walls of Arago	+0.363	+0.107	21.4E	6.1N
	Walls of Lansberg	-0.448	-0.006	26.6W	0.3S
	Walls of Bullialdus	-0.353	-0.354	22.2W	20.7S
	Surface surrounding Kepler	-0.609	+0.141	38.0W	8.0N
	Surface surrounding Aristarchus	-0.676	+0.402	48.0W	24.0N
5.5	Walls of Picard	+0.789	+0.251	54.5E	14.5N
	Walls of Timocharis	-0.202	+0.449	13.1W	26.7N
	Rays of Copernicus	-0.337	+0.168	20.0W	10.0N
6.0	Walls of Macrobius	+0.671	+0.363	46.0E	21.2N
	Walls of Kant	+0.340	-0.184	20.2E	10.6S
	Walls of Bessel	+0.286	+0.370	17.9E	21.7N
	Walls of Mösting	-0.101	-0.012	5.9W	0.7S
	Walls of Flamsteed	-0.696	-0.078	44.3W	4.5S
6.5	Walls of Langrenus	+0.863	-0.155	60.9E	8.9S
	Walls of Thaetetus	+0.084	+0.602	6.0E	37.0N
	Walls of Lahire	-0.349	+0.477	23.4W	28.5N
7.0	Theon	+0.266	-0.014	15.4E	0.8S
	Ariadaeus	+0.296	+0.080	17.2E	4.5N
	Bode B	-0.053	+0.152	3.1W	8.7N
	Wichmann	-0.611	-0.131	38.0W	7.5S
	Kepler	-0.609	+0.141	38.0W	8.1N
7.5	Ukert	+0.024	+0.134	1.3E	7.7N
	Hortensius	-0.466	+0.113	28.0W	6.5N
	Euclides	-0.488	-0.128	29.5W	7.4S
8.0	Walls of Godin	+0.177	+0.032	10.2E	1.8N
	Walls of Bode	-0.042	+0.117	2.4W	6.7N
	Walls of Copernicus	-0.337	+0.168	20.0W	9.7N
8.5	Walls of Proclus	+0.702	+0.278	46.9E	16.1N
	Walls of Bode A	-0.020	+0.156	1.2W	9.0N
	Walls of Hipparchus C	+0.142	-0.129	8.2E	7.4S

APPENDIX E (CONT'D)

ELGER'S ALBEDO SCALE

SCALE	FEATURE	XI	ETA	LONG	LAT
9.0	Censorinus	+0.540	−0.007	32.7E	0.4S
	Dionysius	+0.297	+0.049	17.2E	2.8N
	Mösting A	−0.090	−0.056	5.2W	3.2S
	Mersenius B	−0.731	−0.360	57.6W	21.1S
	Mersenius C	−0.676	−0.338	45.9W	19.8S
9.5	Interior of Aristarchus	−0.676	+0.402	47.6W	23.7N
	Interior of La Perouse	+0.956	−0.185	76.6E	10.7S
10	Central peak of Aristarchus	−0.676	+0.402	47.6W	23.7N

APPENDIX F – LIST OF LUNAR TRANSIENT PHENOMENON SITES

FEATURE	Xi	ETA	LONG	LAT
Agrippa	+0.182	+0.072	4E	10N
Albategnius	+0.070	−0.195	4E	11S
Alfraganus	+0.324	−0.094	19E	5S
Alpetragius	−0.075	−0.276	4W	16S
Alphonsus	−0.046	−0.233	3W	14S
Anaxagoras	−0.050	+0.959	10W	74N
Archimedes	−0.060	+0.496	4W	30N
Aristarchus	−0.676	+0.402	48W	24N
Aristillus	+0.018	+0.557	2E	34N
Arnold	+0.231	+0.919	36E	67N
Arzachel	−0.031	−0.313	2W	18S
Atlas	+0.481	+0.727	44E	47N
A_6 Seismic Site	−0.430	−0.390	27W	24S
A_{14} Seismic Site	−0.580	−0.700	54W	45S
A_{16} Seismic Site	+0.190	+0.130	11E	6N
A_{18} Seismic Site	+0.450	+0.450	30E	26N
A_{20} Seismic Site	−0.480	+0.370	30W	22N
A_{25} Seismic Site	+0.690	+0.400	49E	25N
Babbage	−0.424	+0.862	57W	60N
Baco	+0.206	−0.777	19E	51S
Baillaud	+0.162	+0.964	38E	74N
Baily	+0.328	+0.763	30E	50N
Barocius	+0.205	−0.206	17E	45S
Barrow	+0.043	+0.947	8E	71N
Beaumont	+0.458	−0.310	29E	18S
Bessel	+0.286	+0.370	18E	22N
Biela	+0.449	−0.818	51E	55S
Biot	+0.718	−0.385	51E	23S
Birt	−0.137	−0.380	8W	22S
Blancanus	−0.163	−0.896	22W	64S
Bond, W.C.	+0.026	+0.909	4E	65N
Boussingault	+0.274	−0.942	55E	70S
Bullialdus	−0.353	−0.354	22W	22S
Bürg	+0.334	+0.708	28E	45N
Byrgius	−0.825	−0.418	65W	25S
Calippus	+0.145	+0.629	10E	39N
Cape Agarum	+0.885	+0.225	66E	14N
Capuanus	−0.372	−0.560	27W	34S
Carlini	−0.339	+0.555	24W	34N
Cassini	+0.061	+0.646	4E	40N
Catherina	+0.381	−0.311	24E	18S

APPENDIX F (CONT'D)

FEATURE	Xi	ETA	LONG	LAT
Cauchy	+0.616	+0.167	39E	10N
Cavendish	-0.733	-0.417	54W	25S
Censorinus	+0.540	-0.007	33E	0S
Cepheus	+0.543	+0.653	46E	41N
Challis	+0.029	+0.984	9E	80N
Chevallier	+0.552	+0.706	51E	45N
Chladni	+0.020	+0.070	1E	4N
Clavius	-0.130	-0.852	14W	58S
Cleomedes	+0.730	+0.465	56E	28N
Cleostratus	-0.481	+0.869	76W	60N
Cobra Head	-0.690	+0.415	48W	24N
Conon	+0.032	+0.369	2E	22N
Copernicus	-0.337	+0.168	20W	10N
Cyrillus	+0.397	-0.231	24E	13S
Daniell	+0.422	+0.579	31E	35N
Darwin	-0.878	-0.343	69W	20S
Dawes	+0.424	+0.296	26E	17N
Delambre	+0.300	-0.034	18E	2S
Deseilligny	+0.328	+0.360	20E	21N
Dionysius	+0.297	+0.049	17E	3N
Draper	-0.353	+0.302	22W	18N
Eimmart	+0.826	+0.406	65E	24N
Elger	-0.405	-0.578	30W	35S
Endymion	+0.495	+0.805	56E	54N
Eratosthenes	-0.190	+0.250	11W	14N
Eudoxus	+0.201	+0.698	16E	44N
Fontenelle	-0.145	+0.893	19W	63N
Fontenelle D	-0.183	+0.887	23W	62N
Fracastorius	+0.509	-0.363	33E	21S
Fra Mauro	-0.290	-0.104	17W	6S
Furnerius	+0.701	-0.592	60E	36S
Gärtner	+0.292	+0.858	35E	59N
Gassendi	-0.611	-0.301	40W	18S
Gauss	+0.795	+0.587	79E	36N
Gemma Frisius	+0.191	-0.564	13E	34S
Godin	+0.177	+0.032	10E	2N
Goldschmidt	-0.015	+0.957	3W	73N
Goodacre	+0.205	-0.540	14E	33S
Grimaldi	-0.925	-0.091	68W	5S
Gutenberg	+0.652	-0.151	41E	9S

APPENDIX F (CONT'D)

FEATURE	Xi	ETA	LONG	LAT
Hansteen	−0.771	−0.200	52W	12S
Harbinger Mountains	−0.590	+0.450	43W	26N
Harpalus	−0.416	+0.795	43W	53N
Helicon	−0.298	+0.648	23W	40N
Hercules	+0.434	+0.728	39E	47N
Herodotus	−0.701	+0.394	50W	23N
Herschel	−0.036	−0.099	2W	6S
Herschel J.	−0.308	+0.884	41W	62N
HFT Seismic Site	−0.372	−0.574	27W	35S
Horrocks	+0.102	−0.069	6E	4S
Hyginus N	+0.127	+0.183	7E	10N
Hyginus W	+0.132	+0.168	8E	10N
Janssen	+0.466	+0.234	29E	14N
Kant	+0.340	−0.184	20E	11S
Kepler	−0.609	−0.141	38W	8N
Klein	+0.044	−0.207	3E	12S
Krafft	−0.915	+0.285	73W	17N
Kunowsky	−0.536	+0.056	33W	3N
Lahire	−0.349	+0.477	23W	28N
Lalande	−0.149	−0.078	9W	4S
Lambert	−0.322	+0.435	21W	26N
Landsberg	−0.448	−0.006	27W	1S
Legendre	+0.824	−0.483	70E	29S
Le Monnier	+0.455	+0.447	30E	26N
Letronne	−0.662	−0.184	42W	11S
Lexell	−0.059	−0.584	4W	36S
Lichtenberg	−0.785	+0.527	68W	32N
Linné	+0.181	+0.465	12E	28N
Littrow	+0.485	+0.367	31E	22N
Lubbock	+0.664	−0.068	42E	4S
Lyell	+0.633	+0.236	41E	14N
Maclear	+0.338	+0.183	20E	10N
Macrobius	+0.671	+0.363	46E	21N
Mädler	+0.487	−0.191	30E	11S
Marginus	−0.069	−0.766	6W	50S
Manilius	+0.153	+0.250	9E	14N
Manzinus	+0.171	−0.925	27E	68S
Mare Crisium	+0.800	+0.300	55E	15N
Mare Vaporum	+0.050	+0.200	2E	15N
Marius	−0.758	+0.206	51W	12N
Maskelyne	+0.500	+0.038	30E	2N

APPENDIX F (CONT'D)

FEATURE	Xi	ETA	LONG	LAT
Maurolychus	+0.180	-0.666	14E	42S
McClure	+0.742	-0.264	50E	15S
Mersenius	-0.704	-0.367	49W	22S
Messier	+0.738	-0.033	48E	2S
Messier A	+0.730	-0.035	47E	2S
Moltke	+0.410	-0.010	24E	1S
Moretus	-0.032	-0.943	6W	71S
Mt. Blanc	-0.010	+0.715	1W	46N
Mt. Hadley	+0.070	+0.445	6E	26N
Mt. Huygens	-0.050	+0.340	3W	19N
Nasireddin	+0.003	-0.657	1E	41S
Nicolai	+0.322	-0.674	26E	42S
Nöggerath	-0.472	-0.752	46W	49S
Palus Putredinus	+0.001	+0.450	2E	25N
Parrot	+0.057	-0.252	3E	15S
Parry	-0.269	-0.136	16W	8S
Peirce	+0.761	+0.313	53E	17N
Peirce A	+0.763	+0.310	53E	18N
Philolaus	-0.165	+0.951	32W	72N
Picard	+0.789	+0.251	54E	14N
Piccolomini	+0.464	-0.497	32E	30S
Pico	-0.108	+0.715	9W	46N
Pitatus	-0.203	-0.497	14W	30S
Pitiscus	+0.324	-0.772	31E	50S
Piton	-0.013	+0.650	3W	39N
Plato	-0.100	+0.782	9W	51N
Plinius	+0.387	+0.265	24E	15N
Posidonius	+0.424	+0.528	30E	32N
Prinz	-0.628	+0.430	44W	26N
Proclus	+0.702	+0.278	47E	16N
Prom. Agassiz	+0.030	+0.670	2E	42N
Prom. Heraclides	-0.425	+0.654	34W	41N
Prom. Laplace	-0.300	+0.725	31W	48N
Ptolemaeus	-0.031	-0.161	2W	9S
Purbach	-0.030	-0.430	2W	26S
Pytheas	-0.329	+0.351	21W	20N
Rabbi Levy	+0.329	-0.570	24E	35S
Reiner	-0.812	+0.120	55W	7N
Riccioli	-0.961	-0.054	74W	3S
Rocca	-0.931	-0.225	73W	13S
Römer	+0.537	+0.429	36E	25N
Ross D	+0.386	+0.218	23E	12N

APPENDIX F (CONT'D)

FEATURE	Xi	ETA	LONG	LAT
Sabine	+0.343	+0.024	20E	1N
Sacrobosco	+0.263	-0.401	17E	24S
Schickard	-0.582	-0.700	55W	44S
Schröter's Valley	-0.700	+0.440	48W	24N
Secchi	+0.688	+0.042	44E	2N
Seismic	+0.890	+0.240	67E	17N
Seismic	-0.450	-0.350	28W	21S
Sharp	-0.451	+0.716	40W	46N
Stevinus A	+0.667	-0.528	52E	32S
Stöfler	+0.079	-0.658	6E	41S
Straight Wall	-0.155	-0.370	10W	21S
Sulpicius Gallus	+0.191	+0.336	12E	20N
Taruntius	+0.722	+0.098	46E	6N
Teneriffe Mountains	-0.150	+0.740	17W	54N
Thales	+0.364	+0.881	50E	62N
Theatetus	+0.084	+0.602	6E	37N
Thebit A	-0.079	-0.368	5W	22S
Theophilus	+0.435	-0.198	26E	11S
Timocharis	-0.202	+0.449	13W	27N
Triesnecker	+0.063	+0.073	4E	4N
Tycho	-0.141	-0.685	11W	43S
Ulugh Beigh	-0.832	+0.540	81W	33N
Vieta	-0.726	-0.488	56W	29S
Vitello	-0.525	-0.506	38W	30S
Vitruvius	+0.495	+0.303	31E	18N
Walter	+0.010	-0.545	1E	33S
Wargentin	-0.565	-0.760	0W	50S
Yerkes	+0.759	+0.252	2E	14N

APPENDIX G – SUMMARY OF PHOTOMETRIC PROPERTIES OF SELECTED LUNAR SITES

The data in the following table are summarized from R.W. Shorthill et al., "Photometric Properties of Selected Lunar Features" (NASA CR-1429, 1969), and from R.L. Wildey's "A Digital File of the Lunar Normal Albedo" (The Moon, 1977). Site designations employ letters as follows: D = Dark albedo site, A = Average albedo site, B = Bright albedo site, M = Mare site, C = Crater site, R = Ray site, U = Upland site, T = Scientific site, S = Spacecraft site, and P = Apollo site. Longitudes and latitudes are expressed in degrees and the direction-cosines Xi and Eta are in .0001 lunar radii. The "Hapke Coefficients" are for the least-squares best fit to the Hapke (1966) photometric model for all scans made for the particular site; these are the quantities "Albedo", "H", and "RMS" (root-mean-square error). When either the "F" or the "Gamma" coefficients are non-zero, they are given in parentheses under "Description" (with Gamma in degrees). IAU cardinal directions are abbreviated with periods. The peak spectral sensitivity for the scan is approximately 4400 Å (roughly corresponding to the B spectral band) for the "Albedo" values, with a mean lunar resolution of 14.9 km and is approximately the equivalent to the combined Johnson B and V bandpasses for the '"V" Wildey' values, with a resolution of approximately 6.3 km. (Normal albedo and RMS values were calculated using a brightness reading conversion factor of 0.0016825*B).

Site	Selenographic		Dir-Cosines		Hapke Coefficients				"V"
No.	Long.	Lat.	Xi	Eta	Albedo	H	RMS	Description(F,Gamma)	Wildey
D1	-62.82	+17.81	-8469	+3058	.0581	.2535	.0015	(Darkest point)	.1020
D2	-79.95	+24.68	-8947	+4176	.0680	.4239	.0008	NW. Struve	.1010
D3	-74.07	+21.72	-8933	+3700	.0818	.2318	.0036	E. Struve	.1084
D4	-68.90	+24.45	-8493	+4139	.0606	.3163	.0031	Briggs	.0984
D5	-61.82	+06.23	-8762	+1086	.0636	.2466	.0015	NE. Cavalerius	.0973
D6	-67.20	+04.00	-9196	-0698	.0857	.2088	.0026	Grimaldi	.1133
D7	-56.85	-05.53	-8333	-0964	.0612	.2701	.0012	W. Flamsteed	.0999
D8	-54.85	+32.68	-6882	+5400	.0655	.3027	.0014	W. Gruithuisen	.0955
D9	-46.73	+19.77	-6853	+3382	.0768	.2968	.0018	S. Aristarchus	.1015
D11	-31.15	+19.68	-4871	+3368	.0773	.4104	.0018	NE. Bessarion (0, 4.68)	.1021
D12	-21.05	+24.42	-3271	+4134	.0706	.4827	.0019	S. Lambert	.1008
D13	-09.82	+24.42	-1551	+4134	.0680	.5865	.0013	S. Beer	.1026
D14	-05.65	+12.00	-0963	+2079	.0743	.3950	.0007	SE. Eratosthenes	.1009
D16	+09.40	+18.05	+1553	+3098	.0653	.9290	.0010	N. Manilius	.1046
D17	+19.92	+16.90	+3259	+2907	.0644	.5975	.0011	E. Manilius	.1013
D18	+23.27	+24.22	+3603	+4102	.0629	.4531	.0010	NE. Bessel	.0988
D19	+28.12	+24.20	+4299	+4099	.0617	.4795	.0010	SW. Le Monnier (0, 10.16)	.0984
D20	+36.37	+14.92	+5730	+2574	.0608	.6433	.0013	SW. Franz	.0995
D21	+39.32	+05.87	+6303	+1022	.0616	.5672	.0010	Cauchy (1, 0.02)	.1012
D22	+43.07	+05.85	+6793	+1019	.0684	.6888	.0020	W. Taruntius (1, 0)	.1104
D23	+46.27	-00.05	+7226	-0009	.0670	.5197	.0011	N. Messier	.1021
D24	+51.33	-05.97	+7766	-1039	.0618	.5348	.0013	SE. Messier	.1034
D25	+55.03	-04.23	+8172	-0738	.0659	.5946	.0015	SW. Webb	.1084
D26	+59.35	-00.15	+8603	-0026	.0752	.4473	.0026	W. Webb	.1014
D27	+57.18	+13.58	+8169	+2349	.0640	.5373	.0015	SE. Picard	.1013
D28	+58.23	+16.10	+8169	+2773	.0651	.4603	.0018	Mare Crisium (0, 11.9)	.0996
D29	+63.45	+17.70	+8522	+3040	.0590	.4890	.0015	Mare Crisium E1	.1029

APPENDIX G (CONT'D)

SUMMARY OF PHOTOMETRIC PROPERTIES OF SELECTED LUNAR SITES

Site No.	Selenographic Long.	Lat.	Dir-Cosines Xi	Eta	Albedo	Hapke Coefficients H	RMS	Description (F,Gamma)	"V" Wildey
D30	+59.83	+17.70	+8236	+3040	.0648	.4638	.0017	Mare Cris E2 (.1411, 0)	.1008
D31	+63.30	+11.65	+8750	+2019	.0731	.5489	.0046	Mare Crisium SE.	.1266
D235	-11.42	-19.42	-1862	-3393	.0695	.8800	.0017	NE. Mare Nubium 2	.1045
D236	-11.32	-19.57	-1849	-3349	.0692	.8634	.0016	NE. Mare Nubium 3 (1,01)	1040
D237	-11.00	-20.13	-1791	-3442	.0687	.8780	.0014	NE. Mare Nubium 4	.1030
A1	-73.53	-00.57	-9589	-0099	.1125	.2182	.0033	N. Riccioli	.1788
A2	-62.10	-16.13	-8490	-2779	.1188	.1248	.0022	SW. Sirsalis	.1304
A3	-51.28	-20.48	-7309	-3499	.1109	.2702	.0021	NW. Mersenius	.1275
A4	-50.40	-34.12	-6379	-5609	.1085	.4032	.0017	SE. Fourier (101)	.1321
A5	-26.17	+11.53	-4321	+1999	.1264	.2762	.0020	W. Copernicus	.1690
A6	-26.35	+50.43	-3025	+7709	.0977	.4691	.0026	NE. Maupertius	.1270
A10	-06.40	-19.82	-1049	-3390	.1222	.4766	.0014	NW. Thebit	.1212
A12	-04.63	-17.45	-0771	-2999	.0098	.7521	.0012	W. Arzachel	.1337
A13	-04.60	-04.77	-0799	-0831	.1191	.4221	.0012	SW. Flammarion	.1307
A14	+02.88	-05.73	+0501	-0999	.1309	.1429	.0034	S. Triesnecker	.1340
A15	+10.48	+44.42	+1300	+6999	.1102	.3754	.0020	W. Eudoxus	.1303
A17	+23.28	+46.72	+2710	+7280	.1087	.3589	.0018	NE. Eudox (.4797, 47.61)	.1252
A18	+14.50	+05.73	+2491	+0999	.0927	1.0956	.0024	NE. Whewell	.1260
A19	+31.67	+41.68	+3921	+6650	.1015	.5029	.0028	SE. Mason	.1266
A20	+23.57	-07.82	+3961	-1360	.0917	1.0433	.0022	S. Hypatia	.1364
A21	+37.15	-23.52	+5537	-3990	.1191	.5117	.0022	SE. Fracastorius	.1456
A22	+34.68	-03.38	+5680	-0590	.1030	.6594	.0017	N. Capella	.1317
A23	+38.42	-25.47	+5610	-4300	.1007	.7116	.0031	NE. Weinek (0, 80.2)	.1428
A24	+47.07	+23.58	+6710	+4001	.1067	.5010	.0016	N. Macrobius	.1323
A25	+42.82	+15.85	+6538	+2731	.1048	.4499	.0013	NE. Lyell (1, .02)	.1306
A26	+57.40	+23.95	+7699	+4059	.0970	.5945	.0016	S. Cleomedes	.1226
A27	+59.28	+08.63	+8500	+1501	.1137	.3276	.0011	SE. Lick (.6596, 59.09)	.1295
A28	+55.87	+04.70	+8250	+0819	.1024	.4775	.0030	E. Taruntius	.1300
A29	-64.35	-10.60	-8861	-1840	.1153	.2605	.0028	SE. Grimaldi	.1328
A30	-74.53	-05.73	-9590	-0999	.1015	.2817	.0031	S. Riccioli (0, 55.64)	.1242
B30	-04.15	-32.90	-0607	-5432	.1928	.9640	.0054	(Brightest Point)	.1455
B31	+58.00	+36.00	+6861	+5878	.1393	.2627	.0064	NE. Geminus	.1524
B32	+42.50	+32.50	+5698	+5373	.1345	.3616	.0010	NW. Newco (.9694, 10.28)	.1451
B34	-28.00	+67.50	-1797	+9239	.1348	.4152	.0051	SE. Philolaus	.1609
B35	-67.00	-22.00	-8535	-3746	.1514	.2063	.0049	SE. Darwin	.1511
B36	-60.00	-23.50	-7942	-3987	.1449	.3497	.0041	W. Prosper Henry	.1610
B37	-02.00	-29.00	-0305	-4828	.1404	.4977	.0037	Regiomontanus W.	.1371
B38	-48.50	-31.00	-6420	-5150	.1362	.4331	.0036	E. Fourier (1, .01)	.1598
B39	-12.00	-32.00	-1763	-5299	.1265	.4988	.0013	S. Pitatus	.1486

APPENDIX G (CONT'D)

SUMMARY OF PHOTOMETRIC PROPERTIES OF SELECTED LUNAR SITES

Site	Selenographic		Dir-Cosines			Hapke Coefficients			"V"
No.	Long.	Lat.	Xi	Eta	Albedo	H	RMS	Description (F,Gamma)	Wildey
B40	-19.17	-39.50	-2533	-6361	.1273	.6216	.0018	W. Heinsius	.1561
B41	-19.83	-40.67	-2574	-6517	.1552	.3226	.0009	N. Wilhelm (.3149, 59.04)	.1541
B42	-20.00	-42.50	-2522	-6756	.1391	.4971	.0028	E. Wilhelm	.1516
B43	-19.83	-45.00	-2399	-7071	.1445	.4074	.0025	E. Montanari (.2598, 24.6)	.1552
B44	-18.50	-45.17	-2237	-7092	.1354	.7373	.0034	NE. Montanari	.1570
B45	-17.00	-49.00	-1918	-7547	.1378	.5846	.0030	E. Longomontanus	.1634
B46	-17.50	-52.00	-1851	-7880	.1535	.3574	.0021	N. Clavius (.3884, 77.76)	.1601
B47	-07.50	-52.67	-0792	-7951	.1425	.7028	.0026	NE. Clavius (.541, 87.41)	.1708
B48	-02.50	-58.00	-0231	-8480	.1697	.2603	.0038	E. Clavius (.8361, 83.94)	.1712
B49	-29.00	-57.17	-2629	-8403	.1174	.5591	.0025	W. Clavius	.1469
B50	-37.50	-58.83	-3151	-8557	.1109	.6581	.0023	E. Weigel	.1482
B51	-20.50	-62.33	-1626	-8857	.1380	.4840	.0030	N. Blancan (.7342, 44.4)	.1605
B52	+19.00	-08.00	+3224	-1392	.1358	.6254	.0015	Zöllner	.1518
B54	+21.00	-12.00	+3505	-2079	.1424	.5045	.0026	NW. Cyrillus	.1585
B58	+11.00	-28.00	+1685	-4695	.1355	.5164	.0017	SE. Apianus	.1553
B63	+68.00	-27.67	+8212	-4643	.1004	.7440	.0028	NW. Legendre	.1563
B68	+10.5	-27.50	+1616	-4617	.1445	.5352	.0016	SE. Playfair	.1624
B74	+45.00	-42.00	+5255	-6691	.1142	.8473	.0029	NE. Janssen (0, 0.58)	.1644
B76	+30.00	-47.17	+3399	-7333	.1091	1.0002	.0023	W. Dove	.1537
B79	+08.00	-53.00	+0838	-7986	.1425	.5238	.0018	NE. Lilius (.3505, 56.62)	-------
B80	+11.50	-52.50	+1214	-7934	.1310	.5481	.0040	SE. Cuvier	.1600

M2	-68.00	-05.00	-9237	-0872	.0798	.1000	.0031	Grimaldi	.1079
M3	-54.00	-45.00	-5721	-7071	.1062	.3922	.0010	Schickard (1, 74.24)	.1308
M4	-11.00	+07.00	-1894	+1219	.0896	.3574	.0014	Oceanus Procellarum	.1108
M5	-45.50	-54.50	-4142	-8141	.0787	.7562	.0016	Anonymous No. 1 (1, 0)	.1210
M6	-45.00	+51.00	-4450	+777	1 .0842	.3956	.0024	Sinus Roris (1, 0.01)	.1177
M7	-39.00	-24.00	-5749	-4067	.0668	.3292	.0014	Mare Humorum	.0968
M8	-32.00	+45.00	-3747	+7071	.0712	.3825	.0015	Sinus Iridium (1, 0)	.1059
M9	-23.00	-11.00	-3836	-1908	.0669	.4944	.0014	Mare Cognitum	.0978
M10	-18.00	+39.00	-2402	+6293	.0654	.4928	.0016	Mare Imbrium (0, 3.76)	.0976
M12	-15.00	-21.00	-2416	-3584	.0629	.7087	.0010	Mare Nubium	.1042
M13	-08.00	+12.00	-1361	+2079	.0760	.6080	.0017	Sinus Aestuum	.1076
M14	-01.00	+01.00	-0174	+0175	.0717	.7389	.0015	Sinus Medii	.1065
M15	+03.00	+13.00	+0510	+2250	.0711	.4677	.0007	Mare Vaporum	.0986
M16	+18.00	+26.00	+2777	+4384	.0649	.5537	.0013	Mare Serenitatis	.0994
M17	+27.00	-04.50	+4526	-0785	.0697	1.0519	.0016	Anonymous No. 2	.1140
M18	+26.00	+44.50	+3127	+7009	.0870	.6038	.0019	Lacus Mortis	.1226
M19	+30.00	+07.00	+4963	+1219	.0585	.7585	.0008	Mare Tranquillitatis	.0970

APPENDIX G (CONT'D)

SUMMARY OF PHOTOMETRIC PROPERTIES OF SELECTED LUNAR SITES

Site	Selenographic		Dir-Cosines			Hapke Coefficients			"V"
No.	Long.	Lat.	Xi	Eta	Albedo	H	RMS	Description (F,Gamma)	Wildey
M20	+30.00	+54.00	+2939	+8090	.0745	.6519	.0018	E. M. Frigoris (.5854, 97.4)	.1127
M21	+35.00	-15.00	+5540	-2588	.0737	.8736	.0020	Mare Nectaris	.1135
M22	+36.00	+37.50	+4663	+6088	.0720	.6917	.0017	Lacus Somniorum	.1141
M23	+39.00	+18.50	+5968	+3173	.0820	.3763	.0016	Anonymous No. 3	.1112
M24	+40.83	-46.75	+4480	-7284	.1450	.5090	.0061	Janssen	.1662
M25	+52.75	-20.00	+7480	-3420	.0739	.6156	.0019	Anonymous No. 4	.1270
M26	+52.00	-02.50	+7873	-0436	.0602	.6372	.0012	Mare Fecunditatis	.1032
M27	+59.00	+17.00	+8197	+2924	.0654	.4767	.0018	Mare Crisium (0, 27.4)	.1009
C1	-44.20	-04.50	-6950	-0785	.0677	.1120	.0030	Flamsteed	.0956
C2	-42.92	-07.80	-6746	-1357	.0683	.2830	.0018	Flamsteed A	.0953
C4	-29.55	-07.37	-4891	-1282	.1322	.2917	.0028	Euclides	.1166
C6	+07.03	-02.62	+1223	-0457	.1563	.3135	.0041	Pickering E	.1450
C7	+08.18	-07.42	+1412	-1291	.1548	.8990	.0090	Hipparchus C	.1626
C8	+12.50	+06.25	+2152	+1089	.1451	.1113	.0028	Silberschlag	.1282
C9	+15.10	+03.98	+2599	+0695	.1296	.1109	.0033	Cayley	.1218
C10	+15.40	-00.78	+2655	-0137	.1278	.6625	.0029	Theon Senior	.1445
C31	-09.50	+51.50	-1027	+7826	.0705	.3823	.0018	Plato C	.1130
C36	+03.93	+40.42	+0522	+6483	.1070	.4305	.0017	Cassini NW.	.1287
C39	-49.58	+23.25	-6995	+3947	.0991	.4402	.0042	Herodotus	.1156
C40	-04.00	+29.67	-0606	+4950	.0734	.8156	.0019	Archimedes C	.1108
C44	-15.25	+00.90	-2630	+0157	.0708	.7088	.0015	Gambart	.1081
C50	+69.50	+12.00	+9162	+2079	.0906	.4638	.0035	Condorcet	.1414
C53	-14.00	-11.67	-2369	-2022	.1180	.1158	.0032	Guericke	.1219
C59	+13.92	-13.73	+2336	-2374	.1356	.3178	.0012	Abulfeda (.2270, 56.62)	.1490
C60	+44.08	-12.00	+6805	-2079	.1076	.1629	.0043	Magelhaens	.1353
C62	-66.83	-16.67	-8807	-2868	.0944	.1682	.0028	Cruger	.1236
C64	-23.83	-17.83	-3847	-3062	.0876	.3081	.0014	Lubiniezky (0, 0.30)	.1135
C69	+16.50	+44.25	+2034	+6978	.1264	.4555	.0039	Eudoxus	.1396
C75	+01.47	+30.67	+0220	+5100	.1067	.3128	.0012	Autolychus	.1198
C76	+16.00	+16.25	+2646	+2798	.1359	.4051	.0085	Memelaus	.1332
C79	+56.00	+28.00	+7320	+4695	.1112	.3811	.0034	Cleomedes	.1415
C80	-67.33	+02.00	-9222	+0349	.1197	.2440	.0034	Hevelius (0, 78.2)	.1327
C81	-37.95	+08.08	-6089	+1406	.1310	.2525	.0020	Kepler	.1228
C83	-20.00	+09.67	-3372	+1679	.1635	.2419	.0025	Copernicus	.1506
C84	-11.42	+14.50	-1916	-2504	.0864	.9131	.0016	Erathosthenes	.1170
C88	+46.42	+05.08	+7209	+0973	.0874	.5156	.0021	Taruntius (0, 13.78)	.1165

APPENDIX G (CONT'D)

SUMMARY OF PHOTOMETRIC PROPERTIES OF SELECTED LUNAR SITES

Site	Selenographic		Dir-Cosines		Hapke Coefficients				"V"
No.	Long.	Lat.	Xi	Eta	Albedo	H	RMS	Description (F,Gamma)	Wildey
C91	-02.08	-05.75	-0362	-1002	.1365	.3178	.0033	Herschel	.1355
C94	-39.83	-17.33	-6115	-2979	.0875	1.0512	.0056	Gassendi	.1234
C95	-22.25	-20.70	-3542	-3535	.1126	.3469	.0046	Bullialdus (1, 0.02)	.1149
C99	-32.95	-21.37	-5065	-3643	.0814	.4695	.0021	N. Loewy	.1051
C102	-11.33	-43.00	-1437	-6820	.1705	.6979	.0047	Tycho	.1046
C104	-04.00	-32.50	-0588	-5373	.1815	.7746	.0064	Deslandres	.1870
C112	+10.20	+01.83	+1770	+0320	.1574	.3969	.0026	Godin	.1568
R1	-26.73	+02.00	-4143	+0410	.1120	.1116	.0021	SW. Copernicus 1	.0986
R2	-24.50	+02.35	-4143	+0410	.1120	.1116	.0021	SW. Copernicus 2	.1138
R4	-26.00	+09.23	-4326	+1622	.1188	.1589	.0030	W. Copernicus	.1193
R5	-10.37	+09.67	-1774	+1679	.0755	1.0529	.0022	E. Copernicus	.1135
R6	-20.33	-27.17	-3091	-4566	.0735	1.0463	.0017	NW. Tycho 1	.1153
R7	-19.63	-31.50	-2865	-5225	.1270	.4949	.0024	NW. Tycho 2 (0, 46.94)	.1555
R9	-19.25	-31.67	-2806	-5250	.1227	.4653	.0020	NW. Tycho 4	.1615
R10	-04.00	-31.67	-0594	-5250	.1624	.5840	.0036	NE. Tycho (.42, 29.26)	.1793
R11	-45.00	+22.25	-6545	+3786	.0906	.2528	.0021	E. Aristarchus 1	.1153
R12	-41.17	+24.00	-6013	+4067	.0856	.2744	.0019	E. Aristarchus 2 (1, .04)	.1411
R13	-42.17	+20.42	-6291	+3488	.0858	.2537	.0018	SE. Aristarchus 1 (1, .04)	.1062
R14	-40.17	+19.00	-6099	+3256	.0880	.2082	.0024	SE. Aristarchus 2 (1, .02)	.1083
R15	-38.00	+16.00	-5918	+2756	.0953	.1973	.0022	SE. Aristar. 3 (.0754, 94.7)	.1090
R16	-42.83	+07.17	-6746	+1248	.0876	.1808	.0024	W. Kepler	.1002
R17	-39.75	+09.25	-6311	+1607	.1032	.1358	.0026	NW. Kepler 1	.1087
R18	-32.00	+06.42	-5266	+1118	.1017	.1121	.0025	E. Kepler 2 (1, .01)	.1095
R20	-39.67	+12.00	-6244	+2079	.0900	.2162	.0024	N. Kepler 2 (1, 0)	.1055
R21	+30.83	-10.83	+5034	-1880	.1195	.4071	.0026	E. Mädler	.1277
R22	+00.08	+38.00	+0011	+6157	.1030	.3066	.0028	N. Aristillus	.1168
R23	+54.50	-10.00	+8017	-1736	.0752	.6549	.0018	W. Langrenus	.1114
U1	-02.63	+09.47	-0453	+1645	.0974	.1281	.0022	NW. Bode	.1072
U2	+08.67	+00.65	+1507	+0113	.1327	.4227	.0012	SW. Godin	.1464
U3	+20.68	-04.92	+3519	-0857	.1557	.4784	.0018	W. Hypatia A	.1561
U4	+19.22	-03.02	+3287	-0526	.1318	.7126	.0024	SE. Delambre (1, 0)	.1091
U5	-04.17	+16.48	-0697	+2837	.0837	.7210	.0023	W. Marco Polo	.1200
U6	+03.08	+21.47	+0501	+3660	.1145	.1962	.0024	E. Conon	.1220
U8	-04.83	-04.67	-0840	-0814	.1240	.4060	.0016	E. Lalande R	.1304
U10	+07.67	-00.98	+1334	-0172	.1325	.4551	.0011	NW. Lade S	.1454
U11	+06.50	-01.90	+1131	-0332	.1324	.3768	.0011	NW. Pickering E	.1476
U12	+07.13	-10.80	+1220	-1874	.1203	.5820	.0008	N. Albategnius D	.1390
U13	+39.52	-10.50	+6256	-1822	.1350	.1787	.0057	SW. Gutenberg	.1400
U14	+34.42	-01.28	+5651	-0224	.1180	.3249	.0018	S. Mask A (.8089, 11.13)	.1282

APPENDIX G (CONT'D)

SUMMARY OF PHOTOMETRIC PROPERTIES OF SELECTED LUNAR SITES

Site	Selenographic		Dir-Cosines			Hapke Coefficients			"V"
No.	Long.	Lat.	Xi	Eta	Albedo	H	RMS	Description (F,Gamma)	Wildey
U15	-03.27	+16.77	-0546	+2885	.0867	.7125	.0021	W. Marco Polo P	.1198
U16	-04.47	+20.92	-0727	+3570	.6656	.6779	.0009	N. Huxley	.1006
U17	+06.25	+26.07	+0978	+4394	.0792	.8829	.0012	E. Mount Hadley	.1126
U18	+20.32	-21.13	+3239	-3605	.1292	.3570	.0013	NE. Fermi A (.2131, 56.62)	.1410
U19	+19.00	-16.58	+3120	-2854	.1398	.4100	.0044	S. Tacitus	.1519
U20	+19.67	-26.25	+3018	-4423	.1028	.8402	.0022	SW. Pons	.1499
T1	+60.67	-25.17	+7890	-4253	.0963	.7595	.0087	Petavius Central Peak	.1603
T2	+57.08	-19.42	+7917	-3324	.1089	.9303	.0026	Petavius B	.1430
T3	+51.83	-31.83	+6680	-5275	.2271	.3167	.0075	Sevinus A (.4252, 56.62)	.1707
T4	+47.62	-01.83	+7383	-0320	.0642	.8968	.0027	Messier	.1027
T5	+27.75	-28.00	+4111	-4695	.1267	.4661	.0014	Rupes Altai	.1506
T6	+32.72	-00.43	+5405	-0076	.1420	.9034	.0032	Censorinus	.1337
T7	+29.33	+22.20	+4536	+3778	.0662	1.0651	.0031	Littrow rills	.1054
T11	+13.50	+38.50	+1827	+6225	.1125	.3913	.0019	S. of Alexander	.1244
T12	+09.75	+21.00	+1581	+3584	.0553	.5792	.0011	Sulpicius Gallus rills	.0947
T14	+04.08	-04.75	+0710	-0828	.1200	.5454	.0015	Hipparchus (0, 0.01)	.1334
T18	-04.00	+12.83	-0680	+2221	.0638	.3748	.0013	Rima Bode 2	.0974
T20	-02.67	+49.50	-0302	+7604	.1045	.4624	.0026	Plato, sinu. rill com	.1301
T24	-16.25	+14.67	-2707	+2532	.0980	.3689	.0015	Coper. second craters	.1168
T26	-20.30	+10.42	-3412	+1808	.1455	.2824	.0015	Copernicus	.1417
T27	-22.00	+32.67	-3154	+5398	.0638	.4434	.0014	Imbrium flows (0, 4.48)	.0959
T28	-30.92	+13.17	-5003	+2278	.0764	.5728	.0026	Tobias Mayer dome	.1071
T36	-40.92	+26.50	-5861	+4462	.0837	.3131	.0018	Harbinger Mtn (0, 24.08)	.1099
T50	-45.98	+12.60	-7018	+2181	.0805	.1883	.0015	Marius A	.0998
T69	-04.08	-13.67	-0692	-2363	.0908	.9815	.0023	Alphonsus W	.1203
T70	+17.33	+20.70	+2787	+3535	.0743	.5611	.0011	N. Menelaus	.1021
T71	-17.33	+37.50	-2364	+6088	.0706	.3776	.0012	S. Le Verrier A (.4981, 18.1)	.0970
T72	-38.67	+42.00	-4643	+6691	.0901	.4851	.0026	E. Mairan	.1207
T73	-40.58	+36.42	-5235	+5937	.0900	.3779	.0019	Gruithuisen Gamma (1, 0)	.1141
T74	-39.53	+36.08	-5144	+5890	.0827	.4753	.0021	Gruithuisen Delta (1, 0)	.1128
T75	-39.72	+34.50	-5266	+5664	.0794	.3287	.0018	Gruithuisen Zeta	.1094
T76	+22.00	+13.50	+3643	+2334	.0566	.5906	.0010	N. Ross (1, 0)	.0950
T77	+06.00	+13.00	+1018	+2250	.0660	.4720	.0003	SW. Manilius	.0969
T78	+16.12	+41.37	+2083	+6609	.1119	.4727	.0016	S. Eudoxus (1, 0)	.1303
T79	-19.30	+38.50	-2587	+6225	.0639	.4407	.0012	SE. Le Ver. (0, 86.44)	.0961
T80	-18.70	+40.37	-2443	+6477	.0654	.4680	.0012	E. Le Verrier	.0987
T82	-59.00	+10.00	-8441	+1736	.0602	.3081	.0016	NW. Reiner	.0942
T83	+20.92	-22.58	+3296	-3840	.1177	.4580	.0023	Rupes Altai 1	.1401
T84	+21.40	-22.58	+3369	-3840	.1125	.5597	.0027	Rupes Altai 2 (.7201, 58.66)	.1419

APPENDIX G (CONT'D)

SUMMARY OF PHOTOMETRIC PROPERTIES OF SELECTED LUNAR SITES

Site No.	Selenographic Long.	Lat.	Dir-Cosines Xi	Eta	Albedo	Hapke Coefficients H	RMS	Description (F,Gamma)	"V" Wildey
T85	+22.08	-22.58	+3471	-3840	.1173	.5097	.0021	Rupes Altai 3	.1442
T86	+08.00	+24.25	+1269	+4107	.0649	.4480	.0006	Mare Serenitatis 1	.0987
T87	+10.00	+24.25	+1583	+4107	.0620	.5058	.0008	Mare Serenitatis 2	.0954
T88	+12.00	+24.25	+1896	+4107	.0586	.5422	.0006	Mare Serenitatis 3	.0963
T89	+14.00	+24.25	+2206	+4107	.0625	.6091	.0009	Mare Serenitatis 4	.0984
T90	+16.00	+24.25	+2513	+4107	.0645	.4991	.0007	Mare Serenitatis 5	.0989
T91	+18.00	+24.25	+2817	+4107	.0636	.7088	.0012	Mare Serenitatis 6	.1038
T92	+20.00	+24.25	+3118	+4107	.0696	.4765	.0009	Mare Serenitatis 7	.1006
T94	+24.00	+24.25	+3708	+4107	.0633	.5811	.0007	Mare Serenitatis 9	.0986
T95	+26.00	+24.25	+3997	+4107	.0668	.4986	.0012	Mare Serenitatis 10	.1006
T96	+28.00	+24.25	+4280	+4107	.0615	.4758	.0010	Mare Serenitatis 11	.0978
T97	+29.33	+24.25	+4467	+4107	.0711	.4735	.0020	Mare Serenitatis 12	.1056
T98	+03.00	+26.00	+0470	+4384	.0769	.6298	.0018	Apennines 1	.1147
T99	+04.00	+26.00	+0627	+4384	.0978	.4592	.0030	Apennines 2	.1180
T101	+06.00	+26.00	+0939	+4384	.0814	.7676	.0009	Apennines 4	.1143
T102	+07.00	+26.00	+1095	+4384	.0835	.3551	.0017	Apennines 5	.1096
T103	+08.00	+26.00	+1251	+4384	.0757	.3083	.0020	Apennines 6	.1021
T104	+09.00	+26.00	+1406	+4384	.0619	.6508	.0009	Apennines 7	.0979
T105	-42.00	+34.00	-5547	+5592	.0683	.3714	.0018	NW. Gruithuisen	.1436
T106	-47.50	+12.50	-7198	+2164	.0654	.3394	.0019	W. Marius A	.0950
T107	-14.00	-22.00	-2243	-3746	.0611	.7835	.0013	W. Nicollet	.1073
T108	-13.17	+02.75	-2275	+0480	.0696	.6765	.0017	SW. Gambart C	.1059
T111	-14.42	+05.33	-2479	+0929	.0674	.4060	.0015	SE. Copernicus	.1008

S1	+21.42	+09.35	+3603	+1625	.0563	.6067	.0008	M. Tran. west Side (1,01)	.0942
S2	-20.58	-10.67	-3455	-1851	.0675	.6007	.0016	NW. Mare Nubium 1	.0995
S3	+24.77	+02.67	+4185	+0465	.0590	1.0093	.0012	Mare Tran. west side	.0955
S4	-02.33	-12.92	-0397	-2235	.1132	.4477	.0021	Alphonsus, NE. quarter	.1302
S5	-43.33	-02.33	-6857	-0407	.0604	.3500	.0018	O. Pr. Near Flam.(0,76.16)	.0932
S6	-23.17	-03.33	-3927	-0581	.0716	.3483	.0012	O. Pr. SE. of Lansberg	.1006
S7	+23.18	+01.50	+3935	+0262	.0613	.7333	.0009	Mare Tran. west side	.0991
S8	-01.48	+00.47	-0259	+0081	.0669	.8985	.0015	Sinus Medii	.1089
S9	-11.43	-41.02	-1496	-6563	.1257	.9500	.0036	Tycho, north highlands	.1612
S10	-64.55	+07.00	-8962	+1219	.0723	.2187	.0027	O. Proc. west side	.1037
S11	-62.05	+18.87	-8359	+3234	.0598	.2703	.0014	O. Proc. NW quarter	.0917
S12	-19.83	-11.42	-3325	-1980	.0755	.3491	.0012	Mare Cognitum 1	.1003
S13	-19.57	-11.32	-3284	-1963	.0681	.5350	.0017	Mare Cognitum 2 (0,64)	.0997
S15	-20.10	-10.90	-3375	-1891	.0741	.3921	.0012	Mare Cog. 4 (0, 0.43)	.0994

APPENDIX G (CONT'D)

SUMMARY OF PHOTOMETRIC PROPERTIES OF SELECTED LUNAR SITES

Site	Selenographic		Dir-Cosines			Hapke Coefficients			"V"
No.	Long.	Lat.	Xi	Eta	Albedo	H	RMS	Description (F,Gamma)	Wildey
P1	+42.00	-00.85	+6691	-0148	.0864	.1855	.0023	IP1	.1048
P2	+35.45	+00.10	+5800	+0017	.0954	.6132	.0025	IP2	.1314
P3	+26.08	+00.57	+4397	+0099	.0612	.8113	.0008	IP3	.1006
P4	+13.23	+00.05	+2289	+0009	.1171	.5721	.0010	IP4 (0, 0.44)	.1343
P5	-01.45	+00.02	-0253	+0003	.0678	.8832	.0016	IP5 (0, 0.62)	.1084
P6	-01.93	-03.93	-0337	-0686	.0938	1.1000	.0027	IP6 (0, 0.61)	.1361
P7	-22.10	-03.52	-3755	-0613	.0771	.2726	.0017	IP7 (.0011, 1.79)	.1000
P8	-36.57	-02.98	-5950	-0520	.0645	.3313	.0015	IP8-1 (0, 3.91)	.0939
P9	-43.40	-01.97	-6877	-0343	.0645	.2935	.0014	IP9-2	.0937
P10	+36.92	+04.17	+5991	+0727	.0647	.7009	.0012	IIP1 (.0001, 0.28)	.1006
P11	+34.00	+02.75	+5585	+0480	.0638	.6197	.0011	IIP2	.1061
P12	+21.33	+04.33	+3628	+0756	.0619	.7082	.0008	IIP3	.0975
P14	+24.80	+02.60	+4190	+0454	.0590	1.0361	.0012	IIP5	.0992
P15	+24.17	+00.75	+4094	+0131	.0677	.5557	.0011	IIP6 (1, 0)	.1015
P16	-02.00	+02.17	-0349	+0378	.0725	.8714	.0026	IIP7	.1079
P17	-01.00	+00.08	-0175	+0015	.0692	.7917	.0017	IIP8	.1071
P18	-13.00	+01.00	-2249	+0175	.0697	.6367	.0013	IIP9 (.0001, 0.65)	.1017
P19	-27.11	+03.47	-4557	+0605	.0895	.2433	.0015	IIP10 (0, 44.79)	.1081
P20	-19.92	-00.08	-3407	-0015	.0799	.5589	.0019	IIP11 (0, 0.71)	.1126
P22	-42.33	+01.50	-6732	+0262	.0617	.3235	.0014	IIP13 (.0013, 3.57)	.0954
P23	+35.25	+02.92	+5764	+0509	.0680	.5135	.0015	IIIP1 (0, 0.33)	.1008
P25	+20.25	+03.33	+3455	+0581	.0595	.8320	.0013	IIIP3 (.0013, 4.69)	.0998
P26	-27.45	+00.62	-4609	+0108	.0927	.2215	.0020	IIIP4 (.0004, 0)	.1086
P27	+24.52	+00.45	+4149	+0079	.0586	.6468	.0037	IIIP5 (.8192, 0)	.1022
P28	+21.50	+00.33	+3665	+0058	.0600	1.0794	.0012	IIIP6 (.0001, 0.88)	.1075
P29	-01.33	+00.92	-0233	+0160	.0723	.6340	.0013	IIIP7 (=P37)(0, 0.56)	.1077
P30	-19.83	-00.83	-3382	-0145	.0768	.4622	.0017	IIIP8 (.0010, 3.6)	.1065
P31	-23.25	-03.08	-3942	-0538	.0711	.4316	.0012	IIIP9 (.0002, 3.71)	.1005
P32	-42.00	+01.75	-6688	+0305	.0631	.3352	.0013	IIIP10 (=P44) (0, 0.8)	.0945
P33	-37.17	-03.17	-6032	-0552	.0634	.3280	.0016	IIIP11	.0943
P34	-43.80	-02.42	-6915	-0422	.0602	.3011	.0015	IIIP12 (0, 1.4)	.0942
P36	+13.50	-01.50	+2334	-0262	.1271	.4092	.0012	IIIS2	.1441
P38	-09.00	+05.00	-1558	+0872	.0537	.6332	.0010	IIIS4 (.0017, 4.1)	.0971
P41	-20.00	-00.50	-3420	-0087	.0825	.3761	.0014	IIIS7 (.0010, 3.33)	.1092
P42	-22.08	+01.17	-3759	+0204	.1139	.1603	.0028	IIIS8 (0, 0.55)	.1156
P45	-37.17	-03.50	-6030	-0610	.0628	.3474	.0016	IIIS11	.0943
P46	-43.92	-02.33	-6930	-0407	.0614	.2767	.0016	IIIS12	.0945
P47	+34.00	+02.67	+5586	+0465	.0637	.6239	.0011	Apollo Site I (0, 3.98)	.1072
P48	+23.62	+00.75	+4006	+0131	.0619	.7124	.0009	Apol. Site II (.0003, 1)	.1014
P49	-01.33	+00.42	-0233	+0073	.0674	.8722	.0015	Apollo Site III (0, 0.4)	.1079
P50	-36.42	-03.50	-5925	-0610	.0634	.3506	.0017	Apollo Site IV	.0943
P51	-41.67	+01.67	-6645	+0291	.0661	.3302	.0014	Apol. S. V (.0011, 4.17)	.0947

APPENDIX G (CONT'D)

SITE EVALUATION.

The 298 sites above differ considerably in their usability as photometric standards. Some common problems are abbreviated in the “SITE EVALUATION” listing below as follows:

A = significant albedo variations within scan aperture.
R = significant relief within scan aperture.
S = adjoining relief shades site during portion of the lunar day.
E = RMS error exceeds 2.5% of normal albedo.

Those sites that have none of the above problems are designated "Prime Sites" and are designated "PRIM" in the “SITE EVALUATION” listing below.

SITE EVALUATION

D1	___E	A19	AR_E	M5	AR__	C80	AR_E
D2	AR__	A20	AR__	M6	___E	C81	ARS_
D3	ARSE	A21	_R__	M7	A___	C83	AR_E
D4	___E	A22	AR__	M8	PRIM	C84	ARS_
D5	A___	A23	___E	M9	PRIM	C88	PRIM
D6	___E	A24	AR__	M10	PRIM	C91	ARS_
D7	PRIM	A25	_R__	M12	AR__	C94	AR_E
D8	PRIM	A26	AR__	M13	PRIM	C95	ARSE
D9	A___	A27	AR__	M14	PRIM	C99	AR_E
D11	AR__	A28	___E	M15	PRIM	C102	ARSE
D12	___E	A29	ARS_	M16	PRIM	C104	AR_E
D13	PRIM	A30	_RSE	M17	PRIM	C112	_RS_
D14	PRIM	B30	AR_E	M18	_R__	R1	PRIM
D16	AR__	B31	___E	M19	PRIM	R2	A___
D17	PRIM	B32	_R__	M20	A___	R4	AR_E
D18	PRIM	B34	A__E	M21	A__E	R5	A__E
D19	PRIM	B35	A_SE	M22	PRIM	R6	PRIM
D20	PRIM	B36	ARSE	M23	PRIM	R7	ARS_
D21	PRIM	B37	ARSE	M24	___E	R9	ARS_
D22	AR_E	B38	_R_E	M25	___E	R10	AR__
D23	PRIM	B39	ARS_	M26	PRIM	R11	A___
D24	PRIM	B40	ARS_	M27	___E	R12	PRIM
D25	_R__	B41	_R__	C1	AR_E	R13	PRIM
D26	___E	B42	_RS_	C2	AR_E	R14	___E
D27	PRIM	B43	_R__	C4	AR__	R15	A___
D28	___E	B44	_R_E	C6	AR_E	R16	AR_E
D29	___E	B45	_RS_	C7	AR_E	R17	_R__
D30	___E	B46	_RS_	C8	AR__	R18	A___
D31	AR_E	B47	_R__	C9	AR_E	R20	A__E
D235	AR__	B48	_RS_	C10	AR__	R21	AR__
D236	AR__	B49	_R__	C31	___E	R22	A__E
D237	AR__	B50	AR__	C36	ARS_	R23	PRIM

APPENDIX G (CONT'D)

SUMMARY OF PHOTOMETRIC PROPERTIES OF SELECTED LUNAR SITES

SITE EVALUATION

A1	ARSE	B51	ARS_	C39	ARSE	U1	AR__
A2	AR__	B52	_RS_	C40	___E	U2	_R__
A3	AR__	B54	_RS_	C44	AR__	U3	AR__
A4	ARS_	B58	AR__	C50	___E	U4	ARS_
A5	AR__	B63	___E	C53	___E	U5	_R_E
A6	AR_E	B68	_R__	C59	__S_	U6	_R__
A10	PRIM	B74	_R_E	C60	__SE	U8	_R__
A12	_RS_	B76	AR__	C62	__SE	U10	_R__
A13	AR__	B79	AR__	C64	PRIM	U11	_R__
A14	AR_E	B80	_R_E	C69	_RSE	U12	_R__
A15	PRIM	M2	___E	C75	_RS_	U13	___E
A17	AR__	M3	PRIM	C76	_RSE	U14	A___
A18	_R_E	M4	PRIM	C79	AR_E	U15	A___
U16	A___	T92	PRIM	P16	___E		
U17	AR__	T94	PRIM	P17	___E		
U18	ARS_	T95	PRIM	P18	PRIM		
U19	ARSE	T96	PRIM	P19	PRIM		
U20	PRIM	T97	AR_E	P20	PRIM		
T1	AR_E	T98	ARS_	P22	A___		
T2	ARS_	T99	ARSE	P23	A___		
T3	AR_E	T101	AR__	P25	PRIM		
T4	AR_E	T102	AR__	P26	AR__		
T5	ARS_	T103	AR_E	P27	___E		
T6	AR_E	T104	PRIM	P28	PRIM		
T7	AR__	T105	___E	P29	PRIM		
T11	_R__	T106	___E	P30	PRIM		
T12	_R__	T107	PRIM	P31	PRIM		
T14	PRIM	T108	PRIM	P32	A___		
T18	_R__	T111	AR__	P33	PRIM		
T20	AR__	S1	PRIM	P34	___E		
T24	_R__	S2	A___	P36	_R__		
T26	_RS_	S3	PRIM	P38	PRIM		
T27	PRIM	S4	__S_	P41	PRIM		
T28	ARSE	S5	___E	P42	_R__		
T36	AR__	S6	PRIM	P45	___E		
T50	AR__	S7	PRIM	P46	___E		
T69	ARS_	S8	PRIM	P47	PRIM		
T70	A___	S9	_R_E	P48	PRIM		
T71	PRIM	S10	AR_E	P49	PRIM		
T72	AR_E	S11	PRIM	P50	___E		
T73	AR__	S12	PRIM	P51	A___		

APPENDIX G (CONT'D)

SUMMARY OF PHOTOMETRIC PROPERTIES OF SELECTED LUNAR SITES

SITE EVALUATION

T74	AR_E	S13	PRIM
T75	AR__	S14	PRIM
T76	PRIM	S15	_R__
T77	PRIM	P1	___E
T78	_R__	P2	AR_E
T79	PRIM	P3	PRIM
T80	A___	P4	_R__
T82	___E	P5	PRIM
T83	AR__	P6	_R_E
T84	_RS_	P7	A___
T85	_RS_	P8	_R__
T86	A___	P9	PRIM
T87	PRIM	P10	PRIM
T88	PRIM	P11	PRIM
T89	PRIM	P12	PRIM
T90	PRIM	P14	A___
T91	PRIM	P15	PRIM

APPENDIX H – DATA REDUCTION ALGORITHMS

The following formulae are used for the calculations used in this book and in the computer program [Meeus (1982, 1991); Wilkins & Springett (1961); Wollard & Clemence (1966)]:

1. Average the SKY readings for each set of SKY-COMPARISON-SITE-COMPARISON-SKY measures:

   AVGSKY (SET) = (SKY1 + SKY2) / 2

2. Subtract the averaged SKY readings from the site and comparison measures for each set, "R'":

   R' = COMPARISON – AVGSKY(SET)
   or
   R' = SITE – AVGSKY(SET)

   Then average the COMPARISON1 and COMPARISON2 readings for each set; "R'".

3. Calculate the <u>JULIAN DATE</u>, JD:

   Let YYYY = the year (eg: 1992)
   Let MM = the month (eg: 08)
   Let DD.dd = the day with decimals (eg: 04.08)

   If MM = 1 or 2, subtract 1 from the year, and add 12 to the month.

   If YYYY.MMDD.dd is equal to or greater than 1582.1015, then calculate:

   A = INT (YYYY/100)
   B = 2 – A + INT(A / 4)

   JD = INT(365.25(YYYY + 4716)) + INT(30.6001(MM + 1)) + DD.dd + B – 1524.5

4. Calculate the <u>INTERVAL "T" OF EPHEMERIS TIME</u>:

   $T = (JD - 2451545) / 36525$

   where 2451545 is the fundamental epoch to which the elements of the sun, moon, and planets are referred, and 36525 is the number of days in a Julian Century.

5. Calculate the <u>MEAN LONGITUDE OF THE MOON</u>, "☾":

   ☾ $= 218^\circ.3164591 + 481267^\circ.88134236(T) - 0^\circ.0013268(T^2) + T^3 / 538841 - T^4 / 65194000$

   This is measured in the Ecliptic from the mean Equinox of date to the mean ascending node of the lunar orbit, then along the orbit.

6. Calculate the <u>MEAN ANOMALY OF THE SUN</u>, "g":

$$g = 357°.5291092 + 35999°.0502909(T) - 0°.0001536(T^2) + T^3 / 24490000$$

7. Calculate the <u>MEAN ANOMALY OF THE MOON</u>, "M'":

$$M' = 134°.9634114 + 477198.8676313(T) + 0°.0089970(T^2) + T^3 / 69699 - T^4 / 14712000$$

8. Calculate the <u>MEAN ELONGATION OF THE MOON FROM THE SUN</u>, "D":

$$D = 297°.8502042 + 445267.1115168(T) - 0°.0016300(T^2) + T^3 / 545868 - T^4 / 113065000$$

9. Calculate the <u>MEAN DISTANCE OF THE MOON FROM IT'S ASCENDING NODE</u>, "F":

$$F = 93°.2720993 + 483202.0175273(T) - 0°.0034029(T^2) - T^3 / 3526000 + T^4 / 863310000$$

10. Calculate arguments <u>A1, A2, A3</u>:

$$A_1 = 119°.75 + 131°.849(T)$$

$$A_2 = 53°.09 + 479264°.290(T)$$

$$A_3 = 313°.45 + 481266°.484(T)$$

11. Calculate "<u>e</u>":

$$e = 1 - 0.002516(T) - 0.0000074(T^2)$$

12. Calculate the <u>PERIODIC TERMS FOR THE LONGITUDE</u>, "Σl":

$\Sigma l = 6288774 \sin(M')$	$+ 1274027 \text{SIN}(2D-M')$	$+ 658314 \sin(2D)$	$+ 213618 \sin(2M')$
$- e(185116)\sin(g)$	$- 114332 \sin(2F)$	$+ 58793 \sin(2D-2M')$	$+ e(57066)\sin(2D-g-M')$
$+ 53322 \sin(2D+M')$	$+ e(45758)\sin(2D-g)$	$- e(40923)\sin(g-M')$	$- 34720 \sin(D)$
$- e(30383)\sin(g+M')$	$+ 15327 \sin(2D-2F)$	$- 12528 \sin(2F+M')$	$+ 10980 \sin(M'-2F)$
$+ 10675 \sin(4D-M')$	$+ 10034 \sin(3M')$	$+ 8548 \sin(4D-2M')$	$- e(7888)\sin(g-M'+2D)$
$- e(6766)\sin(2D+g)$	$- 5163 \sin(D-M')$	$+ e(4987)\sin(g+D)$	$+ e(4036)\sin(M'-g+2D)$
$+ 3994 \sin(2D+2M')$	$+ 3861 \sin(4D)$	$+ 3665 \sin(2D-3M')$	$- e(2689)\sin(g-2M')$
$- 2602 \sin(2D-M'+2F)$	$+ e(2390)\sin(2D-g-2M')$	$- 2348 \sin(M'+D)$	$+ e^2(2236)\sin(2D-2g)$
$- e(2120)\sin(2M'+g)$	$- e^2(2069)\sin(2g)$	$+ e^2(2048)\sin(2D-M'-2g)$	$- 1773 \sin(M'+2D-2F)$
$- 1595 \sin(2F+2D)$	$e(1215)\sin(4D-g-M')$	$- 1110 \sin(2M'+2F)$	$- 892 \sin(3D-M')$
$- e(810)\sin(g+M'+2D)$	$+ e(759)\sin(4D-g-2M')$	$- e^2(713)\sin(2g-M')$	$- e^2(700)\sin(2D+2g-M')$
$+ e(691)\sin(g-2M'+2D)$	$+ e(596)\sin(2D-g-2F)$	$+ 549 \sin(M'+4D)$	$+ 537 \sin(4M')$
$+ e(520)\sin(4D-g)$	$- 487 \sin(D-2M')$	$- e(399)\sin(2D+g-2F)$	$- 381 \sin(2M'-2F)$
$+ e(351)\sin(D+g+M')$	$- 340 \sin(3D-2M')$	$+ 330 \sin(4D-3M')$	$+ e(327)\sin(2D-g+2M')$
$- e^2(323)\sin(2g+M')$	$+ e(299)\sin(D+g-M')$	$+ 294 \sin(2D+3M')$	

13. Calculate the **PERIODIC TERMS FOR LATITUDE**, "Σb":

Σb = 5128122 Sin(F) + 280602 Sin(M'+F) + 277693 Sin(M'-F) + 173237 Sin(2D-F)
+ 55413 Sin(2D+F-M') + 46271 Sin(2D-F-M') + 32573 Sin(2D+F) + 17198 Sin(2M'+F)
+ 9266 Sin(2D+M'-F) + 8822 Sin(2M'-F) + e(8216)Sin(2D-g-F) + 4324 Sin(2D-F-2M')
+ 4200 Sin(2D+F+M') - e(3359)Sin(2D+g-F) + e(2463)Sin(2D+F-g-M')+ e(2211)Sin(2D+F-g)
+ e(2065)Sin(2D-F-g-M')- e(1870)Sin(g-M'-F) + 1828 Sin(4D-F-M') - e(1794)Sin(F+g)
- 1749 Sin(3F) - e(1565)Sin(g-M'+F) - 1491 Sin(F+D) - e(1475)Sin(F+g+M')
- e(1410)Sin(g+M'-F) - e(1344)Sin(g-F) - 1335 Sin(D-F) + 1107 Sin(F+3M')
+ 1021 Sin(4D-F) + 833 Sin(F+4D-M') + 777 Sin(M'-3F) + 671 Sin(F+4D-2M')
+ 607 Sin(2D-3F) + 596 Sin(2D+2M'-F) + e(491)Sin(2D+M'-g-F)- 451 Sin(2D-2M'+F)
+ 439 Sin(3M'-F) + 422 Sin(F+2D+2M') + 421 Sin(2D-F-3M') - e(366)Sin(g+F+2D-M')
- e(351)Sin(g+F+2D) + 331 Sin(F+4D) + e(315)Sin(2D+F-g+M')+ e^2(302)Sin(2D-2g-F)
- 283 Sin(M'+3F) - e(229)Sin(2D+g+M'-F)+ e(223)Sin(D+g-F) + e(223)Sin(D+g+F)
- e(220)Sin(g-2M'-F) - e(220)Sin(2D+g-M'-F)- 185 Sin(D+M'+F) + e(181)Sin(2D-g-2M'-F)
- e(177)Sin(g+2M'+F) + 176 Sin(4D-2M'-F) + e(166)Sin(4D-g-M'-F)- 164 Sin(D+M'-F)
+ 132 Sin(4D+M'-F) - 119 Sin(D-M'-F) + e(115)Sin(4D-g-F) + e^2(107)Sin(2D-2g+F)

14. Calculate the **PERIODIC TERMS FOR DISTANCE**, "Σr":

Σr = -20905355 Cos(M') - 3699111 Cos(2D-M') - 2955968 Cos(2D) - 569925 Cos(2M')
+ e(48888)Cos(g) - 3149 Cos(2F) + 246158 Cos(2D-2M') - e(152138)Cos(2D-g-M')
- 170733 Cos(2D+M') - e(204586)Cos(2D-g) - e(129620)Cos(g-M') + 108743 Cos(D)
+ e(104755)Cos(g+M') + 10321 Cos(2D-2F) + 79661 Cos(M'-2F) - 34782 Cos(4D-M')
- 23210 Cos(3M') - 21636 Cos(4D-2M') + e(24208)Cos(2D+g-M') + e(30824)Cos(2D+g)
- 8379 Cos(D-M') - e(16675)Cos(D+g) - e(12831)Cos(2D-g+M') - 10445 Cos(2D+2M')
- 11650 Cos(4D) + 14403 Cos(2D-3M') - e(7003)Cos(g-2M') + e(10056)Cos(2D-g-2M')
+ 6322 Cos(D+M') - e^2(9884)Cos(2D-2g) + e(5751)Cos(g+2M') - e^2(4950)Cos(2D-2g-M')
+ 4130 Cos(2D+M'-2F) - e(3958)Cos(4D-g-M') + 3258 Cos(3D-M') + e(2616)Cos(2D+g+M')
- e(1897)Cos(4D-g-2M')- e^2(2117)Cos(2g-M') + e^2(2354)Cos(2D+2g-M')- 1423 Cos(4D+M')
- 1117 Cos(4M') - e(1571)Cos(4D-g) - 1739 Cos(D-2M') - 4421 Cos(2M'-2F)
+ e^2(1165)Cos(2g+M') + 8752 Cos(2D-M'-2F)

15. Calculate the **ADDITIVE TO Σl**:

Σl = Σl + 3958 Sin(A_1) + 1962 Sin(☾-F) + 318 Sin(A_2)

16. Calculate the **ADDITIVE TO Σb**:

Σb = Σb - 2235 Sin(☾) + 382 Sin(A_3) + 175 Sin(A_1-F) + 175 Sin(A_1+F) + 127 Sin(☾-M') - 115 Sin(☾+M')

17. Calculate the **MOON'S GEOCENTRIC LONGITUDE**, "λ":

λ = ☾ + (Σl / 1000000)

18. Calculate the **MOON'S GEOCENTRIC LATITUDE**, "β":

β = Σb / 1000000

19. Calculate the **MOON'S DISTANCE**, "Δ":

$$\Delta = 385000.56 + (\Sigma r / 1000)$$

20. Calculate the **MOON'S EQUATORIAL HORIZONTAL PARALLAX**, "π":

$$\pi = \mathrm{Sin}^{-1}(6378.14/\Delta)$$

21. Calculate the **LONGITUDE OF THE MEAN ASCENDING NODE OF THE LUNAR ORBIT ON THE ECLIPTIC**, "Ω":

$$\Omega = 125°.0445550 - 1934.1361849(T) + 0.0020762(T^2) + T^3 / 467410 - T^4 / 60616000$$

22. Calculate the **NUTATION IN LONGITUDE**, "$\Delta\psi$":

$$\begin{array}{lll}
\multicolumn{3}{l}{\Delta\psi = (-171996 - 174.2T)\mathrm{Sin}(\Omega) + (-13187 - 1.6T)\mathrm{Sin}(-2D+2F+2\Omega) + (-2274 - 0.2T)\mathrm{Sin}(2F+2\Omega)} \\
+ (2062 + 0.2T)\mathrm{Sin}(2\Omega) & + (1426 - 3.4T)\mathrm{Sin}(g) & + (712 + 0.1T)\mathrm{Sin}(M') \\
+ (-517 + 1.2T)\mathrm{Sin}(-2D+g+2F+2\Omega) & + (-386 - 0.4T)\mathrm{Sin}(2F+\Omega) & - 301\mathrm{Sin}(M'+2F+2\Omega) \\
+ (217 - 0.5T)\mathrm{Sin}(-2D-g+2F+2\Omega) & - 158\mathrm{Sin}(-2D+M') & + (129 + 0.1T)\mathrm{Sin}(-2D+2F+\Omega) \\
+ 123\mathrm{Sin}(-M'+2F+2\Omega) & + 63\mathrm{Sin}(2D) & + (63 + 0.1T)\mathrm{Sin}(M'+\Omega) \\
- 59\mathrm{Sin}(2D-M'+2F+2\Omega) & + (-58 - 0.1T)\mathrm{Sin}(-M'+\Omega) & - 51\mathrm{Sin}(M'+2F+\Omega) \\
+ 48\mathrm{Sin}(-2D+2M') & + 46\mathrm{Sin}(-2M'+2F+\Omega) & - 38\mathrm{Sin}(2D+2F+2\Omega) \\
- 31\mathrm{Sin}(2M'+2F+2\Omega) & + 29\mathrm{Sin}(2M') & + 29\mathrm{Sin}(-2D+M'+2F+2\Omega) \\
+ 26\mathrm{Sin}(2F) & - 22\mathrm{Sin}(-2D+2F) & + 21\mathrm{Sin}(-M'+2F+\Omega) \\
+ (17 - 0.1T)\mathrm{Sin}(2g) & + 16\mathrm{Sin}(2D-M'+\Omega) & + (-16+0.1T)\mathrm{Sin}(-2D+2g+2F+2\Omega) \\
- 15\mathrm{Sin}(g+\Omega) & - 13\mathrm{Sin}(-2D+M'+\Omega) & - 12\mathrm{Sin}(-g+\Omega) \\
+ 11\mathrm{Sin}(2M'-2F) & - 10\mathrm{Sin}(2D-M'+2F+\Omega) & - 8\mathrm{Sin}(2D+M'+2F+2\Omega) \\
+ 7\mathrm{Sin}(g+2F+2\Omega) & - 7\mathrm{Sin}(-2D+g+M') & - 7\mathrm{Sin}(-g+2F+2\Omega) \\
- 7\mathrm{Sin}(2D+2F+\Omega) & + 6\mathrm{Sin}(2D+M') & + 6\mathrm{Sin}(-2D+2M'+2F+2\Omega) \\
+ 6\mathrm{Sin}(-2D+M'+2F+\Omega) & - 6\mathrm{Sin}(2D-2M'+\Omega) & - 6\mathrm{Sin}(2D+\Omega) \\
+ 5\mathrm{Sin}(-g+M') & - 5\mathrm{Sin}(-2D-g+2F+\Omega) & - 5\mathrm{Sin}(-2D+\Omega) \\
- 5\mathrm{Sin}(2M'+2F+\Omega) & + 4\mathrm{Sin}(-2D+2M'+\Omega) & + 4\mathrm{Sin}(-2D+g+2F+\Omega) \\
+ 4\mathrm{Sin}(M'-2F) & - 4\mathrm{Sin}(-D+M') & - 4\mathrm{Sin}(-2D+g) \\
- 4\mathrm{Sin}(D) & + 3\mathrm{Sin}(M'+2F) & - 3\mathrm{Sin}(-2M'+2F+2\Omega) \\
- 3\mathrm{Sin}(-D-g+M') & - 3\mathrm{Sin}(g+M') & - 3\mathrm{Sin}(-g+M'+2F+2\Omega) \\
- 3\mathrm{Sin}(2D-g-M'+2F+2\Omega) & - 3\mathrm{Sin}(3M'+2F+2\Omega) & - 3\mathrm{Sin}(2D-g+2F+2\Omega)
\end{array}$$

$$\Delta\psi = (\Delta\psi / 10000) / 3600$$

23. Calculate the **GEOCENTRIC OPTICAL LIBRATION IN LONGITUDE**, "l'";
AND LATITUDE, "β'":

Let $I = 1°.54242$

This is the inclination of the mean lunar equator to the Ecliptic.

$A\lambda = \lambda + \Delta\psi$

$W = A\lambda - \Delta\psi - \Omega$
$\mathrm{Tan}(A) = (\mathrm{Sin}(W)\mathrm{Cos}(\beta)\mathrm{Cos}(I)-\mathrm{Sin}(\beta)\mathrm{Sin}(I))/(\mathrm{Cos}(W)\mathrm{Cos}(\beta))$

$A = \mathrm{Tan}^{-1}(A)$

If $\mathrm{Cos}(W)\mathrm{Cos}(\beta) < 0$, then $A = A + 180°$

$l' = A - F$

$\mathrm{Sin}(\beta') = -\mathrm{Sin}(W)\mathrm{Cos}(\beta)\mathrm{Sin}(I)-\mathrm{Sin}(\beta)\mathrm{Cos}(I)$

$\beta' = \mathrm{Sin}^{-1}(\beta')$

24. Calculate:

$K_1 = 119.75 + 131.849(T)$

$K_2 = 72.56 + 20.186(T)$

$$\begin{aligned}\rho = {} & -0.02752\mathrm{Cos}(M') - 0.02245\mathrm{Sin}(F) + 0.00684\mathrm{Cos}(M'-2F) - 0.00293\mathrm{Cos}(2F) \\ & - 0.00085\mathrm{Cos}(2F-2D) - 0.00054\mathrm{Cos}(M'-2D) - 0.00020\mathrm{Sin}(M'+F) - 0.00020\mathrm{Cos}(M'+2F) \\ & - 0.00020\mathrm{Cos}(M'-F) + 0.00014\mathrm{Cos}(M'+2F-2D)\end{aligned}$$

$$\begin{aligned}\sigma = {} & -0.02816\mathrm{Sin}(M') + 0.02244\mathrm{Cos}(F) - 0.00682\mathrm{Sin}(M'-2F) - 0.00279\mathrm{Sin}(2F) \\ & - 0.00083\mathrm{Sin}(2F-2D) + 0.00069\mathrm{Sin}(M'-2D) + 0.00040\mathrm{Cos}(M'+F) - 0.00025\mathrm{Sin}(2M') \\ & - 0.00023\mathrm{Sin}(M'+2F) + 0.00020\mathrm{Cos}(M'-F) + 0.00019\mathrm{Sin}(M'-F) + 0.00013\mathrm{Sin}(M'+2F-2D) \\ & - 0.00010\mathrm{Cos}(M'-3F)\end{aligned}$$

$$\begin{aligned}\tau = {} & +0.02520(e)\mathrm{Sin}(g) + 0.00473\mathrm{Sin}(2M'-2F) - 0.00467\mathrm{Sin}(M') + 0.00396\mathrm{Sin}(K_1) \\ & + 0.00276\mathrm{Sin}(2M'-2D) + 0.00196\mathrm{Sin}(\Omega) - 0.00183\mathrm{Cos}(M'-F) + 0.00115\mathrm{Sin}(M'-2D) \\ & - 0.00096\mathrm{Sin}(M'-D) + 0.00046\mathrm{Sin}(2F-2D) - 0.00039\mathrm{Sin}(M'-F) - 0.00032\mathrm{Sin}(M'-g-D) \\ & + 0.00027\mathrm{Sin}(2M'-g-2D) + 0.00023\mathrm{Sin}(K_2) - 0.00014\mathrm{Sin}(2D) + 0.00014\mathrm{Cos}(2M'-2F) \\ & - 0.00012\mathrm{Sin}(M'-2F) - 0.00012\mathrm{Sin}(2M') + 0.00011\mathrm{Sin}(2M'-2g-2D)\end{aligned}$$

25. Calculate the **PHYSICAL LIBRATION IN LONGITUDE**, " l" ":

$l'' = -\tau + (\rho\mathrm{Cos}(A) + \sigma\mathrm{Sin}(A))\mathrm{Tan}(\beta')$

26. Calculate the **PHYSICAL LIBRATION IN LATITUDE**, " b" ":

$$b'' = \sigma \mathrm{Cos}(A) - \rho \mathrm{Sin}(A)$$

27. Calculate the **TOTAL LIBRATION IN LONGITUDE**,"l":

$$l = l' + l''$$

This is the geocentric selenographic longitude of the Earth.

28. Calculate the **TOTAL LIBRATION IN LATITUDE**, "b":

$$b = \beta' + b''$$

This is the geocentric selenographic latitude of the Earth.

29. Calculate the **MEAN AND TRUE OBLIQUITY OF THE ECLIPTIC**, "ε_0", ε":

Let U = T / 100

$$\begin{aligned}\varepsilon_0 = {} & 23°.44484667 - 1°.300258333U - 0E.0004305556U^2 + 0°.5553472222U^3 \\ & - 0°.0142722222U^4 - 0°.0693527778U^5 - 0°.0108472222U^6 + 0°.0019777778U^7 \\ & + 0°.0077416667U^8 + 0°.0016083333U^9 + 0°.0006805556U^{10}\end{aligned}$$

$$\begin{aligned}\Delta\varepsilon_0 = {} & (92025 + 8.9T)\mathrm{Cos}(\Omega) + (5736 - 3.1T)\mathrm{Cos}(-2D+2F+2\Omega) + (977 - 0.5T)\mathrm{Cos}(2F+2\Omega) \\ & + (-895 + 0.5T)\mathrm{Cos}(2\Omega) + (54 - 0.1T)\mathrm{Cos}(g) - 7\mathrm{Cos}(M') \\ & + (224 - 0.6T)\mathrm{Cos}(-2D+g+2F+2\Omega) + 200\mathrm{Cos}(2F+\Omega) + (129 - 0.1T)\mathrm{Cos}(M'+2F+2\Omega) \\ & + (-95 + 0.3T)\mathrm{Cos}(-2D-g+2F+2\Omega) - 70\mathrm{Cos}(-2D+2F+\Omega) - 53\mathrm{Cos}(-M'+2F+2\Omega) \\ & - 33\mathrm{Cos}(M'+\Omega) + 26\mathrm{Cos}(2D-M'+2F+2\Omega) + 32\mathrm{Cos}(-M'+\Omega) \\ & + 27\mathrm{Cos}(M'+2F+\Omega) - 24\mathrm{Cos}(-2M'+2F+\Omega) + 16\mathrm{Cos}(2D+2F+2\Omega) \\ & + 13\mathrm{Cos}(2M'+2F+2\Omega) - 12\mathrm{Cos}(-2D+M'+2F+2\Omega) - 10\mathrm{Cos}(-M'+2F+\Omega) \\ & - 8\mathrm{Cos}(2D-M'+\Omega) + 7\mathrm{Cos}(-2D+2g+2F+2\Omega) + 9\mathrm{Cos}(g+\Omega) \\ & + 7\mathrm{Cos}(-2D+M'+\Omega) + 6\mathrm{Cos}(-g+\Omega) + 5\mathrm{Cos}(2D-M'+2F+\Omega) \\ & + 3\mathrm{Cos}(2D+M'+2F+2\Omega) - 3\mathrm{Cos}(g+2F+2\Omega) + 3\mathrm{Cos}(-g+2F+2\Omega) \\ & + 3\mathrm{Cos}(2D+2F+\Omega) - 3\mathrm{Cos}(-2D+2M'+2F+2\Omega) - 3\mathrm{Cos}(-2D+M'+2F+\Omega) \\ & + 3\mathrm{Cos}(2D-2M'+\Omega) + 3\mathrm{Cos}(2D+\Omega) + 3\mathrm{Cos}(-2D-g+2F+\Omega) \\ & + 3\mathrm{Cos}(-2D+\Omega) + 3\mathrm{Cos}(2M'+2F+\Omega)\end{aligned}$$

$$\varepsilon = \varepsilon_0 + (\Delta\varepsilon_0 / 10000) / 3600$$

30. Calculate the **APPARENT RIGHT ASCENSION**, "α":

$$\mathrm{Tan}(\alpha) = (\mathrm{Sin}(\lambda)\mathrm{Cos}(\varepsilon) - \mathrm{Tan}(\beta)\mathrm{Sin}(\varepsilon)) / \mathrm{Cos}(\lambda)$$

$$\alpha = \mathrm{Tan}^{-1}(\alpha)$$

If $\mathrm{Cos}(\lambda) < 0$, then $\alpha = \alpha + 180°$

31. Calculate the **APPARENT DECLINATION**, "δ":

$$\sin(\delta) = \sin(\beta)\cos(\varepsilon) + \cos(\beta)\sin(\varepsilon)\sin(\lambda)$$

$$\delta = \sin^{-1}(\delta)$$

32. Calculate the **MEAN LONGITUDE OF THE LUNAR PERIGEE**, "Γ'":

$$\Gamma' = 83°.3532430 + 4069.0137111(T) - 0.0103238(T^2) - T^3 / 80053 + T^4 / 18999000$$

This is measured in the Ecliptic from the Mean Equinox of Date to the Mean Ascending Node of the lunar orbit, then along the orbit.

33. Calculate the **GEOMETRIC MEAN LONGITUDE OF THE SUN**. "λ_{υ}":

$$\lambda_{\upsilon} = 280°.46645 + 36000°.76983(T) + 0°.0003032(T^2)$$

This is measured from the Mean Equinox of Date.

34. Calculate the **GEOCENTRIC POSITION OF THE MOON**,"M":

$$M = 0°.040\sin(\Gamma'-\Omega) - 0°.003\sin(☾-\Omega)$$

35. Calculate the **POSITION OF THE MOON'S NORTH CELESTIAL POLE**, "N":

$$N = 0°.020\cos(\Gamma'-\Omega) + 0°.003\cos(☾-\Omega)$$

36. Calculate the **PHYSICAL LIBRATION OF THE POSITION ANGLE OF THE MOON'S AXIS**, "δC":

$$\delta C = M \sin(l') - (N \cos(l')\sec(\beta'))$$

37. Calculate the **SUN'S EQUATION OF CENTER**, "C":

$$C = (1°.914600 - 0°.004817(T) - 0°.000014(T^2))\sin(g) + (0°.019993 - 0°.000101(T))\sin(2g) + 0°.000290\sin(3g)$$

38. Calculate the **TRUE LONGITUDE OF THE SUN**,"$\odot$":

$$\odot = \lambda_{\upsilon} + C$$

39. Calculate the **ECCENTRICITY OF THE EARTH'S ORBIT**, "e":

$$e = 0.016708617 - 0.000042037(T) - 0.0000001236(T^2)$$

40. Calculate the **SUN'S TRUE ANOMALY**, "V":

$$V = g + C$$

41. Calculate the **RADIUS VECTOR OF THE SUN**, "R":

$$R = 1.000001018(1 - e^2) / (1 + e\ \mathrm{Cos}(V))$$

42. Calculate the **HELIOCENTRIC LONGITUDE OF THE MOON**, "λ_h":

$$\lambda_h = \lambda_\odot + 180° + (8.794/((3600)(\pi)(R))(57°.296\mathrm{Cos}(\beta)\ \mathrm{Sin}(\lambda_\odot - \lambda))$$

43. Calculate the **HELIOCENTRIC LATITUDE OF THE MOON**, "β_h":

$$\beta_h = (8.794 / ((3600)(\pi)(R)))(\beta)$$

44. Calculate the **AUXILIARY QUANTITIES FOR THE SELENOGRAPHIC POSITION OF THE SUN**, "l_h'", "b_h'":

$$W_h = \lambda_h - \Delta\psi - \Omega$$

$$\mathrm{Tan}(A) = \mathrm{Sin}(W_h)\mathrm{Cos}(\beta_h)\mathrm{Cos}(I) - \mathrm{Sin}(\beta_h)\mathrm{Sin}(I)) / \mathrm{Cos}(W_h)\mathrm{Cos}(\beta_h))$$

$$A = \mathrm{Tan}^{-1}(A)$$

If $\mathrm{Cos}(W_h)\mathrm{Cos}(\beta) < 0$, then $A = A + 180°$

$$l_h' = A - F$$

$$\mathrm{Sin}(b_h') = -\mathrm{Sin}(W_h)\mathrm{Cos}(\beta_h)\mathrm{Sin}(I) - \mathrm{Sin}(\beta_h)\mathrm{Cos}(I)$$

$$b_h' = \mathrm{Sin}^{-1}(b_h')$$

45. Calculate the **SELENOGRAPHIC LONGITUDE OF THE SUN**, "ls":

$$ls' = -\tau + (\rho\mathrm{Cos}(A) + \sigma\mathrm{Sin}(A))\mathrm{Tan}(b_h')$$

$$ls = l_h' + ls'$$

46. Calculate the **SELENOGRAPHIC LATITUDE OF THE SUN**, "bs":

$$bs' = \tau\mathrm{Cos}(A) - \rho\mathrm{Sin}(A)$$

$$bs = b_h' + bs'$$

47. Calculate the **SELENOGRAPHIC COLONGITUDE**, "cls":

$$cls = 90° - ls$$

48. Calculate the **GEOCENTRIC LATITUDE**, "ϕ'":

$Tan(U) = 0.99664719Tan(\phi)$

$U = Tan^{-1}(U)$

Let H_o = Observer's elevation in meters

$\rho Sin(\phi') = 0.99664719Sin(U) + (H_o / 6378140)Sin(\phi)$

$\rho Cos(\phi') = Cos(U) + (H_o / 6378140)Cos(\phi)$

$Tan(\phi') = \rho Sin(\phi') / \rho Cos(\phi')$

$\phi' = Tan^{-1}(\phi')$

49. Calculate the **GREENWICH MEAN SIDEREAL TIME AT 0h U.T.**, "θ_0":

$\theta_0 = 100.46061837 + 36000.770053608(T) + 0.000387933(T^2) - T^3 / 38710000$

50. Calculate the **LOCAL SIDEREAL TIME**, "LST":

$LST = \theta_0 - \lambda$

51. Calculate the **GEOCENTRIC LOCAL HOUR ANGLE**, "H":

$H = LST - \alpha$

52. Calculate the **TOPOCENTRIC CORRECTION FOR PARALLAX IN R.A. AND THE TOPOCENTRIC DECLINATION**, "$\Delta\alpha$", "$\Delta\delta$":

$Tan(\Delta\alpha) = (-\rho Cos(\phi')Sin(\pi)Sin(H)) / (Cos(\delta)-(\rho Cos(\phi') Sin(\pi)Cos(H)))$

$\Delta\alpha = Tan^{-1}(\Delta\alpha)$

$T\alpha = \alpha + \Delta\alpha$

$Tan(\Delta\delta) = ((Sin(\delta) - (\rho Sin(\phi')Sin(\pi)))Cos(\Delta\alpha)) / (Cos(\delta) - (\rho Sin(\phi')Sin(\pi)Cos(H)))$

$T\delta = Tan^{-1}(\Delta\delta)$

53. Calculate the **APPARENT LOCAL HOUR ANGLE**, "AH":

$AH = LST - T\alpha$

54. Calculate the **TOPOCENTRIC LONGITUDE AND LATITUDE**, "Tλ", "Tβ":

$\mathrm{Tan}(T\lambda) = (\mathrm{Sin}(T\alpha)\mathrm{Cos}(\varepsilon) + \mathrm{Tan}(T\delta)\mathrm{Sin}(\varepsilon)) / \mathrm{Cos}(T\alpha)$

$T\lambda = \mathrm{Tan}^{-1}(T\lambda)$

If $\mathrm{Cos}(T\alpha) < 0$, then $T\lambda = T\lambda + 180°$

$\mathrm{Sin}(T\beta) = \mathrm{Sin}(T\delta)\mathrm{Cos}(\varepsilon) - \mathrm{Cos}(T\delta)\mathrm{Sin}(\varepsilon)\mathrm{Sin}(T\alpha)$

$T\beta = \mathrm{Sin}^{-1}(T\beta)$

55. Calculate the **TOPOCENTRIC OPTICAL LIBRATIONS IN LONGITUDE**, "Tl'", **AND LATITUDE**, "Tb'":

Let I = 1.54242

$W = T\lambda - \Delta\psi - \Omega$

$\mathrm{Tan}(A) = (\mathrm{Sin}(W)\mathrm{Cos}(T\beta)\mathrm{Cos}(I) - \mathrm{Sin}(T\beta)\ \mathrm{Sin}(I)) / (\mathrm{Cos}(W)\mathrm{Cos}(T\beta))$

$A = \mathrm{Tan}^{-1}(A)$

If $\mathrm{Cos}(W)\mathrm{Cos}(T\beta) < 0$, then $A = A + 180°$

$Tl' = A - F$

$\mathrm{Sin}(Tb') = -\mathrm{Sin}(W)\mathrm{Cos}(T\beta)\mathrm{Sin}(I) - \mathrm{Sin}(T\beta)\mathrm{Cos}(I)$

$Tb' = \mathrm{Sin}^{-1}(Tb')$

56. Calculate **ΔTl"** and **ΔTb"** using steps 25 & 26.

57. Calculate the **TOPOCENTRIC LIBRATIONS IN LONGITUDE AND LATITUDE**, "TLONG", "TLAT":

$TLONG = Tl' + \Delta Tl''$

$TLAT = Tb' + \Delta Tb''$

58. Calculate the **MOON'S ALTITUDE**, "ALT":

$\mathrm{Sin}(ALT) = \mathrm{Sin}(\phi)\mathrm{Sin}(\delta) + (\mathrm{Cos}(\phi)\mathrm{Cos}(\delta)\mathrm{Cos}(H))$

$ALT = \mathrm{Sin}^{-1}(ALT)$

59. Calculate the **ZENITH DISTANCE**, "ZD":

$ZD = 90° - ALT$

60. Calculate the **AIR MASS CORRECTION**, "X":

$Sec(ZD) = 1 / ZD$

$X = (Sec(ZD) - 0.0018167(Sec(ZD)-1) - 0.002875(Sec(ZD)-1)^2 - 0.0008083(Sec(ZD)-1)^3)^{-1}$

NOTE: Steps 1 through 60 should be performed for each site and comparison site.

61. Multiply the measures for each site, R' by the air mass correction, " R" ".

62. Average the sun's colongitude, sun's latitude, and the Earth's selenographic longitude and latitude, "Acls", "Abs", ATLONG", "ATLAT".

63. Calculate the **SUN'S ALTITUDE**, "SA":

$Sin(SA) = Sin(bs)Sin(\beta_s) + Cos(bs)Cos(\beta_s)Cos(\eta\text{-}cls)$

Where η is the site's longitude; + = East (toward Mare Crisium), and β_s is the site's latitude; + = North (toward Plato).

$SA = Sin^{-1}(SA)$

64. Calculate the **EARTH'S ALTITUDE**,"EA":

$Sin(EA) = Sin(b)Sin(\beta_s) + Cos(b)Cos(\beta_s)Cos(\eta - cls)$

$EA = Sin^{-1}(EA)$

65. Calculate the **MOON'S PHASE ANGLE**, "PA":

$Sin(PA) = Sin(bs)Sin(b) + Cos(bs)Cos(b)Cos(cls\text{-}l)$

$PA = Sin^{-1}(PA)$

PA is between 0° and 180°.

$PAA = |PA|$

If PA < 0, then add 180° to PAA.
If PAA > 180°, then subtract 360 from PAA.

If l < cls, then multiply PAA by -1.

This is the angle between the direction of incidence and observation.

66. Calculate the **BRIGHTNESS LONGITUDE**, "BL":

$$BL = |Sin(EA)/\sqrt{(1-Cos(EA)^2+((Sin(SA)-(PA)Sin(EA))/Sin(PA)^2))}|$$

If $l > ls$, then $BL = -1$ if $(\eta - l) < 0$
$BL = 0$ if $(\eta - l) = 0$
$BL = +1$ if $(\eta - l) > 0$

If $l < ls$, then $BL = -1$ if $(l - \eta) < 0$
$BL = 0$ if $(l - \eta) = 0$
$BL = +1$ if $(l - \eta) > 0$

67. Calculate the **PHOTOMETRIC FUNCTION**, "PFT":

Let BF = 1, where "BF" is the backscatter factor.

Let $H = 0.4$, $f = 0.9$, and $\gamma = 45°$. The values for H, f, and γ are the recommended values for Hapke's model.

If $|PA| = 0$, then $BF = 2$; for a Lambert surface.

If $|PA| > 0$ and $< 45°$, then

$$BF = 2 - (Tan(|PA|)/2H)(1 - exp(-H/Tan(|PA|)))(3 - exp(- H/Tan(|PA|)))$$

where "H" is Hapke's "H" function indicating the porosity of the soil and the sharpness of the backscatter peak.

If $|PA| = 0$ or $|PA| >= 45°$, then

$$S = (Sin(|PA|) + (180° - |PA|)(Cos(|PA|)))/180° + 0.1(1 - Cos(|PA|)^2)$$

This is the average angular scattering function of a single particle. The $(0.1(1 - Cos(|PA|)^2))$ term results from diffraction of light around the small irregularities on the limbs of the particles.

Let $PABL = |BL| + |PA|$

Determine Hapke's region, "R":

Let R = 0.
If $PABL < 45°$, then R = 1.
If $PABL < (45° - \gamma)$, then R = 2.

where γ is Hapke's γ function, which represents the angle of the surface to the incident light.

If R = 2 and $|BL| < -\gamma$, then R = 3.

If R = 1 and $|BL| < -\gamma$, then R = 4.

If R = 4 and $|PA| > (45° - \gamma)$, then R = 5.

Determine the constants for the photometric function:

Let K1 = 1 and K2 = 1.

If R = 0, then K1 = 0.
If R = 0, or R = 5, then K2 = 0.
Let J = 0 and K3 = 0.
If R = 1, then J = 1.
If R = 2 or R = 4, then J = 0.5.
If R = 4, then K3 = 1.
If R = 1 or R = 3, then K3 = 0.5.

$$L1 = K1(1 - f)/(1 + \mathrm{Cos}(|BL|)/\mathrm{Cos}(PABL)))$$

where "f" is Hapke's f function, which represents the number of troughs on the surface of the particle.

$$L2 = K2(f)/(2\mathrm{Cos}(|PA|/2)\mathrm{Cos}(|BL|)\mathrm{Sin}(\gamma))$$

$$L3 = \mathrm{Cos}(|BL| + J(|PA|))\mathrm{Sin}(\gamma + K3(|PA|))$$

$$L4 = (\mathrm{Cos}(|BL| + J(|PA|)) + \sin(\gamma + K3(|PA|)))/(\mathrm{Cos}(|BL| + J\ |PA|)) - \mathrm{Sin}(\gamma + K3(|PA|)))$$

$$L5 = 0.5(\mathrm{Sin}(|PA|/2)^2\ln(|L4|))$$

$$L = L1 + L2(L3 - L5)$$

$$PFT = (L)(S)(BF)$$

NOTE: The H, f, and γ functions are the recommended default values. Values other than these will significantly alter the results, since these parameters are very sensitive to observational errors.

**** Steps 63 through 67 should be performed for each site's "Acls", "Abs", "ATLONG", and "ATLAT" sets.

68. Determine the albedo from Shorthill's list (Appendix G).

69. Calculate **A(0)PFT(0)**, where PFT(0) is the PFT for the comparison site.

70. For each set, for each site, calculate the **PHOTOMETRIC FUNCTION** "PF", and the **ALBEDO**,"A":

$$PF = (PFT(0)A(0)R'' / R''(0))$$

where R"(0) is the R" of the comparison site.

$$A = PF/PFT$$

where PFT is the photometric function of the site.

71. Average the A values, "AVGA".

72. Plot AVGA versus PA.

73. Average the PF values, "AVGPF".

74. Plot AVGPF versus PA.

THE FOLLOWING STEPS ARE FOR MULTIBAND PHOTOMETRY.

75. Calculate instrumental magnitude of the standard and extinction stars:

$V = -2.5 \text{ Log}(R'_{V\text{-STAR}})$

$B = -2.5 \text{ Log}(R'_{B\text{-STAR}})$

$R = -2.5 \text{ Log}(R'_{R\text{-STAR}})$

76. Calculate the magnitude difference between the site and the standard star:

$\Delta V = -2.5 \text{ Log}(R'_{V\text{-SITE}} / R'_{V\text{-STAR}})$

$\Delta B = -2.5 \text{ Log}(R'_{B\text{-SITE}} / R'_{B\text{-STAR}})$

$\Delta R = -2.5 \text{ Log}(R'_{R\text{-SITE}} / R'_{R\text{-STAR}})$

77. Calculate the difference in color indices:

$\Delta(B\text{-}V) = \Delta B - \Delta V$

$\Delta(V\text{-}R) = \Delta V - \Delta R$

78. Calculate the first-order extinction correction:

Plot V versus X, B versus X, and R versus X;

where V, B, and R = the instrumental magnitudes of the extinction star, and X = the air mass correction.

Calculate the slope ("k'_V", "k'_B", "k'_R") of the line:

$k'_V = ((N)\, \Sigma(X_i V_i) - \Sigma\, (X_i)\, \Sigma\, (V_i)) / ((N)\, \Sigma\, (X_i^2) - (\Sigma\, (X_i))^2)$

$k'_B = ((N)\, \Sigma\, (X_i B_i) - \Sigma\, (X_i)\, \Sigma\, (B_i)) / ((N)\, \Sigma\, (X_i^2) - (\Sigma\, (X_i))^2)$

$k'_R = ((N)\, \Sigma\, (X_i R_i) - \Sigma\, (X_i)\, \Sigma\, (R_i)) / ((N)\, \Sigma\, (X_i^2) - (\Sigma\, (X_i))^2)$

where N = the number of measurements,
I = 1 to N,
X_i = the air mass correction, and
V_i, B_i, R_i = the V, B, and R instrumental magnitudes.

This is the first-order extinction correction.

79. Calculate the **INTERCEPT OF THE LINE**, "a_V", "a_B", and "a_R":

$$a_V = \overline{V}_{STAR} - k'_V(\overline{X}_{STAR})$$

$$a_B = \overline{B}_{STAR} - k'_B(\overline{X}_{STAR})$$

$$a_R = \overline{R}_{STAR} - k'_R(\overline{X}_{STAR})$$

where $\overline{V}_{STAR}$, $\overline{B}_{STAR}$, and $\overline{R}_{STAR}$ = the average instrumental magnitudes, and $\overline{X}_{STAR}$ = the average air mass correction.

80. Calculate $\mathbf{V_i^L}$**,** $\mathbf{B_i^L}$**, and** $\mathbf{R_i^L}$:

$$v_i^L = a_V Cos(X_{STARi})$$

$$B_i^L = a_B Cos(X_{STARi})$$

$$R_i^L = a_R Cos(X_{STARi})$$

This is the linear least-square fit for the instrumental magnitudes.

81. Calculate the **STANDARD ERROR**, "Σ_V", "Σ_B", and "Σ_R":

$$3_V = \sqrt{(\Sigma\ (V_i - V_i^L)^2 / (N - 2))}$$

$$3_B = \sqrt{(\Sigma\ (B_i - B_i^L)^2 / (N - 2))}$$

$$3_R = \sqrt{(\Sigma\ (R_i - R_i^L)^2 / (N - 2))}$$

82. Calculate the **GOODNESS OF FIT**, "r":

$$r_V = 1 / (N - 1)\ \Sigma\ ((X_{STARi} - \overline{X}_{STAR})(V_{STARi} - \overline{V}_{STAR}))\ /$$

$$(\sqrt{1 / (N - 1)\ \Sigma\ (X_{STARi} - \overline{X}_{STAR})^2}\sqrt{1 / (N - 1)\ \Sigma\ (V_{STARi} - \overline{V}_{STAR})^2})$$

$$r_B = 1 / (N - 1)\ \Sigma\ ((X_{STARi} - \overline{X}_{STAR})(B_{STARi} - \overline{B}_{STAR}))\ /$$

$$(\sqrt{1 / (N - 1)\ \Sigma\ (X_{STARi}\ \overline{X}_{STAR})^2}\sqrt{1 / (N - 1)\ \Sigma\ (B_{STARi} - \overline{B}_{STAR})^2})$$

$r_R = 1 / (N - 1)\ \Sigma\ ((X_{STARi} - X_{STAR})(R_{STARi} - R_{STAR}))\ /$

$(\sqrt{1 / (N - 1)\ \Sigma\ (X_{STARi} - \bar{X}_{STAR})^2}\ \sqrt{1 / (N - 1)\ \Sigma\ (R_{STARi} - \bar{R}_{STAR})^2})$

"r" should be as close to 1.0 as possible.

83. Calculate the **CORRECTED MAGNITUDE DIFFERENCE**, "ΔV_0", "ΔB_0", and "ΔR_0":

$\Delta V_0 = \Delta V - k'_V(X_{SITE} - X_{STAR})$

$\Delta B_0 = \Delta B - k'_B(X_{SITE} - X_{STAR})$

$\Delta R_0 = \Delta R - k'_R(X_{SITE} - X_{STAR})$

84. Calculate the **CORRECTED COLOR INDEX DIFFERENCES**:

$\Delta(B\text{-}V)_0 = \Delta(B - V) - (k'_B - k'_V)(X_{SITE} - X_{STAR})$

$\Delta(V\text{-}R)_0 = \Delta(V - R) - (k'_V - k'_R)(X_{SITE} - X_{STAR})$

85. Calculate the **APPARENT MAGNITUDE OF THE SITE**, "SM(V)", "SM(B)", and "SM(R)":

$SM(V) = M(V)_{STD\ STAR} - 2.5\ \mathrm{Log}(V_{SITE} / V_{STAR})$

$SM(B) = M(B)_{STD\ STAR} - 2.5\ \mathrm{Log}(B_{SITE} / B_{STAR})$

$SM(R) = M(R)_{STD\ STAR} - 2.5\ \mathrm{Log}(R_{SITE} / R_{STAR})$

86. Calculate the **COLOR INDEX OF THE SITE**:

$CI(B\text{-}V) = SM(B) - SM(V)$

$CI(V\text{-}R) = SM(V) - SM(R)$

ACKNOWLEDGMENTS

I wish to thank the person whose encouragement and support made this handbook possible:

Dr. John E. Westfall, Director of the Association of Lunar and Planetary Observers. Dr. Westfall wrote the original "Lunar Photoelectric Photometry Handbook", copyright 1984, and has graciously permitted me to include material from his handbook. He has consistently been available to answer the many questions that I have had at the beginning of my attempt at lunar photometry. His encouragement has been most welcome and appreciated.

I would also like to thank Charlie Lemon and Scott Ziesel for their help in scanning the diagrams. This is an art which I am not that familiar with. So, thanks guys!!!

A special thanks to my wife who has suffered through my research, and who helped in putting this handbook together.